Surfactant Pseudophases for Open-tubular Liquid Chromatography and Electrochromatography

by

Faustino Tarongoy Jr.

School of Natural Sciences

Submitted in fulfilment of the requirements for the Doctor of Philosophy

(Physical Science)

University of Tasmania

June, 2018

Declaration of Originality

This thesis contains no material which has been accepted for a degree or diploma by the University or any other institution, except by way of background information and duly acknowledged in the thesis, and to the best of my knowledge and belief no material previously published or written by another person except where due acknowledgement is made in the text of the thesis, nor does the thesis contain any material that infringes copyright.

1st June 2018

Authority of Access

This thesis may be made available for loan and limited copying and communication in accordance with the Copyright Act 1968.

Statement regarding published work contained in thesis

The publishers of the papers comprising Chapters 1 and 4 hold the copyright for that content, and access to the material should be sought from the respective journals. The remaining non-published content of the thesis may be made available for loan and limited copying and communication in accordance with the Copyright Act 1968.

1st June 2018

Statement of co-authorship

The following people and institutions contributed to the publication of the work undertaken as part of this thesis:

Candidate:	Faustino Tarongoy Jr., Australian Centre for Research on Separation Science, School of Natural Sciences, University of Tasmania
Author 1:	Joselito P. Quirino (primary supervisor), Australian Centre for Research on Separation Science, School of Natural Sciences, University of Tasmania
Author 2:	Paul R. Haddad (secondary supervisor), Australian Centre for Research on Separation Science, School of Physical Sciences, University of Tasmania

Author details and their roles:

Paper 1: Tarongoy, F. M., Jr.; Haddad, P. R.; Quirino, J. P., Recent developments in open tubular capillary electrochromatography from 2016 to 2017. *Electrophoresis* **2018,** *39* (1), 34-52. Journal impact factor: 2.744

Located in Chapter 1

Candidate was the primary author and Author 1 and Author 2 contributed to the idea, its formalisation and revision.

Paper 2: Quirino, J. P.; Tarongoy, F. M., Liquid chromatography with micelles in open-tube capillaries. *Green Chemistry* **2018,** *20* (11), 2486-2493. Journal impact factor: 9.125

Located in Chapter 4

Candidate was the secondary author and contributed 65% to the execution and experimental studies and drafted significant parts especially the preparation of figures and tables of the paper.

Author 1 was the primary author, contributed to the conception, planning and design of the project, writing and revisions. He contributed approximately 35% to the experimental work.

Paper 3 (manuscript for submission): Tarongoy, F. M., Jr.; Haddad, P. R.; Quirino, J. P., Open-tubular admicellar liquid chromatography and electrochromatography.

Located in Chapter 3

Candidate was the primary author and executed the experimental studies.

Author 1 was the secondary author and contributed to the conception, planning and design of the project, analysis and interpretation of the research data, writing and revisions.

Author 2 contributed to the conception, planning, design of the project and to the interpretation of the work by critically revising the paper.

We the undersigned agree with the above stated "proportion of work undertaken" for each of the above published (or submitted) peer-reviewed manuscripts contributing to this thesis:

Signed: _____ _____

./Prof. Joselito P. Quirino	**Prof. Mark Hunt**
ervisor	*Head of School*
hool of Natural Sciences	*School of Natural Sciences*
College of Science and Engineering	*College of Science and Engineering*
University of Tasmania	University of Tasmania
Date: 31/5/2018	5/6/18

Acknowledgments

This dissertation would not have been possible without the generous support of advisors, colleagues, friends, and family, to whom I am very, very grateful.

The curiosity and keen interest in science have been planted, nurtured and tended by my extraordinary teachers and mentors who have been huge influences and outstanding examples that helped shape my career choices towards Chemistry and direction in life —Ms.Carmen de la Cruz, Dr. Ciriaco Gillera, Ms. Christine Avancena, Dr. Lina Kwong, my college mentor, model administrator and later colleague and friend, and Dr. Fabian Dayrit, my MS adviser, scientist and a stalwart of Chemistry in the Philippines.

My deepest gratitude and most profound respect I give to Associate Professor Joselito Quirino, first for acknowledging that I might have something yet more to contribute even with my "late" entry to postgraduate life and so accepted me for his PhD project, for his sharp mind to guide me in the direction of my PhD, for his careful supervision for quality research work and communication, helping me improve my writing style and awareness of the world of research publications, for his keen guidance to gain critical awareness and appreciation of my own work and of other researchers, and for his subtle but constant support to keep on amidst the challenges, difficulties and also successes. Professor Paul Haddad also deserves my next biggest thanks for his sharp-minded insights that helped me so much to improve my work and my writing, and for placing his undeserved reassurance and confidence on me and my work.

I will also be forever grateful to everyone in UTAS Chemistry that helped me make my postgraduate work and life possible and fruitful. To the administrative staff, to Murray Frith for making sure our needs regarding research facilities are always met; to Trish McKay, for her able and very kind assistance in addressing our paper work needs; to Brendon Schollum and Andrew Grosse, for their constant availability to assist us with lab supplies and ensuring our safety always; to Petr Smejkal, for his valued assistance in keeping our instruments up to performance; and to Marina Lanz, Umme Kalsoom, Carol Jacobs and Aimee Scott, for their immeasurable help to coordinate our endeavors in ACROSS. I also wish to extend my deepest appreciation and admiration to all the academics in ACROSS while I was present in UTAS, for this extraordinary pool of intellect and talent, and their outstanding body of work that greatly influenced my work and dedication towards Chemistry and science.

I wish to deeply thank all my colleagues in ACROSS – my fellow postgrads, for the exciting presentation and exchange of ideas, comments and good times that helped influence my own work and life balance; most especially to my fellow workers in Lito's group: Alain Wuetrich, Marni Tubaon-Amuno, Wojciech Grochocki, Mojtaba Mostafavi, Alireza Ghiasvand, Mitch Zimmerman and Kurt Debuille (including the amazing Angus Olding), for their inspiring dedication, helpful collaboration, and enduring bonds of friendship.

My gratitude is extended to the financial support provided by the Australian Research Council Discovery Grant DP180102810. and the University of Tasmania for the International Postgraduate Scholarship. I am also greatly indebted for the

support granted by my home institution, Xavier University, Cagayan de Oro, Philippines, particularly for the study leave grant with pay to pursue PhD studies.

My life and the completion of my studies here in Hobart, Tasmania, would not have been also fulfilling and memorable if not for the tremendous support and friendship of the Filipino community in Tasmania, particularly in Hobart, who have welcomed me and now have become part of my life forever. I am also very grateful for the constant support extended to me by my colleagues in my home department and other faculty friends in Xavier University, particularly Drs. Aileen Angcajas and Juliet Dalagan, for helping sustain me with unceasing encouragement and logistical and administrative support.

I am always deeply indebted to my family: my loving mother Estefania, and ever supportive siblings, Maria Fe, Fely and Bernie and their own families, for keeping me grounded and connected as a family, and most especially for their unceasing love and support in every moment of my life. I am especially grateful for the generous love and confidence of my beloved aunt, Nelia, for her willingness to help me out financially sometime during this PhD studies.

Finally, I owe everything to my Lord and God, for His benevolence and unconditional love, for His never-ending guidance and consolation, for His Spirit of inspiration, courage, hope and resilience, and for His gifts of joy, people and experiences to help me continue to go where He leads me.

Content

List of abbreviations

ACN	acetonitrile
AFM	atomic force microscopy
AIBN	azobisisobutyronitrile
APS	ammonium persulphate
APTES	3-aminopropyltriethoxysilane
APTMS	3-aminopropyltrimethoxysilane
BET	Brunauer–Emmett–Teller
BGE	background electrolyte
BGS	background solution
BHA	butylhydroxyanisole
BSA	bovine serum albumin
BTC	1,3,5-benzenetricarboxlic acid
β-CD	β-cyclodextrin
CE	capillary electrophoresis
CEC	capillary electrochromatography
cmc	critical micelle concentration
COF	covalent organic framework
csac	critical surface aggregation concentration

CTAB	hexadecyl- or cetyltrimethylammonium bromide
CZE	capillary zone electrophoresis
DCM	dichloromethane
DMEAPL	dimethylethanolamine-aminated polychloromethylstyrene nanolatex
EDS	energy dispersive X-ray spectrometry
EDMA	ethylene glycol dimethacrylate
EOF	electroosmotic flow
FT-IR	Fourier transform-infra red spectroscopy
G	graphene
GLYMO	3-glycidoxy-propyl-trimethoxysilane
GNPs	gold nanoparticles
GO	graphene oxide
GOOH	reduced graphene oxide
GPTMS	3-glycidoxypropyl-trimethoxysilane
HILIC	hydrophilic interaction liquid chromatography
LbL	layer-by-layer
LODs	limits of detection
γ-MAPS	γ-methacryloxypropyltrimethoxysilane
MEKC	micellar electrokinetic chromatography

MeOH	methanol
MIP	molecularly imprinted polymers
MLC	Micellar liquid chromatography
MOF	metal organic framework
MPTMS	3-mercaptopropyl-trimethoxysilane
NCCs	nanocellulose crystals
NP	nanoparticles
NSAIDs	non-steroidal anti-inflammatory drugs
OT-AMEC	open-tubular admicellar electrochromatography
OT-AMLC	open-tubular admicellar liquid chromatography
OT-CEC	open-tubular capillary electrochromatography
OT-LC	open-tubular liquid chromatography
OT-MLC	open-tubular micellar liquid chromatography
PAA	poly(acrylic acid)
PAHs	polyaromatic hydrocarbons
PDA	polydopamine
PDADMAC	poly(diallyldimethylammonium chloride)
PDMAEMA	poly(2-dimethylaminoethylmethacrylate)
PDMS	poly(dimethylsiloxane)

PEI	polyethyleneimine
PLOT	porous layer open tubular
PMMA	polymethyl methacrylate
RAFT	reversible addition-fragmentation chain transfer polymerisation
RPLC	reversed-phased liquid chromatography
RRT	relative retention time
RSD	relative standard deviation
SDS	sodium dodecylsulfate
SEM	scanning electron microscopy
SP	stationary phase
TEM	transmission electron microscopy
TMAPL	trimethylamine-aminated polychloromethylstyrene nanolatex
XRD	X-ray diffraction
XPS	X-ray photoelectron spectroscopy
ZIF	zeolitic imidazolate framework

List of figures

List of tables

List of included publications

Peer-reviewed articles

1. Tarongoy, F. M., Jr.; Haddad, P. R.; Quirino, J. P., Recent developments in open tubular capillary electrochromatography from 2016 to 2017. *Electrophoresis* **2018,** *39* (1), 34-52. Journal mpact factor: 2.744 (Chapter 1)
2. Quirino, J. P.; Tarongoy, F. M., Liquid chromatography with micelles in open-tube capillaries. *Green Chemistry* **2018,** *20* (11), 2486-2493. Journal impact factor: 9.125 (Chapter 4)

Manuscript for publication

1. Tarongoy, F. M., Jr.; Haddad, P. R.; Quirino, J. P., Open-tubular admicellar liquid chromatography and electrochromatography. (Chapter 3)

Poster presentations

Tarongoy, F. M., Jr.; Haddad, P. R.; Quirino, J. P., 2nd ACROSS International Symposium on Advances in Separation Science. 2 (ASASS 2), Hobart, Tasmania, 30 November – 2 December 2016, Title: *Static and dynamic coating materials for electrodriven separations*

Tarongoy, F. M., Jr., Haddad, P. R., Quirino, J. P., RACI R&D Topics 2017 Conference, University of Tasmania, Hobart, Tasmania, Australia, 3 – 6 December 2017. Title: *Surfactant admicelles for open tubular capillary electrochromatography.*

Abstract

Chromatographic science continues to take great interest in column development, particularly in discovering new materials for stationary phases that are efficient, stable, robust and selective. Open-tubular formats for microcolumns are regarded as advantageous due to the improved increased mass transfer, with very good chromatographic performance shown by theoretical studies. Surfactant-based separations by liquid chromatography and electrophoresis have long been established with surfactants above the critical micelle concentration (cmc). New liquid chromatography and electrochromatographic techniques are introduced here that exploit the molecular aggregates of surfactants below and above the cmc as immobile pseudophases suitable for open-tubular capillary columns. Electroosmotic flow measurements were used to characterise surface aggregation of two common ionic surfactants, hexadecyl- or cetyltrimethylammonium bromide (CTAB) and sodium dodecylsulfate (SDS), determining the cmc and the critical surface aggregation concentration (csac) that define admicelle and micellar formation. Admicelles formed between the csac and cmc were employed as soft and immobile pseudophases for the open-tubular admicellar liquid chromatography (OT-AMLC) and admicellar electrochromatography (OT-AMEC) of neutral (alkyl phenyl ketones, pesticides) and ionic (sulfonamides) analytes. Retention behaviour was ascertained using the relative retention times (RRT) showing similar values within the csac-to-cmc range, confirming admicelles were unaltered by pressure and electric field forces. Interfacial and solution micelles formed above the cmc govern the separation behaviour in open-tubular micellar liquid chromatography (OT-MLC) applied to neutral and ionic (food antioxidants) analytes and real sample

matrices. Mobile phase conditions (pH, ionic strength, added salts and organic solvents) affected chromatographic behaviour. Analytical figures of merit (linearity, LOD, repeatability) have indicated acceptable employability of these techniques. This thesis introduces a new area of interest in separation science research.

Introduction

Chromatography as a separation technique has evolved into a mature science with a diversity of specific techniques and advanced instrumentation technology. The diversity comes from the elucidation of the nature of the mobile phase (gas or liquid), types of stationary phases (liquid, bonded liquid or solid) used and the various mechanisms of separation (partition, adsorption, modified partition, ion-exchange or exclusion, etc.). Column development continues to be a driving force in research in separation sciences and the need to discover novel or innovative and more selective, efficient, and green stationary phases remains. A particular area in microcolumn development has been to develop new stationary phases that can be introduced into columns of much smaller inner diameters, either in packed, monolithic or open-tubular column formats. Open-tubular formats have been of great interest due to increased mass transfer[1-3] and has demonstrated more advantageous chromatographic performance, at least theoretically.[4,5] The advent of capillary electrophoresis (CE) in separation science has further diversified the ability of moving analytes within a mobile phase along a stationary phase from using conventional fluid pressure forces to introduction of an applied electric field.

Over the past decade, capillary electrochromatography (CEC) has been generally recognized for its strength as a separation technique that combines the high separation efficiency of capillary electrophoresis (CE) with the high selectivity and increased sample loadings of capillary liquid chromatography (cLC). Diverse types of capillary column formats can be employed in CEC, ranging from packed, monolithic or open-tubular systems. The open tubular format remains desirable

because of its inherent advantages over the other formats – easy preparation, simple instrumental handling, absence of back-pressure problems and bubble formation, and avoidance of cumbersome frit fabrication.

Open tubular capillary electrochromatography (OT-CEC) was first reported by Tsuda *et al.*[6] using an octadecylsilane-(C_{18})-coated narrow bore (30-µm i.d.) capillary to separate benzene-related and polyaromatic hydrocarbons. The discovery and employment of novel stationary phase (SP) materials to manipulate separation continues to be the driving motivation in the development of OT-CEC technology and a wide diversity of materials have been introduced. These materials are often chosen for their ability to provide selectivity based on known chromatographic separation mechanisms. This gives the advantage of OT-CEC over other CEC modes to readily enhance separation selectivity using innovative coating materials. These novel SPs include functionalised polymers, polyelectrolyte layers, chiral selective materials, nanoparticles, graphene-based materials, and more recently metal-organic frameworks, covalent organic frameworks, molecularly imprinted polymers, hybrid materials, biological/biochemical materials like nanocellulose, platelets and oligonucleotides. These materials were also previously identified as SP developments in published reviews covering the years 2013 until 2017.[7,8]

In analytical separation science, surfactants have been extensively studied and employed for their ability to solubilise many organic compounds that pose separation challenges, especially in aqueous media. The chemical structure of surfactants, *i.e.*, having a hydrophobic (water-hating) "tail" made of carbon chain and a hydrophilic (water-loving) "head" made of an ionic or polar group, renders them suitable to incorporate hydrophobic substances within a water-based

environment. This structure enables surfactant molecules (or monomers) to orient themselves into microstructures or aggregates in a self-assembly manner, forming micelles within a bulk solution. The spherical form of micelles as microemulsions generates an inner hydrophobic core of clustered hydrocarbon tails which enable nonpolar or hydrophobic components of sample mixtures to incorporate into (solubilisation) while remaining in suspension. Surfactant solutions are made up of free surfactant molecules or monomers and micelle aggregates when the surfactant amounts are above their critical micelle concentration (cmc).

Surfactant-based separations have been well-known and summarised in literature reviews and book chapters.[9,10] The solubilising activity of surfactants is the basis for its use in sample preparation methods, where surfactants have been extensively studied and utilised as emulsifiers, extraction media, and as carrier for liquid phase extractions,[11] as well as hemimicelle/admicelle adsorbents coated on solid surfaces, e.g. mineral oxide surfaces like silica[12] or alumina,[13] magnetic nanoparticles,[14] for solid-phase extraction techniques[15] or as desorbing agents[16] to replace organic solvents in solid-phase microextractions.

Surfactant-mediated separations by chromatography and electrophoresis are also well-documented and summarised in reviews,[17,18] involving techniques that employ mobile phases made up of surfactant solutions above the cmc to generate micelles as pseudophases. Micellar liquid chromatography (MLC), introduced by Armstrong and Henry,[19] is a mode of reversed-phased liquid chromatography (RPLC) which employs mobile phases containing a surfactant above its cmc instead of just organic solvents. MLC, as alternative to conventional RPLC, operates similarly with common RPLC systems using a nonpolar stationary phase and a polar aqueous mobile phase but made of micellar aggregates and free

surfactant monomers in the surrounding bulk solution. The mobile phase in MLC requires use of surfactants of low cmc to avoid viscous solutions, with chromatographic separations being carried out at temperatures above the surfactants' Krafft point temperature to prevent precipitation, pH control within the limited working range of the RPLC columns (2.5 – 7.5), and inclusion of selective organic modifiers/solvents of controlled amounts to maintain homogeneity and more importantly to preserve micelle integrity.[20] MLC has demonstrated efficient analytical determination of varying pharmaceutical and biological samples,[21,22] antitumoral and antiretroviral drugs in plasma,[23] and drug monitoring of urine and serum samples.[24] In MLC, the porous surface of the stationary phase can also be modified by the adsorption of surfactant monomers which affect chromatographic retention by reducing interactions with uncoated silanols, reduction of pore volume,[25] production of net charge (using ionic surfactants), and masking of bonded-stationary phase.[26] Solute retention has been attributed to the partitioning effect of interactions of the solute with bulk solution and suspended micelles or with surface-adsorbed surfactants on the stationary phase.[27,28]

It is also the ability of surfactants to solubilise neutral or hydrophobic compounds that is exploited in the technique of *micellar electrokinetic chromatography* (MEKC) whereby surfactants in the buffer solution at concentrations exceeding the cmc (as micelles) act as suspended pseudostationary phases in partitioning uncharged analytes.[29-33] As a mode of CE, introduced by Terabe, *et al.*,[34,35] MEKC employs ionic micelles incorporated into the electrophoretic buffer solution that, by micellar equilibrium processes, solubilise part of neutral or hydrophobic analytes and migrates by its own micellar mobility (electrophoretic) along an applied electric field, usually in a direction opposite to

the EOF, while the solubilised analyte moves at a velocity between that of the EOF and the micelles (Figure I). The surfactant micelles act as pseudostationary phases being able to influence migration of uncharged solutes while not being fixed onto the capillary column wall like usual stationary phases. MEKC continues to be a significant and extensively used technique for separation of pharmaceutical drugs,[36,37] chiral compounds of interest,[38] of polluting compounds in environmental samples,[39,40] in metabolomics using urine[41] and serum[42] samples, in natural products,[43] in food[44] and agriculture[45] and even in forensics.[46]

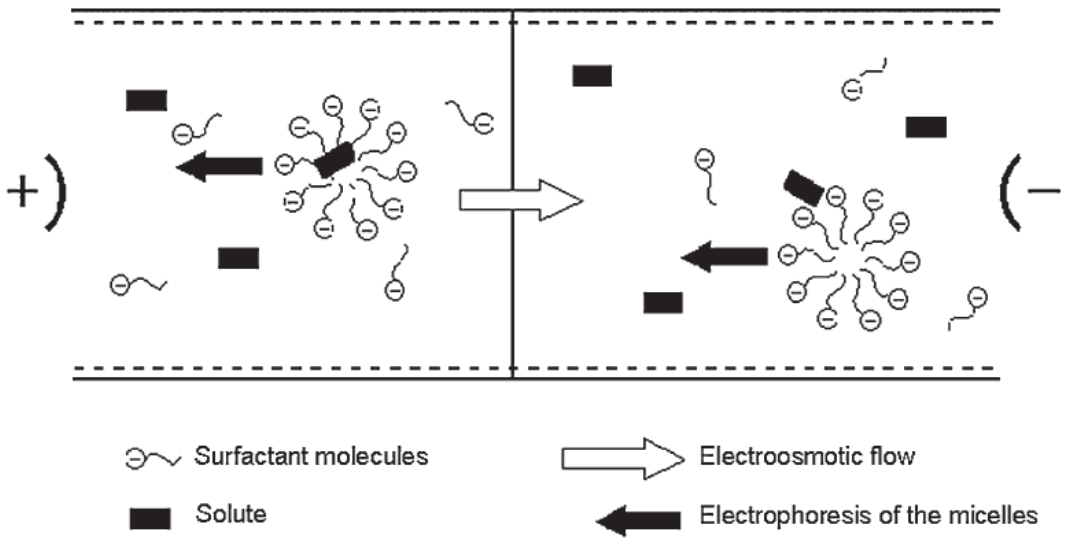

Figure I. Schematic illustration of the separation principle of micellar electrokinetic chromatography. Reproduced from ref 29.

Surfactants have also been well used as dynamic coatings for electrodriven separations like capillary zone electrophoresis (CZE). The bulk flow inside the separation channel is driven by electroosmosis and this electroosmotic flow is an essential force that influences the apparent velocity of charged analytes dissolved in electrolyte when moving along an applied electric field. Separation of charged

analytes in CZE is influenced by the inherent electrophoretic mobility of the analytes resulting from their charge-to-mass ratio and the flow velocity and direction produced by the EOF. EOF velocity is governed by the dielectric constant (ε), the viscosity (η) of the solution, the electric field strength (E), and the zeta potential (ζ), wherein the velocity is correlated with the zeta potential by $V_{EOF} = \frac{-\varepsilon \zeta_{(\sigma)} E}{\eta}$. The zeta potential is the parameter reflecting the magnitude and polarity of the capillary surface charge upon which the EOF mobility (μ_{EOF}) is dependent. Separation behaviour can therefore be modified by employing techniques of manipulating the EOF. Coating materials attached statically, dynamically and covalently on the inside wall of channels (in capillaries or microchips) have been used to manipulate EOF. The separation performance is also improved by coatings which introduce analyte-wall interaction for retention (electrochromatography) or reduce this interaction to prevent adsorption (e.g., of proteins). Employment of surfactants in electrodriven separation is largely focused on using surfactants as dynamic coatings (usually at concentrations well above their cmc) on a fused-silica capillary wall to modulate the EOF[47] and/or to suppress the strong adsorption of positively charged peptides and proteins on the negatively charged inner wall of the capillary.[48] Ionic surfactants like hexadecyltrimethylammonium bromide (CTAB) adsorbing onto charged silica surfaces can modify the electroosmotic flow in capillary electrophoresis by affecting the surface charge.

So far, surfactant-mediated separations have always involved micellar structures to extract or retain solute analytes, that is, pressure-driven and electrodriven chromatographic separations have been demonstrated for mobile phases or background buffer solutions containing surfactants above their cmc.

However, at conditions below the cmc where micelles are not formed and only surfactant aggregates exist on the liquid/solid interface as hemimicelles and admicelles, there exists a gap in investigation of any significant separation performance where electrodriven or liquid chromatographic analyses are employable. As far as we know, surfactants as semipermanent and stationary pseudophase coatings below and just above cmc have never been systematically studied for chromatographic and electrochromatographic separations on capillary column dimensions (column i.d. < 100 μm) on an open-tubular format.

Research Aims

The research project reported in this thesis intends to accomplish the following aims:

1) To understand the molecular aggregation of two common long-chain ionic surfactants at the solid (fused-silica) – solution interface using EOF measurements by capillary electrophoresis, particularly on admicelle and micelle formation, and to define the critical surface aggregation concentration (csac) and critical micelle concentration (cmc) from the electroosmotic mobility as a function of surfactant concentration;
2) To introduce the concept of admicellar pressure- and electric field-driven chromatography in open tubular format, denoted as open-tubular admicellar liquid chromatography (OT-AMLC) and open-tubular admicellar electrochromatography (OT-AMEC), to describe the mobile phase parameters affecting separation performance, and to demonstrate separation of charged and neutral analytes for application with real sample matrices;

3) To introduce open-tubular micellar liquid chromatography (OT-MLC) as a novel technique employing interfacial micellar and solution micellar aggregates at surfactant concentrations just above the cmc as pseudophases for pressure-driven separations of neutral and charged analytes, to determine the mobile phase parameters that affect the chromatographic performance, to demonstrate separation in real samples, and highlight the technique as a green innovation compared to conventional liquid chromatography.

The project was subdivided into three work phases: (1) electroosmotic mobility measurements against a range of surfactant concentrations for profiling of aggregation behaviour on the solid-solution interface of a fused-silica capillary inner wall and determination of cmc and csac; (2) evaluation of selectivity and applicability of an ionic surfactant (*i.e.*, CTAB) above the csac and below cmc as soft stationary pseudophases (admicelles) for chromatographic and electrochromatographic separations in open tubes, and (3) investigation of micellar solubilisation behaviour of ionic surfactants just above the cmc for open-tubular capillary liquid chromatography.

To investigate the selectivity and applicability for practical admicellar-based analytical separations, the project necessitated exploring the aggregational structure and behaviour of representative surfactants adsorbed on the inner wall of fused silica capillaries of varying internal diameters from 25 to 100 µm. An important preliminary parameter to define was the determination of the cmc of selected surfactants (CTAB, sodium dodecyl sulfate or SDS) as this is essential to gauge the admicellar range of surfactant concentration. Electrodriven[49] and

pressure-driven[50] techniques were employed in this project to determine the cmc[51,52] for micelle formation and the csac that define the hemimicellar-admicellar self-assembly (Chapter 2). Open-tubular capillary chromatography and electrochromatography were employed for selected analytes using surfactant concentrations above the csac and below the cmc to explore feasibility, applicability and limitations of admicellar-mediated separations in open-tubular capillary column formats (Chapter 3). The project also investigated the factors that will influence or alter hemi/admicellar properties and separation capabilities including pH, buffer ionic strength, influence of organic solvents and added salts.[53-56] Representative test analytes (neutrals, cations and anions) were utilised to characterise the separation capabilities of selected surfactant models, and separation performance was evaluated for standard analytical figures-of-merit including linearity, limits of detection and quantification, as well as repeatability.[47,55,57] Further exploration was carried by capillary liquid chromatography (pressure-driven) using a dynamic surfactant coating just above the cmc for similar sets of analytes to study the potential for open-tubular coatings of surfactants in the presence of bulk solution micelles (Chapter 4). To understand the variables that influence the admicelle/micelle mediated separation behaviour, the effects of the same parameters of pH, buffer ionic strength, added organic solvents and salts were also examined.

Surfactant models were assessed for application potential using real samples of pharmaceutical, food and environmental interest[13,50,58] particularly in the detection of active pharmaceutical ingredients, food additives (e.g., antioxidants) and organic environmental pollutants (e.g. pesticides, PAHs).

References

(1) Hibi, K.; Ishii, D.; Fujishima, I.; Takeuchi, T.; Nakanishi, T. *J High Resolut Chromatogr* **1978**, *1*, 21-27.

(2) Jorgenson, J. W.; Guthrie, E. J. *J Chromatogr A* **1983**, *255*, 335-348.

(3) Forster, S.; Kolmar, H.; Altmaier, S. *J Chromatogr A* **2012**, *1265*, 88-94.

(4) Knox, J. H.; Gilbert, M. T. *J Chromatogr A* **1979**, *186*, 405-418.

(5) Causon, T. J.; Shellie, R. A.; Hilder, E. F.; Desmet, G.; Eeltink, S. *J Chromatogr A* **2011**, *1218*, 8388-8393.

(6) Tsuda, T.; Nomura, K.; Nakagawa, G. *J Chromatogr A* **1982**, *248*, 241-247.

(7) Tarongoy, F. M., Jr.; Haddad, P. R.; Boysen, R. I.; Hearn, M. T.; Quirino, J. P. *Electrophoresis* **2016**, *37*, 66-85.

(8) Tarongoy, F. M., Jr.; Haddad, P. R.; Quirino, J. P. *Electrophoresis* **2018**, *39*, 34-52.

(9) Scamehorn, J. F.; Harwell, J. H. In *Surfactant-Based Separations*; American Chemical Society, 1999, pp 1-14.

(10) Hinze, W. L. In *Ordered Media in Chemical Separations*; American Chemical Society, 1987, pp 2-82.

(11) Moradi, M.; Yamini, Y. *J Sep Sci* **2012**, *35*, 2319-2340.

(12) Wangchareansak, T.; Keniry, M. A.; Liu, G.; Craig, V. S. *Langmuir* **2014**, *30*, 6704-6712.

(13) Saitoh, T.; Nakayama, Y.; Hiraide, M. *J Chromatogr A* **2002**, *972*, 205-209.

(14) Wang, H.; Zhao, X.; Meng, W.; Wang, P.; Wu, F.; Tang, Z.; Han, X.; Giesy, J. P. *Anal Chem* **2015**, *87*, 7667-7675.

(15) Arnnok, P.; Patdhanagul, N.; Burakham, R. *Chromatographia* **2015**, *78*, 1327-1337.

(16) Santana, C. M.; Padron, M. E.; Ferrera, Z. S.; Rodriguez, J. J. *J Chromatogr A* **2007**, *1140*, 13-20.

(17) Khaledi, M. G. *J Chromatogr A* **1997**, *780*, 3-40.

(18) Nishi, H. *J Chromatogr A* **1997**, *780*, 243-264.

(19) Armstrong, D. W.; Henry, S. J. *J Liq Chromatogr* **1980**, *3*, 657-662.

(20) Rambla-Alegre, M. *Chromatogr Res Int* **2012**, *2012*, 1-6.

(21) Esteve-Romero, J.; Carda-Broch, S.; Gil-Agustí, M.; Capella-Peiró, M.-E.; Bose, D. *TrAC, Trends Anal Chem* **2005**, *24*, 75-91.

(22) Kawczak, P.; Bączek, T. *Cent Eur J Chem* **2012**, *10*, 570-584.

(23) Peris-Vicente, J.; Casas-Breva, I.; Roca-Genovés, P.; Esteve-Romero, J. *Bioanalysis* **2014**, *6*, 1975-1988.

(24) Esteve-Romero, J.; Albiol-Chiva, J.; Peris-Vicente, J. *Anal Chim Acta* **2016**, *926*, 1-16.

(25) Borgerding, M. F.; Hinze, W. L.; Stafford, L. D.; Fulp, G. W.; Hamlin, W. C. *Anal Chem* **1989**, *61*, 1353-1358.

(26) Lavine, B. K.; Hendayana, S.; He, Y. F.; Cooper, W. T. *J Colloid Interf Sci* **1996**, *179*, 341-349.

(27) Ruiz-Angel, M. J.; Carda-Broch, S.; Torres-Lapasio, J. R.; Garcia-Alvarez-Coque, M. C. *J Chromatogr A* **2009**, *1216*, 1798-1814.

(28) Rambla-Alegre, M. *Chromatogr Res Int* **2012**, *2012*, 1-5.

(29) Terabe, S. *The Chemical Record* **2008**, *8*, 291-301.

(30) Otsuka, K.; Terabe, S. *Bull Chem Soc Jpn* **1998**, *71*, 2465-2481.

(31) Terabe, S. *Anal Chem* **2004**, *76*, 240 A-246 A.

(32) Terabe, S. *Annu Rev Anal Chem* **2009**, *2*, 99-120.

(33) Terabe, S. *Procedia Chem* **2010**, *2*, 2-8.

(34) Terabe, S.; Otsuka, K.; Ichikawa, K.; Tsuchiya, A.; Ando, T. *Anal Chem* **1984**, *56*, 111-113.

(35) Terabe, S.; Otsuka, K.; Ando, T. *Anal Chem* **1985**, *57*, 834-841.

(36) Stăcescu, Ș.; Hancu, G.; Gagyi, L.; Soare, R. M.; Kelemen, H. *Stud Univ Babes-Bolyai, Chem* **2017**, *62*, 189-198.

(37) Nishi, H.; Terabe, S. *J Pharm Biomed Anal* **1993**, *11*, 1277-1287.

(38) Otsuka, K.; Terabe, S. *J Chromatogr A* **1990**, *515*, 221-226.

(39) Quirino, J. P.; Iwai, Y.; Otsuka, K.; Terabe, S. *Electrophoresis* **2000**, *21*, 2899-2903.

(40) Aranas, A. T.; Guidote, A. M.; Haddad, P. R.; Quirino, J. P. *Talanta* **2011**, *85*, 86-90.

(41) Oledzka, I.; Kowalski, P.; Plenis, A.; Baczek, T. *Electrophoresis* **2017**, *38*, 1632-1643.

(42) Wang, J.; Cao, Y.; Wu, S.; Wang, S.; Zhao, X.; Zhou, T.; Lou, Y.; Fan, G. *Molecules* **2017**, *22*, 538.

(43) Rabanes, H. R.; Guidote, A. M.; Quirino, J. P. *Microchemical Journal* **2014**, *112*, 153-158.

(44) Marti, R.; Valcarcel, M.; Herrero-Martinez, J. M.; Cebolla-Cornejo, J.; Rosello, S. *Food Chem* **2017**, *221*, 439-446.

(45) Quirino, J. P.; Inoue, N.; Terabe, S. *J Chromatogr A* **2000**, *892*, 187-194.

(46) Copper, C.; Brensinger, K.; Rollman, C.; Clark, A.; Perez, M.; Genzman, A.; Rine, J.; Moini, M. *Electrophoresis* **2016**, *37*, 2554-2557.

(47) Erny, G. L.; Goncalves, B. M.; Esteves, V. I. *J Chromatogr A* **2012**, *1256*, 271-275.

(48) Melanson, J. E.; Baryla, N. E.; Lucy, C. A. *TrAC, Trends Anal Chem* **2001**, *20*, 365-374.

(49) Bellmann, C.; Synytska, A.; Caspari, A.; Drechsler, A.; Grundke, K. *J Colloid Interface Sci* **2007**, *309*, 225-230.

(50) Merino, F.; Rubio, S.; Perez-Bendito, D. *Anal Chem* **2004**, *76*, 3878-3886.

(51) Cifuentes, A.; Bernal, J. L.; DiezMasa, J. C. *Anal Chem* **1997**, *69*, 4271-4274.

(52) Dominguez, A.; Fernandez, A.; Gonzalez, N.; Iglesias, E.; Montenegro, L. *J Chem Educ* **1997**, *74*, 1227-1231.

(53) Weston, J. S.; Harwell, J. H.; Shiau, B. J.; Kabir, M. *Langmuir* **2014**, *30*, 6384-6388.

(54) Hankins, N. P.; O'Have, J. H.; Harwell, J. H. *Ind Eng Chem Res* **1996**, *35*, 2844-2855.

(55) Lucy, C. A.; Underhill, R. S. *Anal Chem* **1998**, *70*, 1045.

(56) Okamoto, N.; Yoshimura, T.; Esumi, K. *J Colloid Interface Sci* **2004**, *275*, 612-617.

(57) Liu, Q.; Shi, J.; Wang, T.; Guo, F.; Liu, L.; Jiang, G. *J Chromatogr A* **2012**, *1257*, 1-8.

(58) Adak, A.; Pal, A. *Desalin Water Treat* **2012**, *6*, 269-275.

Chapter 1

Recent Developments in Open Tubular Capillary Electrochromatography from 2016 – 2017

1.1 Abstract

Interest in open-tubular capillary electrochromatography (OT-CEC) continues to thrive because of the inherent advantage of OT-CEC combining the high efficiency of capillary electrophoresis (CE) and the high selectivity of high performance liquid chromatography (HPLC). For the period 2016 to 2017, novel materials have been developed as first-time stationary phases (SP) for OT-CEC and are grouped in this review as polymer-based materials, frameworks, nanoparticles, graphene-based materials, and biomaterials. Coating and fabrication methods mostly rely on covalent coating strategies while non-covalent immobilisation strategies like electrostatic assembly are notably still being employed. The concern of overcoming phase ratio challenges in OT-CEC coatings have also generated adoption of combined coating strategies including multi-layering, layer-by-layer self-assembly and methods adapted from nanofilm fabrications like epitaxial growth, liquid phase deposition, or nucleation of crystal growth. The emergence of non-conventional coating characterisation methods such as TEM, XRD or XPS are also discussed.

*Most of this chapter has been published as Tarongoy, F. M., Jr.; Haddad, P. R.; Quirino, J. P., Recent developments in open tubular capillary electrochromatography from 2016 to 2017. *Electrophoresis* **2018,** *39* (1), 34-52.

1.2 Introduction

Capillary electrochromatography (CEC) employs the high separation efficiency of capillary electrophoresis (CE) and high selectivity of high-performance liquid chromatography (HPLC). CEC takes on different formats for stationary phases in capillary columns – packed, monolithic and open tubular. The open tubular format remains desirable because of its inherent advantages over the other formats – easy preparation, simple instrumental handling, absence of back-pressure problems and bubble formation, and avoidance of cumbersome frit fabrication. The discovery and employment of novel stationary phase (SP) materials to manipulate separation continues to be the driving motivation in the development of open tubular capillary electrochromatography (OT-CEC) technology and a wide diversity of materials have been introduced. These include functionalised polymers, polyelectrolyte layers, chiral selective materials, nanoparticles, graphene-based materials, and more recently metal-organic frameworks, covalent organic frameworks, molecularly imprinted polymers, hybrid materials, biological/biochemical materials like nanocellulose, platelets and oligonucleotides. Following a recent review on developments and highlights on OT-CEC[1], this technique continues to sustain interest in analytical separation science.

Polymeric materials in diverse physical forms, such as block polymers, porous polymers, tentacles, dendrimers, sol-gel matrices or imprinted polymers, have been studied most frequently. The significance of polymer-based materials has been sustained due to the availability of chemistries for *in situ* synthesis and/or

preparation of new types of coatings, their functionalisation to enable retention behaviour to be better defined, and with increased porosity to augment surface area dependencies that are needed in OT-CEC. Continued interest in nanomaterial application to OT-CEC has also been significantly based on the utilisation of a growing diversity of nanomaterials ranging from latex nanoparticles, polystyrene, gold NPs, titanium dioxide NPs to silica, poly(glycidyl methacrylate) nanoparticles, magnetic nanocomposites, molecularly imprinted magnetic NPs and more recently graphene and graphene derivatives. This focus on NPs is noteworthy because of the perceived benefits of their increased surface area, the relatively straightforward manner of their synthesis including ways to chemically control NP size, and flexibility in their functionalisation. Furthermore, the use of NPs in OT-CEC has been increasingly favoured over other CEC modes since no frits are needed and difficulties in column-packing and SP carry over are avoided. Besides, NP modified OT-CEC columns can be regenerated in less time.[2]

The utilisation of metal-organic frameworks (MOFs) or their composites in OT-CEC is a very recent development considering that MOFs have been investigated for many years as sorbents for sampling, solid-phase extraction, and as SPs in gas chromatography and HPLC. The remarkable properties of MOFs such as tunable pore volume and high specific surface area have garnered much interest in OT-CEC to address problems of low phase ratio and sample capacity. The ease of immobilising MOFs *in situ* undoubtedly will lead to more investigations with other MOFs. Also, chiral OT-CEC column development will continue to flourish due to the availability of an increasing range of suitable chiral selectors and advances in molecular imprinting.

The limited amount of stationary phase coating results in low sample loading capacity and low phase ratio, which remain as the most significant challenges for OT-CEC development. The use of capillaries of smaller internal diameter (2–25 μm) is also required to allow very efficient solute diffusion into and from the SP, thus leading to high plate numbers, *N*, and narrow peak widths. Coating stability is required for separations to be repeatable for numerous runs. Thus, regarding SP immobilisation strategies, the ability to increase surface area, improve the phase ratio, enhance the stability and robustness of the coating and employ more facile manufacturing procedures are primary considerations. Several coating strategies have been introduced to address these challenges. In the literature, these approaches are classified as physical adsorption, electrostatic interaction (e.g., multiple ionic layer) and covalent approaches (e.g., polymerisation reactions like reversible addition-fragmentation chain transfer polymerisation (RAFT), silanisation, and sol-gel reactions. Some coating methods use combinations such as electrostatic and covalent strategies.

As was pointed out in a previous review,[1] although *in situ* polymerisations still constitute the most frequently employed method, more layer-by-layer (LbL) assembly strategies will be increasingly explored because of their simplicity, versatility and facility to control the surface of any planar or particulate substrate with nanoscale dimensionality. This will allow the preparation of more diverse ranges of OT-CEC columns. The feasibility of constructing and attaching MOFs on capillary walls *via in situ* LbL assembly or by forming multilayers as single-cycle coatings with enhanced layer thickness are indications of opportunities ahead. Novel applications based on the use of LbL assembly will undoubtedly stimulate further interest in OT-CEC applications. A recent innovation for nanoparticle non-

covalent coatings involved transient fixing of magnetic coating materials, particularly magnetic nanoparticles (MNPs), to the surface of the capillary wall using an external magnetic field.

Continuous improvements are expected over the next few years in the design and synthesis of new SP materials with structural modifications that are better tailored for selective interaction with the relevant analytes under the desired separation mode. Understanding the retention mechanism of these new materials will facilitate the optimisation of experimental conditions for high-resolution OT-CEC separations. Materials that show mixed-mode separations or stimuli-responsive behaviour will continue to gain attention because of their ability to fine-tune the chromatographic selectivity. These materials are also very promising candidates since they can also be used for a wider range of structurally more complex analytes than it is currently the case. Separation mechanisms have been documented for reversed-phase, ion-exchange, hydrophilic partitioning, enantio-selective recognition and ligand affinity behaviour. Applications have largely focused on small, low molecular weight molecules relevant to the pharmaceutical, environmental monitoring, food and consumer goods industries, as well as on natural products research and chemical analysis more generally.

The main emphasis in OT-CEC (including microchip) research continues to be on the preparation and characterisation of columns. However, many of the OT-CEC SPs are also finding their way into various other fields of applications, indicating that the future directions of OT-CEC research will move more towards solving real world analytical challenges.

This chapter, taken primarily from our recent review[3] as a follow-up to a previous review in 2015, highlights emerging trends in areas of interest around

OT-CEC development from 2016 to the present. Within this updated review, a total of 38 articles which include 30 research articles and 8 review papers have been covered. Succeeding sections will discuss the developed SP materials, coating strategies and fabrication techniques, characterisation methods, previous reviews, and the prospects and direction of OT-CEC.

1.3 Developments in stationary phase materials

The variety of SP materials that were developed has coincided with the growth of discovery of new materials which have adequate porosity and/or possess structure and functionality that can demonstrate retentive properties for separation. Most of these are novel in terms of being employed for OT-CEC purposes for the first time. They are grouped accordingly as polymer-based, frameworks, nanoparticles, graphene-based, and biomaterials.

1.3.1 Polymer-based

Many novel polymer-based materials can be employed since they are easily designed with monomers with functionalities that express specific chromatographic interactions. Table A1.1 (see chapter Appendix) provides a summary of these materials. Synthesised co-polymers have been used predominantly to attain multi-functionality and therefore establish either selectivity or versatility in separating various analytes.

The characteristics of styrene as an important component in RAFT polymerisation, methacrylic acid (MAA) to generate electroosmotic flow (EOF), and N-phenylacrylamide to synthesise the N-phenylacrylamide-styrene-methacrylic acid tri-copolymer by RAFT polymerisation for separation of peptides was utilised by Ali and Cheong.[4] In their work, nonpolar (styrene)

monomers and polar (N-phenylacrylamide) were utilised with an aromatic ring from the polar monomer contributing to the selectivity. Using a long OT-CEC column (112 cm of 50 μm i.d.), high electrochromatographic separation efficiency > 1,700,000 theoretical plates per column was achieved for a synthetic mixture of five peptides, compared to 286,700 for the same column used in the liquid chromatography mode. These results reinforced previous findings from the same group using a shorter 60-cm capillary coated with the same tri-copolymer. This shorter column yielded the separation of about 20 peptide peaks from the tryptic digest sample of cytochrome C with high separation efficiency close to 500,000 plates/column and acceptable peak capacity of over 220.[5]

A poly(2-dimethylaminoethylmethacrylate)-*block*-poly(acrylic acid) (PDMAEMA-b-PAA) Y-shaped block copolymer was fabricated by Seperifhar and co-workers using two dissimilar polymer chains linked onto a tri-functional 1,3,5-sym-triazine core.[6] The introduction of the weakly charged functional groups of PAA and PDMAEMA enabled the manipulation of the magnitude and direction of the EOF as a response to pH changes in the background electrolyte (BGE). They proposed that the hydrophilicities of the stimuli-responsive polymers could be altered as a function of pH to influence the direction of migration of acidic and basic analytes as well as their interaction with the analytes to produce controlled selectivity and resolution. However, in the absence of analyte retention factor or effective electrophoretic mobility values that will indicate interactions between analytes and the di-block SP, the selectivity aspect becomes speculative. As such, the test acidic and basic compounds were essentially separated by virtue of electrophoretic mobilities under different pH conditions.

Molecularly imprinted polymers (MIPs) continue to be utilised because of their porous three-dimensional structure with recognition sites formed by template synthesis. These sites could be tuned to recognise specific chiral compounds for enantiomeric separations. MIPs based on polyhedral oligomeric silsesquioxanes (POSS) with the formula $(RSiO_{1.5})_n$ synthesized with a mixture of PSS-(1-propylmethacrylate)-heptaisobutylsubstituted (MA0702), S-amlodipine (template), methacrylic acid (functional monomer), and 2-methacrylamidopropylmethacrylate (crosslinker), have been used to separate racemic mixtures of small molecule drugs.[7] An organic-inorganic hybrid MIP column was developed using 3-(trimethoxysilyl)propyl methacrylate as the cross-linking monomer by Chen and co-workers for the chiral separation of propranolol enantiomers.[8] The MIP was prepared *in situ* using S-(–)-propranolol as template molecule and MAA as the functional monomer at 1:4 ratio dissolved in a mixed porogen of toluene and methanol (1:1).

An MIP in porous layer open tubular (MIP-PLOT) format was fabricated by Kulsing and co-workers for the chiral separation and peak sharpening of a Z-Asp-OH racemates.[9] Using a traditional dilution polymerisation method with Z-L-Asp-OH as the template, 4-vinylpyridine (4VP) was the choice functional monomer which increased ionic interactions with the negatively charged analytes. Layer-on-layer coating method, functional monomer amounts, and selection of porogenic solvents and amounts in the polymerisation process were optimised.

Polymerisation processes that produce monoliths with macropore sizes of at least 10 μm have been of interest lately, particularly polymeric high-internal-phase emulsion (polyHIPE) materials. These emulsions, with an internal droplet phase (aqueous) greater than 74% of the total emulsion volume[10], usually form

monoliths. Choudhury and co-workers coated multiple polystyrene-co-divinylbenzene polyHIPE layers onto 100 μm i.d. x 20 cm long column.[11] After three sequential coatings of thin films, a lace pore structure was observed by scanning electron microscopy (SEM), and the optimised coating regimen produced baseline separation of two alkylbenzenes (resolution, $R_s = 2.80$).

1.3.2 Metal-organic and covalent organic frameworks

Metal-organic and covalent organic frameworks are highly innovative materials that are currently of great research interest. A summary of these materials is shown in Table A1.2. The methods of linking the MOF (and zeolite imidazolate frameworks [ZIF]) materials with the capillary wall are by electrostatic interaction (Section 1.3.2) and covalent attachment (Section 1.3.3).

1.3.2.1 Metal-organic frameworks

MOFs are a class of hybrid inorganic and organic microporous structures constructed from self-assembly of metal ions and organic linkers bonded through coordination. MOFs remain of great interest because of their properties of high porosity, diverse structures, and tunable pore sizes, resulting in large surface area and adsorption affinity, making them promising SPs for chromatography[12] and particularly for OT-CEC.[1]

The use of MOF-180 was studied by Tang and co-workers as a novel SP material to investigate the influence of aperture and pore size on OT-CEC separation.[13] MOF-180 is made of an octahedral $Zn_4O(CO_2)_6$ and 4,4',4" -[benzene-1,3,5-triyl-tris(ethyne-2,1-diyl)] tribenzoate (BTE) with a cage size of 15 × 23 Å and 89% void volume from the total crystal volume. The separation of mixtures of acidic or basic analytes was ascribed to hydrophobicity effects from the ethyne and benzene ring groups of MOF-180. Moreover, aperture size was

believed to affect elution based on analyte molecular size as shown by the order of their retention times.

Bao and co-workers employed MOF-5, also named as isoreticular MOF (IRMOF-1), for the separation of substituted benzenes and small aromatic acidic and basic compounds.[14] The MOF-5 structure, built from the reticulating organic dicarboxylate group and the octahedral Zn-O-C lattice, utilised the dicarboxylate benzene struts to interact with the benzene structures of the analytes for their separation.

The homochiral MOF $[Zn(s\text{-}nip)_2]_n$ was used by Pan and co-workers as a novel SP by immobilising the MOF via an *in situ* coating strategy involving ZnO nucleating agents.[15] The fabricated MOF demonstrated separation ability for monoamine neurotransmitters (including enantiomers of epinephrine, isoprenaline and synephrine), diastereoisomers of ephedrine and pseudoephedrine, the isomers of nitrophenols and analogues of bisphenols.

1.3.2.2 Zeolite imidazolate frameworks

ZIFs are a subclass of MOFs consisting of *M–Im–M* links (*M* stands for Zn or Co cation and *Im* for the imidazolate linker) formed with a resulting zeolite-like structure.[16] With the ZIFs having the combined advantage from the properties of MOFs and zeolites, it showed great promise in numerous applications in catalysis, sensing, and separation since 2010.[17] The ZIF-90 framework was the initial model of a ZIF employed for the OT-CEC separation of three groups of isomers, neutral and basic compounds and nonsteroidal anti-inflammatory drugs.[18]

The ZIF-8 material evaluated by Qu and co-workers was ascertained to have increased phase ratio due to the layer-by-layer coating strategy.[19] A thick

porous layer with larger ZIF-8 nanocrystals was developed that allowed unsaturated Zn sites of the framework to interact well with phenolic isomers under separation.

Li and co-workers also employed ZIF-8 framework to separate diphenol isomers, alkylbenzenes, PAHs, chlorobenzenes and aromatic amines[20] while Pan and colleagues were able to demonstrate the viability of ZIF-8 to simultaneously separate two different analyte groups (cationic monoamine neurotransmitters and neutral flavonoids) using the same mobile phase or BGE.[21] Their one-dimensional (1-D) CEC method (Figure 1.1) was anchored on the imidazolium framework of ZIF-8 interacting with the amine and hydroxy groups of the cationic analytes and the microporous network interacting with the neutral analytes through hydrophobic and π -π interactions.

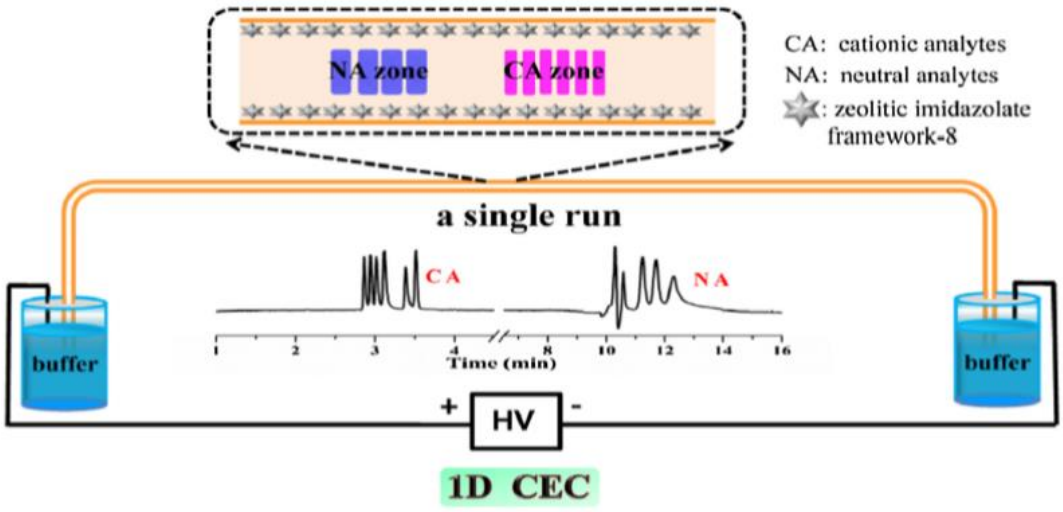

Figure 1.1 Schematic diagram of the simultaneous separation of neutral and cationic analytes on ZIF-8 coated capillary column by 1D OT-CEC. Reproduced with permission from ref 21.

1.3.2.3 Covalent organic frameworks

Covalent organic frameworks (COFs) have been introduced in 2005 as extended highly porous covalently linked two- and three-dimensional organic structures entirely composed of light elements (H, B, C, N, and O) held together by strong covalent bonds.[22,23] Their high surface area, low density, good thermostability and structured cavities have rendered them useful in applications in hydrogen storage, catalysis and gas separations, but they have only recently been exploited for chromatographic separations.

Covalent organic framework-LZU1 (COF-LZU1) was the first COF studied as a potential stationary phase for OT-CEC by Chen's group by attaching the COF via imine links with the glycidoxypropyltrimethoxysilane (GLYMO)-coated capillary.[24] The COF had a pore size and specific surface area of 18 Å and 410 m^2g^{-1}, respectively, and the presence of multiple benzene rings exhibited the size selectivity and the hydrophobicity needed to separate alkylbenzenes, polyaromatic hydrocarbons, and anilines. The same COF was also used by Kong and co-workers and was grafted into a capillary using an in-situ synthesis based on epitaxial growth by Schiff reaction.[25] The separation of neutral analytes alkylbenzenes and PAHs were mainly attributed to their hydrophobic interactions and π-interactions with COF-LZU1. In contrast to the fabrication approach in Ref. 24, the *in situ* preparation in Ref. 25 was more expedient (synthesis and immobilisation on a single process).

COF-5, a boron-based COF introduced by Yaghi's group[22] was employed by Bao and co-workers[26] as a SP for separation of neutral alkylbenzenes and PAHs. The polydopamine (PDA)-supported multilayering of COF-5 resulted to

the baseline separation attributed to the π-π interaction between the aromatics and aromatic framework in COF-5.

1.3.3 Nanoparticles

The large surface-to-volume ratio of nanoparticles (NPs) is the major property that draws continued interest in the development of NPs as either a SP support or as the SP itself[27] and a number of NPs have been applied to OT-CEC.[1,28] Table A1.3 shows a summary of the recent nanoparticle and graphene-based materials as SP.

Among the various NPs, gold nanoparticles (GNPs) have been applied primarily as SP support to exploit the large surface area it provides. Aside from their stability and chemical inertness, the ability of GNPs for self-assembly to form uniform monolayers have been recognised as highly beneficial in improving the phase-to-volume ratio that promotes better analyte-stationary phase interactions needed in OT-CEC.[2,29] Furthermore, GNPs can also be easily functionalised with specific groups to enhance selectivity, e.g. alkylthiol functionalised GNPs. Fang and co-workers employed GNPs fixed on a 3-mercaptopropyl-trimethoxysilane (MPTMS)-modified capillary through layer-by-layer assembly and later functionalised with thiols β-cyclodextrin (SH-β-CD) to fabricate a chiral SP.[30] Under optimised conditions, three-layered GNPs enabled enantioselective separation of meptazinol and its three intermediate enantiomers (intermediates II, III and IV) within 20 min. The same group initially employed a monolayer of chemically immobilised β-CD modified GNPs but failed to show enantioselectivity under strict OT-CEC conditions in which no chiral selector is added to the BGE.[31]

Titanium dioxide (TiO_2) nanoparticles immobilised through deposition on a PDA-coated capillary were used by Zhang, *et al*. for the separation of five model

proteins. This approach was also used to separate eight glycoisoforms of ovalbumin (OVA) in a standard mixture and five glycoisoforms of OVA in chicken egg white sample.[32]

Mesoporous silica nanoparticles (MSNs) have been characterised with high surface area (>700 m^2g^{-1}) and pore volume (>1 cm^3g^{-1}), tunable pore diameter (2–10 nm), stable mesopore structure, two functional surfaces (exterior particle and interior pore faces), and modifiable morphology (controllable particle shape and size).[33] Liu and co-workers developed a novel fibrous mesoporous silica nanoparticles ($fSiO_2$) SP grafted with poly(2-(dimethylamino) ethyl methacrylate (PDMAEMA).[34] By using $fSiO_2$/MSN functionalised with octadecylsilane (P-fSiO2@C18 column), three neutral analytes showed significant increase in retention compared to bare silica and C18-modified capillary without the $fSiO_2$. Three proteins were also separated.

Yang and co-workers improved their trimethylamine amination polychloromethyl styrene nanolatex (TMAPL)-coated column[35] with methyldiethanolamine amination polychloromethyl styrene nanolatex (MDEAPL) particles.[36] Aside from achieving higher yield of the synthesised SP material, improved stability, reproducibility, lower EOF and better separation of phytohormone analytes were observed compared to the original column.

1.3.4 Graphene-based materials

Graphene-based materials – graphene, graphene oxide (GO), reduced graphene oxide (GOOH) – has been popular as a SP because of their high surface area and a structure that produces strong π-π stacking interactions for selective separation of aromatic compounds. However, the same interaction, in combination with a hydrophilic effect, π-π electron-donor-acceptor, and hydrogen bonding have been

attributed to undesirable peak tailing effects that ultimately reduced separation performance.

Qu and co-workers proposed to address this problem by fabricating a GO and silica nanoparticles hybrid nanostructure (GO/SiO_2 NPs)-coated capillary by infusing a silanised column with a mixture of GO and silica sol.[37] When this column (GO/SiO_2 NPs@column) was compared with other prepared columns [GO-SiO_2 NPs@column (prepared by layer-by-layer method), and the SiO_2 NPs@column, all derivatized with octadecyltrichlorosilane (C18-)], a significant increase in resolution between naphthalene and biphenyl demonstrated the effect of increasing SiO_2 coverage on the GO surface. Furthermore, the typical peak tailing observed with GO as SP was significantly reduced by addition of SiO_2 to the nanostructure, and yet retaining the high shape selectivity with an appropriate amount of GO.

1.3.5 Biomaterials

Biochemical and biological materials have increasingly been explored as novel SPs because of their unique interactions with target analytes being separated. Many of them have distinct microenvironments that render them enantioselective or display selective affinities to specific types of molecules. These materials are summarised in Table A1.4.

The potential enantioselectivity of nanocellulose crystals (NCCs) was investigated by Dong and co-workers by employing an organic and inorganic hybrid of NCC derivatised with 3,5-dimethylphenyl isocynate (DMPC) as SP material.[38] The DMPC/NCCs hybrid, introduced layer-by-layer by a sol-gel method, demonstrated individual separations of 13 pairs of enantiomers that included chiral amino acids, drugs, and pesticide residues. The separation was

attributed to the chiral structure of the hybrid material and the high homogeneity resulting from the coating method. The employment of β-cyclodextrin as SP material for enantioseparations is well known, whereby Guo and co-workers developed a direct method of immobilisation on the capillary wall by forming a β-CD/PDA composite utilising the adhesive properties of PDA.[39] Separation performance was validated with good separations of seven pairs of chiral isomers with resolutions (R) from 1.23 (carvedilol enantiomers) to 3.45 (terbutaline enantiomers) and column efficiencies (number of theoretical plates, N) from 53,833 and 64, 718 (tryptophan enantiomers) to 190,336 and 440,250 (epinephrine enantiomers).

Proteins have been used as CEC stationary phases for enantiomeric separations, being amphoteric and possessing varied functional moieties. Bovine serum albumin (BSA) has been a well-studied biomaterial due to its enantioselective abilities. The group of Jia fabricated a BSA-coated poly(diallydimethylammonium chloride) (PDDA) column to investigate the selectivity of BSA in separating the charge variants of monoclonal antibodies (mAbs) for their heterogeneity characterisation.[40] The same group conducted further improvements in simplifying column preparations by adopting fibrin as a novel SP for characterisation of the same mAbs charge variants.[41] The coating strategy involved *in situ* polymerisation of fibrin in the presence of the catalyst thrombin and immobilised by physical adsorption. Fibrin was of interest as a potential SP material due to the fibrin network's inherent biocompatibility, adsorptivity, porosity and capacity for functionalisation.

Certain living organisms like bacteria have been well observed to possess instrinsic chirality in the microscopic and macroscopic scale and therefore being

chiral systems themselves, they can exhibit properties as chiral selectors for enantioselective separations. Xia's group employed a non-pathogenic *E. coli* strain DH5a adhered to a positively charged polyethyleneimine (PEI)-coated capillary for the enantioseparation of fluoroquinolone enantiomers and simultaneous separation of six fluoroquinolone antibiotics.[42] A bacterial concentration of 2 x10^9 cells/mL in 12 h of coating was adopted.

On the other hand, biomaterials have been utilised as SP materials not solely for separation capabilities but also as interesting materials to study binding affinities and to characterise specific SP and analyte interactions. Wang and co-workers used rabbit platelets physically adsorbed to the capillary column to study interactions of the platelets with adenosine diphosphate (ADP) (positive control), protocatechuic acid (negative control), and seven natural products.[43] The interactions assessed based on retention factors and binding constants were then correlated with anti-platelet aggregation activities that indicated the compounds with higher binding constants with platelets exhibited higher aggregation activities.

Double-stranded (dsDNA) and single-stranded DNA (ssDNA) were coated electrostatically by D'Ulivo and Feng on a capillary derivatised with 3-(aminopropyl)-triethoxysilane (APTES) to study the interaction of chemicals with DNA through binding.[44] These DNA oligonucleotide probes were used to characterise the binding affinities of three environmental contaminants based on their retention factors that showed 2,4-diaminotoluene with the highest binding affinity, positively correlating with its International Agency for Research on Cancer (IARC) ranking as class 2B (possibly carcinogenic to humans).

Kong and Chen utilised a PDA-immobilised hydroxyapatite (HAP) coating to study the interaction between hydroxyapatite with bisphosphonates by nonlinear chromatography.[45] They determined the association rate constants of zoledronate in hydroxyapatite-modified capillary and bare capillary as 642.3 and 195/M/min, respectively showing that zoledronate has high affinity and strong interaction with HAP by the P–C–P structure.

1.4 Developments in coating strategies and fabrication techniques

Coating methods in OT-CEC are herein classified as physical (adsorption), electrostatic and covalent based on the type of inter-atomic or intermolecular interactions that bind the coating material to the inner capillary wall. The choice of coating method largely depends on the available chemistry of the SP material and on establishing the balance of expediency of the process and the desired stability of the coating. A number of the fabrication techniques involve a combination of strategies, and the advantages of multi-layer coating have now been widely applied. In this section, salient aspects of these coating techniques will be featured. A summary of characterisation methods will be highlighted.

1.4.1 Coating by physical adsorption

Although considered the least stable, physical adsorption is the most simple and straightforward coating method as it involves facile steps of pressure-controlled introduction of the coating mixture into the column using a syringe pump or the CE instrument.[41,43] The SP in solution adheres onto the capillary surface by physical adsorption involving hydrophilic interactions, such as dipole-dipole interactions or hydrogen bonding. Xiao and co-workers enabled fibrin to

physically adsorb onto the capillary after allowing fibrinogen solution to polymerise in the presence of thrombin solution inside the capillary for 5h at 37ºC to form a fibrin network coating with an average thickness of 1.13 μm.[41]

1.4.2 Electrostatic coating

Electrostatic coating is also a non-covalent coating approach which may pose problems on the stability of the coating due to pH and ionic buffer concentrations affecting the adhesion strength of the coating. However, it continues to attract usage as a coating strategy because of the simplicity of the coating protocol which has similar advantages to coating by physical adsorption, i.e. direct injection of coating mixture, short preparation times, less rigorous coating conditions, minimal usage of solvents and relatively low temperature conditions. Electrostatic coating can be employed for direct immobilisation of the SP material, or by utilising surface modifying materials that electrostatically adhere to the capillary wall and can then be used to attach SP materials noncovalently or covalently to it.

1.4.2.1 Direct electrostatic coating

Several complex SP materials like frameworks and nanoparticles were successfully immobilised onto the capillary wall by direct electrostatic coating.[19,21,36] An interesting coating was proposed by Yang et al. where nanolatex MDEAPL material was directly coated onto the inner wall surface of capillary.[36] A MDEAPL solution was flushed three times through a pretreated capillary, with 30 min standing time in between flushing. The coating was allowed to stabilise for 24 h at 80ºC to allow the ionised silanols to establish electrostatic absorption with hydroxyl groups of methyl diethanolamine in the nanolatex particles.

1.4.2.2 Polydopamine-supported coating

Polydopamine (PDA) continues to be significantly employed as surface modifying agent to immobilise SP substrates onto capillary columns for OT-CEC. Easily formed *in situ* through the self-polymerisation of dopamine, this mussel-inspired material exhibits strong adhesive quality while easily forming thin layer films on surfaces,[46] allowing hydrophilic interactions to embed frameworks [20,26] nanoparticles [32] and biomaterials.[39,45] An innovative approach was used by Zhang and co-workers for the deposition of TiO_2 nanoparticles into a column by a liquid phase deposition (LPD) process.[32] This involved filling a PDA-modified capillary with an aqueous solution of $(NH_4)_2TiF_6$ and H_3BO_3 and the NPs were made to grow and deposit onto the surface over a certain period (Figure 1.2A and 1.2B). The extent of the deposition was evaluated by SEM images (Figure 1.2C) and EOF measurements over various LPD times wherein a minimum 1 h LPD time indicated complete NP coverage of the column when a constant EOF was achieved. The TiO_2@PDA columns coated for 1 h or more also allowed separation of four protein analytes, verifying complete coating of TiO_2 over the PDA film (Figure 1.2D).

1.4.2.3 Polyelectrolyte-assisted coating

Exploiting the charged state of ionised polymers or polyelectrolytes to adhere to a pre-treated inner capillary wall has also been employed for the fabrication of SPs from nanoparticles[34] and biomaterials.[40,42] Poly(diallydimethylammonium chloride) (PDDA) was used by Zhang and co-workers to support the fabrication of a BSA-coated OT column by electrostatic self-assembly.[40] This was achieved by sequential flushing of PDDA solution in Tris-HCl buffer (pH 8.3) containing 0.2 M NaCl, followed by BSA solution in

Tris-HCl buffer (pH 7.4). Positively charged PDDA will adhere onto the negatively charged capillary wall and likewise electrostatically attract the negatively charged BSA particles, effectively immobilising the BSA.

In a contrasting approach, D'Ulivo and Feng first covalently modified the capillary with 3-(aminopropyl)-triethoxysilane (APTES) solution to form amino groups that created a positively charged surface.[44] This enabled the negatively charged DNA oligonucleotide probes to adsorb onto the oppositely charged APTES-coated wall. A reversal of EOF direction opposite to that observed in an APTES-derivatised column indicated coating of the DNA probes.

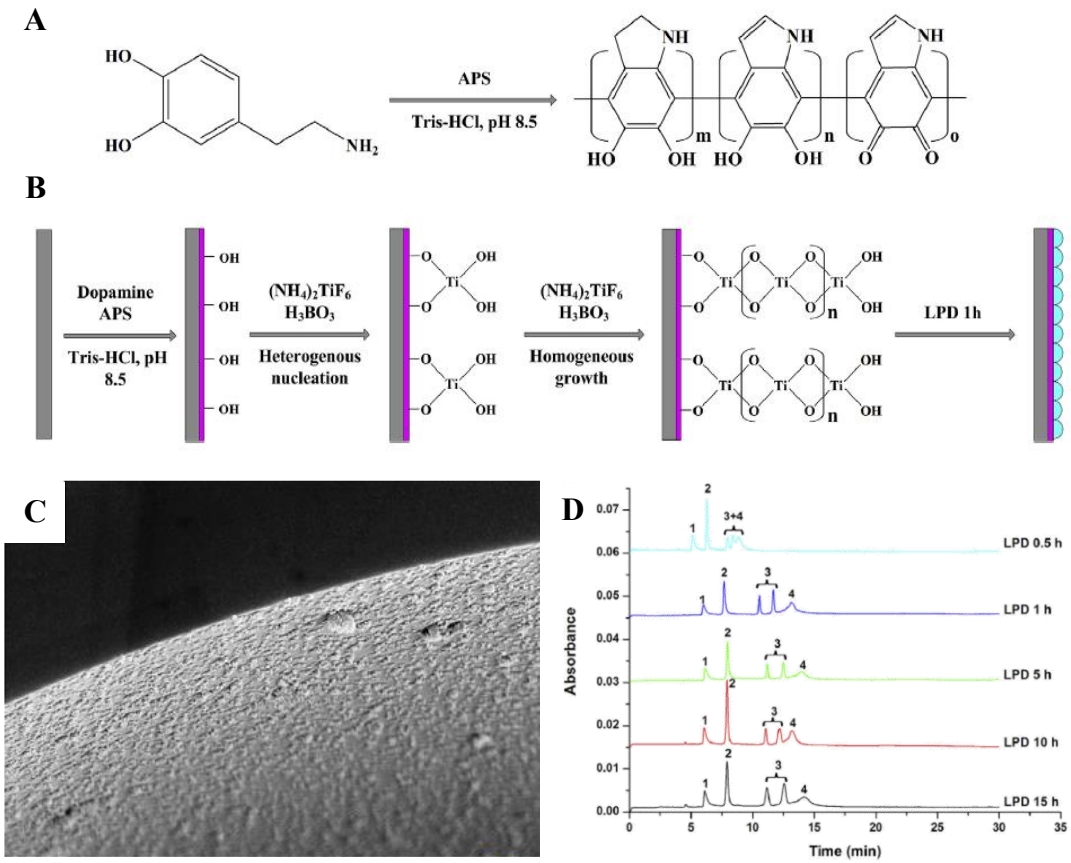

Figure 1.2 (A) Schematic illustration of the formation of PDA and (B) TiO_2 NPs deposited on the PDA coated OT column. (C) SEM image of TiO_2@PDA coated OT column (LPD 1 h). (D) Electrochromatograms for separation of proteins in TiO_2@PDA coated OT columns at different LPD times. Conditions: capillary, 50 µm i.d. x 29.2 cm effective length; BGE, 40 mM phosphate (pH 9.0); electric field strength, 383 Vcm^{-1}. Reproduced with permission from ref 32.

1.4.3 Covalent coatings

Attachment of SPs by direct covalent bonds onto the inner capillary wall or through a covalently-bonded functionalised layer are the common modes of covalent coatings that remain the most preferred, albeit most tedious, among the different coating strategies. Major setbacks of the covalent coating approach are: (1) long fabrication times with multiple synthetic steps of long reaction times and complexity, (2) numerous rinsing times, (3) problems on viscosity and/or homogeneity of reagents and mixtures that can cause blockages during pressure-driven infusion into the μm-i.d. of capillaries, (4) control of coating time to ensure film formation and (5) control of removal of unreacted or excess reagents. A coated layer with good phase ratio or surface area remains a challenge. Synthesis conditions need to be optimised according to relative amounts of reacting components, reaction temperature, stabilisation time, role and amount of solvents and clean-up. Many strategies now employ repetition of coating process, e.g. layer-by-layer process, to ensure complete coverage over the surface and generate an acceptable phase ratio.

1.4.3.1 Pre-modification via silanisation

Silanisation of the inner wall of fused silica capillaries is a well-known derivatisation reaction using organofunctional alkoxysilanes to react with the hydroxyl groups of silica and establish covalent bonds between the inorganic silicate surface with an organic functionality. For example, the use of aminosilanes (3-aminopropyl)triethoxysilane (APTES) or (3-aminopropyl)-trimethoxysilane (APTMS) generate terminal aminopropyl- groups whereby other condensation reactions can take place to covalently attach the SP.[13,14,25] An elegant coating approach was proposed by Bao and co-workers for the immobilisation of MOF-5

framework. The process involved initial silanisation with APTES, functionalisation with aldehyde groups by reaction with glutaraldehyde, then further oxidation to form carboxyl terminated surface.[13,14] The MOF was built onto the surface by an epitaxial growth process utilising the COOH- terminals as reaction points to bind the Zn clusters of the MOF. The process simply required first depositing Zn^{2+} to the COOH- covered surface, then allowing the organic ligand to bind with the Zn after introduction of a solution of 1,4-benzenedicarboxylic acid. This was to respond to the technical challenge of immobilising dicarboxylate-based MOF-5 since the ligands as framework connectors would block coordination sites of the metal ions from anchoring to the wall.

Another notable example was the derivatisation with a mercaptosilane (3-mercaptopropyl)trimethoxysilane (MPTMS) to generate a thiol-functionalised wall to bind GNPs in a multilayering process.[30] In another report, 3-(trimethoxysilyl) propyl methacrylate was used as silanisation agent to provide methacrylate groups to polymerise with the polystyrene-co-divinylbenzene (PS-co-DVB) polyHIPE emulsion.[11] Glycidoxypropyltrimethoxysilane (GLYMO) was also used to functionalise the wall with epoxy groups to form an imine link with amino groups of the COF-LZU1.[24] Chen and co-workers also employed 3-(trimethoxysilyl)propyl methacrylate (γ-MPS) as a cross-linking monomer for MIP synthesis since its bifunctional groups (–Si–OH and –C = C–) can simultaneously form hybrid polymers as well as provide linkage with the inner capillary wall.[8]

1.4.3.2 Polymerisation reactions

Polymer synthesis design is a crucial task in the fabrication of novel polymers as SP materials. The process of forming the polymer material itself requires elaborate reaction processes, long reaction times and rigorous conditions. Developing an *in situ* synthesis protocol that can readily form the polymer inside the capillary and chemically immobilise it simplifies the whole fabrication process.

The *in situ* synthesis and immobilisation of N-phenylacrylamide-styrene-methacrylic acid copolymer layer onto the capillary by RAFT polymerization was developed.[4,5] The reaction scheme started with reacting a pre-treated capillary with 4-(chloromethyl)phenyl isocyanate in the presence of dibutyltin dichloride as catalyst followed by sodium diethyl dithiocarbamate as the initiator moiety. The subsequent RAFT polymerisation of monomers N-phenylacrylamide, styrene and methacrylic acid (MAA) was then designed and modified according to relative amounts of the monomers, choice of polymerisation solvents, conditions for infusion to the capillary and reaction time.

In their column prepared to separate cytochrome C tryptic digests, Ali and Cheong decreased levels of MAA to reduce very strong interactions of the SP with the analyte that caused band broadening.[5] Toluene was employed as solvent in place of p-xylene and included 4-methyl-2-pentanone as a co-solvent to improve compatibility of the polymerization mixture. Extensive washing steps removed polar and nonpolar monomer residues. Ali and Cheong reduced the relative amount of N-phenylacrylamide (responsible for control of polarity and compatibility or stickiness of the SP) to overcome partial clogging over a longer column.[4] They decreased the amount of the mixed solvent and employed high-

performance syringe for faster introduction of reaction mixture and reduced polymerisation time from 15 to 8 h.

1.4.3.3 Synthesis by crystal growth involving nucleation

An exciting development in SP preparation is *in situ* synthesis by crystal growth involving nucleation. This was exploited by Pan and co-workers to expedite the synthesis and immobilisation of MOF $[Zn(s\text{-}nip)_2]_n$ onto the inner capillary wall.[15] The method employed introduction of an ethanol suspension of ZnO nanoparticles for nucleation on a pre-treated capillary, left at 200°C for 1 h, then the precursor mixture of $Zn(NO_3)_2 \cdot 6H_2O$ and organic ligand (S)-2-(1,8-naphthalimido)-3-(4-imidazole) propanoate (s-nip) was delivered and allowed to form the MOF in 1h (Figure 1.3). The 1-h optimum reaction time was determined based on thickness effects on the enantioseparation ability of the material. The performance of $[Zn(s\text{-}nip)_2]_n$ -coated capillaries prepared with or without using ZnO showed no significant difference.

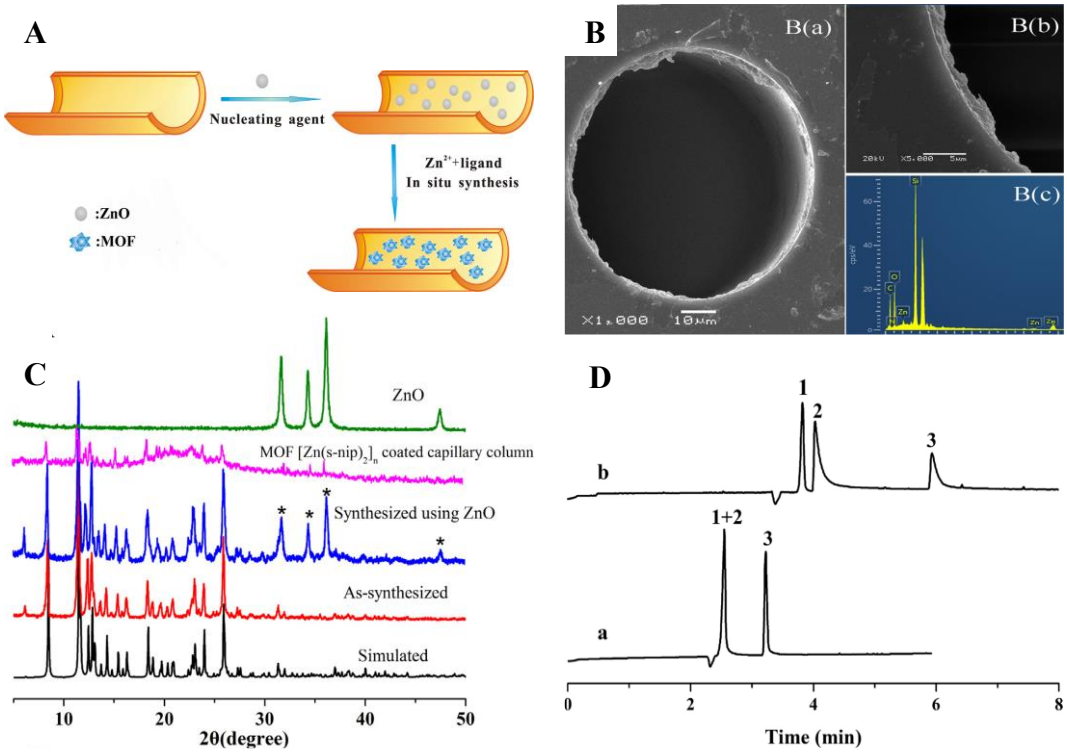

Figure 1.3 (A) Schematic diagram for the preparation process of $[Zn(s\text{-}nip)_2]_n$ coated capillary column. (B) SEM images of the MOF $[Zn(s\text{-}nip)_2]_n$ coated capillary (a, b), EDS spectra of the MOF $[Zn(s\text{-}nip)_2]_n$ coated capillary (c). (C) XRD patterns of the simulated XRD patterns of MOF $[Zn(s\text{-}nip)_2]_n$, the ZnO nanoparticles, the synthesized $[Zn(s\text{-}nip)_2]_n$ using ZnO nanoparticles and the MOF $[Zn(s\text{-}nip)_2]_n$ synthesized according to the literature. Reproduced with permission from ref 15.

1.4.3.4 Layer-by-layer assembly

Layer-by-layer (LbL) assembly is a method of incorporating molecules with complementary properties *via* their sequential application onto a surface. Typically, the layers are held in place by electrostatic interaction or chemical bonding. Repeated cycles of application are carried out to form a number of layers of the desired thickness, properties, structures and function. This technique, based on the pioneering work of Decher and co-workers,[47] has been widely applied due to its ease of use, efficiency, versatility and robustness to form nano-structured assemblies, like nano-films and nano-composites. LbL assembly can be applied to any type of substrate morphology (*e.g.* planar, porous or spherical) and can utilise a wide range of molecules as building blocks. Not only are electrostatic interactions used to influence the formation of thin film coatings but also other molecular interactions have been employed to facilitate formation of multilayer films of desired thickness.[48] Coating of open tubular capillaries by LbL assembly principally follows the general scheme of fluidic assembly technology described by Richardson *et al.*.[49] Multilayers are deposited on the wall of fluidic channels or on a substrate attached to a channel wall using pressure or vacuum delivery to sequentially deliver coating materials (*e.g.* polymers) or to allow washings. Thus, LbL assembly is one of the most powerful tools available to the separation scientist to fabricate SPs or alter chromatographic and electrophoretic behaviour.

By exploiting LbL approaches, Pédehontaa-Hiaa and co-workers have prepared poly-electrolyte multilayers using the cationic polymer, trimethylammonium-β-cyclodextrin (CD) and the anionic polymers poly(sodium 4-styrenesulfonate), polycarboxymethyl-β-CD or chondroitin sulfate.[50] LbL methods have also been used by Pan and co-workers to fabricate homochiral

MOFs,[51] whilst Bao and co-workers have produced a face-centred cubic MOF material.[52] Figure 1.4 shows the method of Xu and co-workers[53] for the preparation of an innovative class of iron(III) carboxylate MOF-coated capillaries. This procedure involved chemically modifying the bare silica surface with 3-glycidoxypropyl-trimethoxysilane-iminodiacetic acid-silane (GLYMO-IDA-silane) and the layer-by-layer assembly by alternate infusion of solutions of $FeCl_3 \cdot 6H_2O$ and 1,3,5-benzenetricarboxlic acid (BTC) / ethanol. This approach was claimed by the authors to be a key development for the *in situ* MOF synthesis of OT-CEC for use in the separation sciences. The dependency of separation efficiency for neutral analytes on the number of assembly cycles was demonstrated with 10 cycles producing highest peak efficiency for respectively optimised conditions (including buffer concentration, pH and organic modifier). The prepared capillary columns demonstrated good stability and performance with intra-day reproducibility RSDs (n=3) for migration time and peak area of < 4.6% and < 6.6%, respectively, and inter-day RSDs (n=3) of < 8.0% and < 9.5%, respectively.

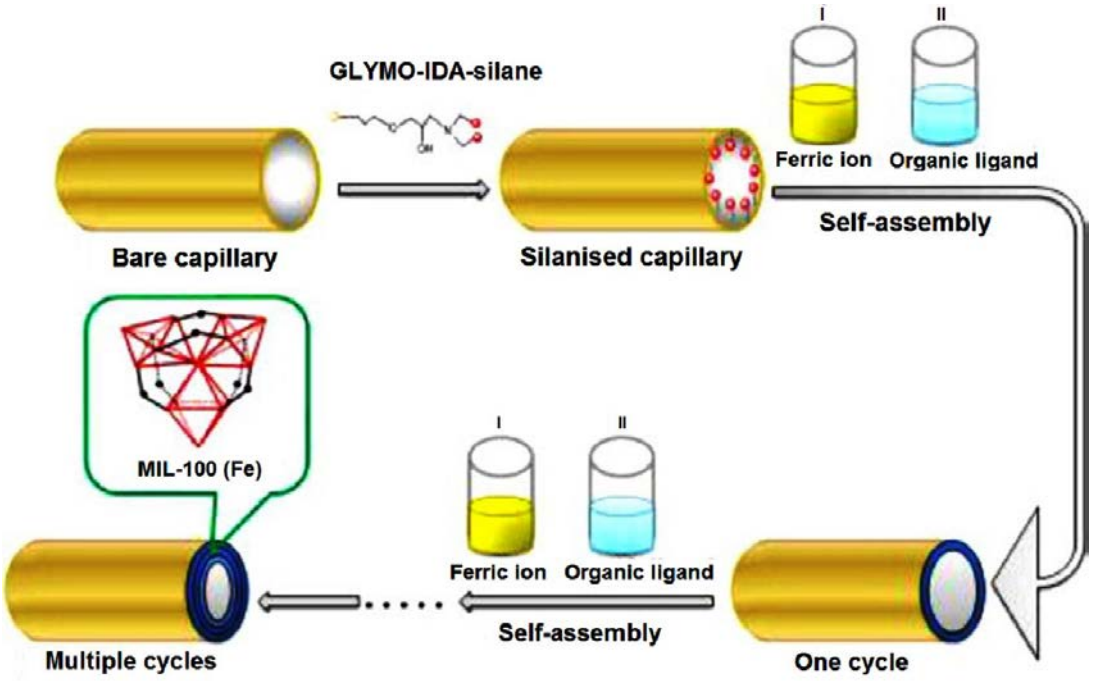

Figure 1.4 Schematic diagram for the preparation of MIL-100(Fe). Reproduced with permission from ref 53.

1.4.4 Immobilisation approach using external magnetic field

A new approach for attachment of MNPs onto capillary walls was introduced by Zhu and co-workers[54] by fixing magnetic NPs to the inner capillary wall using an external magnetic field. The coating can simply be regenerated by application and removal of the magnetic field. The same research group extended their initial work to core/shell magnetic NPs by modifying these materials with amino- or octadecyl (C_{18})-functionalities (Fe_3O_4@SiO_2-NH_2 or Fe_3O_4@SiO_2–C_{18}).[55] Figure 1.5 illustrates how the amino- and C_{18}-functionalised NPs were separately loaded from opposite ends of the capillary and arranged in series along the whole capillary length.

A mixed SP was also prepared by introducing a mixture of both functionalised MNPs and fixed using an externally applied magnetic field. In these applications, the relative column efficiency of salicylic acid was 420,000 plates/m, while benzoic acid reached 480,000 plates/m by using mixed SPs. Five organic acids were best separated using a 2:1 ratio of Fe_3O_4@SiO_2–NH_2 to Fe_3O_4@SiO_2–C_{18} in both series/mixed SPs. Retention time RSDs were less than 0.44% and 1.65% for five consecutive runs and 10.20% and 4.29% for five columns using series/mixed SPs, respectively, with no change in resolution observed for at least 30 consecutive runs. The transport properties of the organic acids were subsequently investigated using isocratic and double stepwise gradient elution.[56] On the other hand, Wang and co-workers have used externally placed magnets to pack dopamine-imprinted magnetic NPs (Fe_3O_4@PDA) into PDMS microchannels.[57]

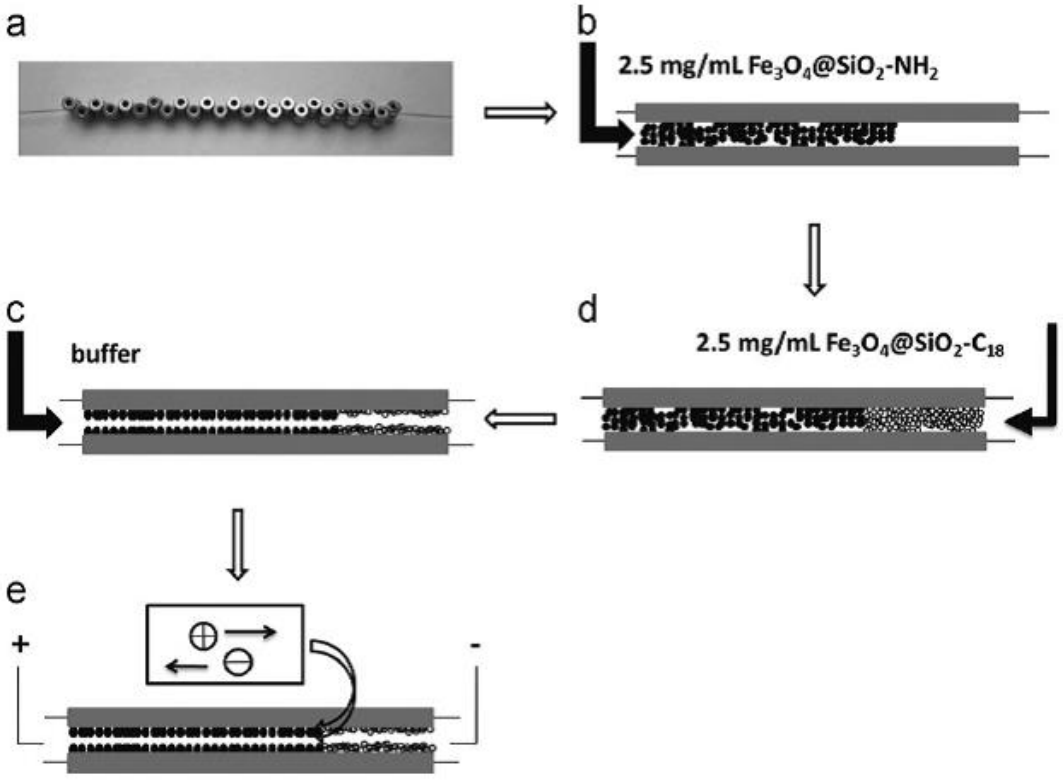

Figure 1.5. Preparation of OT-CEC column with magnetically responsive series SPs: (a) Placement of magnets, (b) loading of Fe_3O_4@SiO_2–NH_2, (c) loading of Fe_3O_4@SiO_2–C_{18}, (d) column cleaning, (e) electric balance. Grey rectangles represent magnets. Solid ball represents Fe_3O_4@SiO_2–NH_2, and hollow ball represents Fe_3O_4@SiO_2–C_{18}. Reproduced with permission from ref 55.

1.5 Characterisation methods

Characterisation of the coating materials in OT-CEC can provide information on the confirmation of actual formation of the SP material and the success of its immobilisation on the inner surface of the capillary. Characterisation of SP materials included surface charge (EOF measurements), surface morphology and area (e.g. SEM, TEM), elemental analysis (EDS), chemical structure (vibrational and absorbance spectroscopy) and crystal structure (XRD). During this review period, a noticeable increase in the number of techniques to characterise coatings has emerged. Selection of characterisation technique was dependent on the nature of the SP material.

1.5.1 EOF measurements

The measurement of EOF mobility (μ_{EOF}) is a standard CEC tool that gives surface charge profile. EOF measurements are performed by determining the elution of an unretained compound (e.g. thiourea). When the inner surface is coated with a layer of another material, the change in surface charge will lead to variations in the magnitude and direction of the EOF. If the coating material has a cationic functional group, the EOF direction is expected to become anodic (bare fused silica produces cathodic EOF). The EOF magnitude is dependent on the coating coverage and pH of the BGE. Also, the repeatability of the EOF in several runs is an important indicator of coating success as well as stability.

EOF measurements become more valuable when evaluating pH-responsiveness of the SP. The grafting of poly(2-dimethylaminoethylmethacrylate)-block-poly(acrylic acid) (PDMAEMA-b-PAA) was characterised with EOF measurements at different pH values.[6] Lower EOF magnitude at all pH values compared to that in a bare fused silica capillary

was observed to demonstrate actual attachment of the SP. A pH-dependent EOF inversion was also observed around pH 5.0 as the surface became predominantly positive due to the protonation of more tertiary amine groups of PDMAEMA chain, resulting to an anodic EOF at lower pH. Above pH 5.0, the deprotonated amine groups of PDMAEMA, the carboxylic acid groups of PAA, and any residual silanols contributed to the net negative charge, producing a cathodic EOF.

1.5.2 Surface morphology and area characterisation

Scanning electron microscopy (SEM) has become an indispensable characterisation method for a visual confirmation of the surface morphology of coated surfaces. SEM images of successfully coated surfaces were described to show rough surfaces, [6,9,13-15,24,25,30-32,34,36-38,41,42] hilly or bumpy surfaces,[4,5] with distinct shapes of the embedded material,[11,13,19-21,42,43] good layer density and homogeneity or uniformity,[20,21,25,32,38,40] and more importantly significant layer thickness[7-9,11,15,19-21,26,30,39] as opposed to the smooth surfaces seen in bare silica surfaces. Some SEM scans were performed on flat silica surfaces for detailed characterisation because of the inherent difficulty in successfully imaging wall coatings for a capillary format. Although SEM images of coatings formed on flat silica were observed to appear similar to capillary depth scan images, replication of the fabrication on two different platforms is not definitive.

An interesting application of SEM characterisation is the monitoring of the stability of the *E. coli* coating by obtaining SEM images before and after repeated runs.[42] Together with SEM, elemental analysis by energy dispersive X-ray spectrometry (EDS) provided information of material composition of certain elements like metallic Zn and gold or carbon in graphene in SP materials such as MOFs and nanoparticles.[15,30,37] Transmission electron microscopy (TEM) has also

been employed to characterise the microstructure, particle size and surface features of coated particles or layers.[24,30,31,32,37,38] Other coated layer characterisation methods employed were bio-microscope[43], contact-angle to monitor changes in hydrophobicity from the coating,[21] Brunauer-Emmett-Teller (BET) analysis via nitrogen adsorption isotherms to characterise surface area and pore size and structure of the samples,[7,34] atomic force microscopy (AFM) for coating thickness based on height profile,[42] and thermogravimetric analysis for assessing the thermal stability of the coating.[15]

1.5.3 Chemical and crystal structure and composition characterisations

Fourier transform-infra red spectroscopy (FT-IR) has become requisite to ascertain formation of desired covalent bonds, verifying the chemical structure of the synthesised SP [7,13-15,20,21,25,26,31,36,38,39] and to confirm actual attachment of the material onto the capillary.[25,26,31,36,39] Two structural characterisations emerging as support to elucidate the chemical structures of embedded SP are X-ray diffraction (XRD) and X-ray photoelectron spectroscopy (XPS). XRD analysis has been important for elucidation and confirmation of crystal structure of crystalline SPs [14,15,19,21,24,26] while XPS analyses were used to identify formation of covalent bonds forming the SP or attachment to the capillary wall.[24,38]

Results obtained using different characterisation methods are exemplified in Figure 1.6. Figure 1.6A shows the fabrication scheme of GO/SiO_2 nanoparticles in different schemes and the resulting coatings were characterised by SEM (Figure 1.6B), by EDS for carbon composition of graphene (Figure 1.6C), and EOF measurements (Figure 1.6D). The separation performance of each coating on seven neutral analytes is shown in Figure 1.6E.

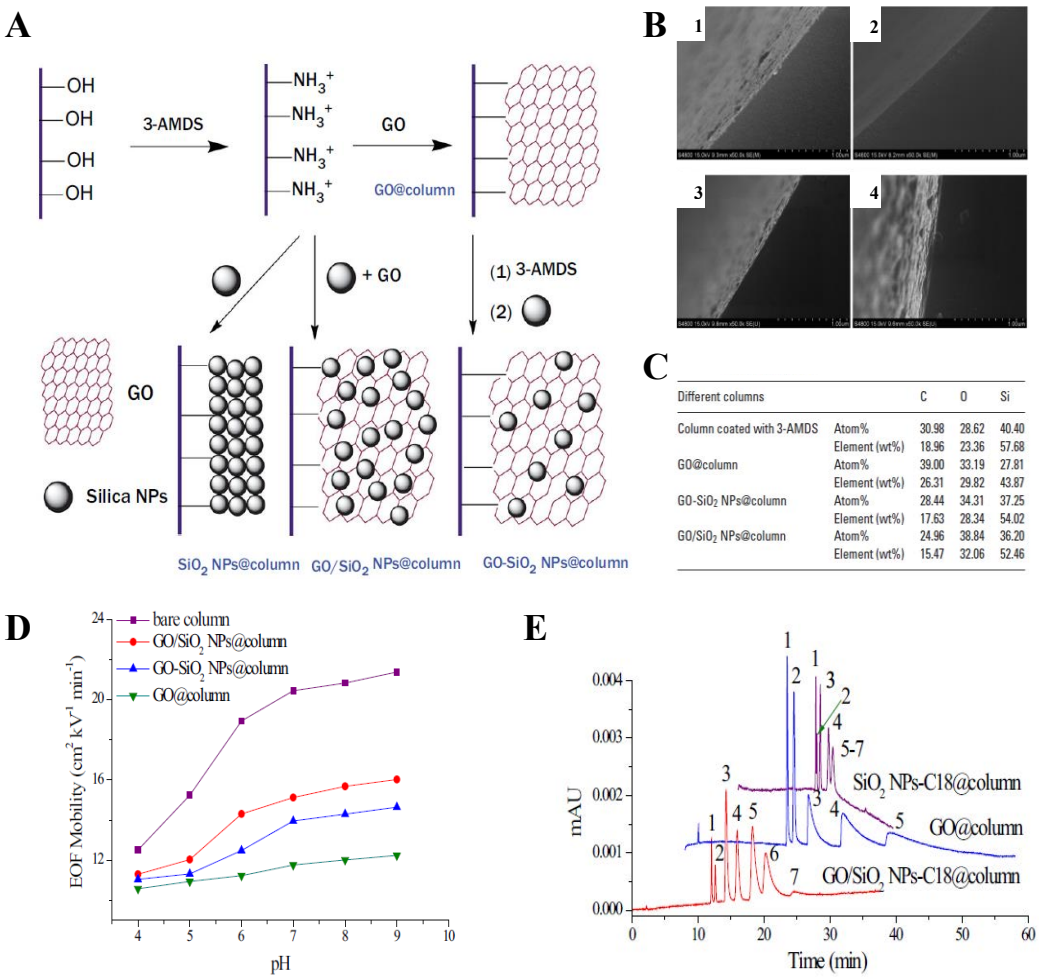

Figure 1.6 (A) Schematic representation of the fabrication processes of the GO@column, GO/SiO_2 NPs@column, GO-SiO NPs@column, and SiO_2 NPs@column. (B) SEM images of (1) GO@column, (2) SiO_2 NPs@column, (3) GO-SiO_2 NPs@column, and (4) GO/SiO_2 NPs@column. (C) Element analyses of columns modified with GO and silica NPs by EDS. (D) Effect of pH value of the buffer on the EOF mobility for various columns. Experimental conditions: MeOH−5 mM Na_2HPO_4 (50:50); capillary column, 75 μm id × 50 cm effective length; temperature, 25°C; detection, 254 nm; electric field strength, 333 Vcm^{-1}; injection, 0.5 psi × 3 s. (E) Separation of seven neutral analytes on the GO@column, GO/SiO_2 NPs-C18@column, and SiO_2 NPs-C18@column. Conditions: detection at 214 nm; MeOH−5 mM Na_2HPO_4 (30:70, v/v). Other conditions were identical to (D). Peak identities: 1, thiourea; 2, mesitylene; 3, toluene; 4, naphthalene; 5, 2-methylnaphthalene; 6, acenaphthene; 7, fluorene. Reproduced with permission from ref 37.

1.6 Other reviews

Since 2000, a number of review papers have been published that have discussed developments in SP materials for CEC. The review on OT-CEC by Jinno and Sawada published in 2000[58] described different types of open tubular capillaries according to their method of preparation. Subsequently, the innovative use of new classes of materials as SPs (including early nanoparticle phases and microchip channel CEC) was summarised by Guihen and Glennon in 2004.[59] Three reviews published during 2013-2015 have described the more general developments of SP materials and their applications in the separation sciences, including OT-CEC. These reviews have documented progress in the use of nanoparticles,[2] molecularly imprinted polymers[60] and porous layer open tubular (PLOT) capillaries.[61] Another review has discussed advances in CEC involving capillary design, detectors and two-dimensional CEC techniques.[62]

Cheong *et al.*[63] published a review in 2013 related to OT-CEC developments from 2007 to 2012. These authors described findings with new SP materials used in OT-CEC. These materials included *in situ* prepared polymers, molecular imprinted polymers, brush polymers and ligands, tentacle polymers, host ligands, block polymers, carbon nanotubes, biomolecules such as poly-saccharides and proteins, nanoparticles, monoliths and polyelectrolyte multilayers.

Review papers that appeared during this review period have addressed the need to look at recent specific OT-CEC separations and applications. Guihen made a focused review on applications of alkylthiol based gold nanoparticles for electrochromatographic separations,[29] while D'Orazio *et al.* highlighted OT-CEC separations in food analysis as mainly on separation of extracted analytes from food samples or matrices for general assessment of food quality.[64] Kapnissi-

Christodoulou *et al*. gave a comprehensive examination of developments in enantioseparations by OT-CEC featuring innovations in chiral SP preparation approaches like chiral nanomaterials, porous layers, molecular imprinting, polymeric coatings, among others.[65] Kašička presented an extensive review on recent capillary and microchip electroseparations of peptides[66] while Mikšík made a thorough review of CEC applications for proteins and peptides covering the past decade, also highlighting OT-CEC developments of various SPs that were chemically bonded, sol-gel prepared, porous layers and physically coated.[67] Though strictly not pertinent to OT-CEC but quite relevant to mention, two other reviews have discussed the progress in capillary coatings for enhancing CE protein separations[68] and for open-tubular CE-integrated immobilised enzyme reactors (IMER).[69] These reviews indicate the importance and dynamic progress of OT-CEC in versatility and applicability in separation science.

1.7 Conclusion

OT-CEC still is an active and exciting research area in separation science. Major focus remains on the development of SP materials and less on applications. For new materials, column performance was assessed mainly on resolutions, linearity, repeatability and stability. Although a few studies included evaluation of column efficiencies, only one paper reported notable column efficiencies.[4] Most OT-CEC analyses done during this review period have employed conventional separation of test analytes and few applications on real samples like chicken egg white,[32,34,37] human urine,[21,30] wheat plant parts,[36] and commercial drugs.[42] However, there has been an interest in using OT-CEC for binding and affinity studies, e.g. to investigate interaction dynamics of focused analytes like natural

products[43] and environmental pollutants[44] with embedded host biomaterial SPs. There was an increase in using non-conventional characterisation of coatings by TEM, AFM, XRD, XPS, and contact angle, amongst others. This is because of the development of highly innovative materials as SP that require sophisticated characterisation. We continue to expect further SP developments in line with current active efforts in material science.

1.8 References

(1) Tarongoy, F. M., Jr.; Haddad, P. R.; Boysen, R. I.; Hearn, M. T.; Quirino, J. P. *Electrophoresis* **2016**, *37*, 66-85.

(2) Guihen, E. *TrAC, Trends Anal Chem* **2013**, *46*, 1-14.

(3) Tarongoy, F. M., Jr.; Haddad, P. R.; Quirino, J. P. *Electrophoresis* **2018**, *39*, 34-52.

(4) Ali, A.; Cheong, W. J. *J Sep Sci* **2017**, *40*, 2654-2661.

(5) Ali, F.; Cheong, W. J. *B Korean Chem Soc* **2016**, *37*, 1374-1377.

(6) Sepehrifar, R.; Boysen, R. I.; Danylec, B.; Yang, Y.; Saito, K.; Hearn, M. T. *Anal Chim Acta* **2016**, *917*, 117-125.

(7) Zhao, Q. L.; Zhou, J.; Zhang, L. S.; Huang, Y. P.; Liu, Z. S. *Talanta* **2016**, *152*, 277-282.

(8) Chen, G. N.; Li, N.; Luo, T.; Dong, Y. M. *J Chromatogr Sci* **2017**, *55*, 471-476.

(9) Kulsing, C.; Yang, Y.; Chowdhury, J. M.; Boysen, R. I.; Hearn, M. T. W. *Electrophoresis* **2017**, *38*, 1179-1187.

(10) Silverstein, M. S. *Polymer* **2014**, *55*, 304-320.

(11) Choudhury, S.; Connolly, D.; White, B. *J Appl Polym Sci* **2016**, *133*, 1-6.

(12) Gu, Z. Y.; Yang, C. X.; Chang, N.; Yan, X. P. *Acc Chem Res* **2012**, *45*, 734-745.

(13) Tang, P.; Bao, T.; Chen, Z. *Electrophoresis* **2016**, *37*, 2181-2189.

(14) Bao, T.; Tang, P.; Mao, Z.; Chen, Z. *Talanta* **2016**, *154*, 360-366.

(15) Pan, C.; Wang, W.; Chen, X. *J Chromatogr A* **2016**, *1427*, 125-133.

(16) Chen, B.; Yang, Z.; Zhu, Y.; Xia, Y. *J Mater Chem A* **2014**, *2*, 16811-16831.

(17) Phan, A.; Doonan, C. J.; Uribe-Romo, F. J.; Knobler, C. B.; O'Keeffe, M.; Yaghi, O. M. *Acc Chem Res* **2010**, *43*, 58-67.

(18) Yu, L. Q.; Yang, C. X.; Yan, X. P. *J Chromatogr A* **2014**, *1343*, 188-194.

(19) Qu, Q.; Xuan, H.; Zhang, K.; Ding, Y.; Xu, Q. *Electrophoresis* **2016**, *37*, 2175-2180.

(20) Li, Y.; Bao, T.; Chen, Z. *J Sep Sci* **2017**, *40*, 954-961.

(21) Pan, C.; Lv, W.; Wang, G.; Niu, X.; Guo, H.; Chen, X. *J Chromatogr A* **2017**, *1484*, 98-106.

(22) Cote, A. P.; Benin, A. I.; Ockwig, N. W.; O'Keeffe, M.; Matzger, A. J.; Yaghi, O. M. *Science* **2005**, *310*, 1166-1170.

(23) Diercks, C. S.; Yaghi, O. M. *Science* **2017**, *355*, 1-8.

(24) Niu, X.; Ding, S.; Wang, W.; Xu, Y.; Xu, Y.; Chen, H.; Chen, X. *J Chromatogr A* **2016**, *1436*, 109-117.

(25) Kong, D. Y.; Bao, T.; Chen, Z. L. *Microchim Acta* **2017**, *184*, 1169-1176.

(26) Bao, T.; Tang, P.; Kong, D.; Mao, Z.; Chen, Z. *J Chromatogr A* **2016**, *1445*, 140-148.

(27) Duan, A.-H.; Xie, S.-M.; Yuan, L.-M. *TrAC, Trends Anal Chem* **2011**, *30*, 484-491.

(28) Hu, W.; Hong, T.; Gao, X.; Ji, Y. *TrAC, Trends Anal Chem* **2014**, *61*, 29-39.

(29) Guihen, E. *Electrophoresis* **2017**.

(30) Fang, L. L.; Wang, P.; Wen, X. L.; Guo, X.; Luo, L. D.; Yu, J.; Guo, X. J. *Talanta* **2017**, *167*, 158-165.

(31) Fang, L.; Yu, J.; Jiang, Z.; Guo, X. *PLoS One* **2016**, *11*, e0146292.

(32) Zhang, Y.; Wang, W.; Ma, X.; Jia, L. *Anal Biochem* **2016**, *512*, 103-109.

(33) Kwon, S.; Singh, R. K.; Perez, R. A.; Abou Neel, E. A.; Kim, H. W.; Chrzanowski, W. *J Tissue Eng* **2013**, *4*, 2041731413503357.

(34) Liu, Y.; Liu, Q.; Yu, H.; Sun, S.; Xue, Y.; Wang, Y.; Qu, Q.; Yan, C. *J Chromatogr A* **2017**, *1499*, 196-202.

(35) Guo, Y.; Xu, F.; Meng, L.; Tang, W.; Xia, Y.; Wu, Y.; Zhang, S. *Electrophoresis* **2013**, *34*, 1312-1318.

(36) Yang, L.; Chen, Y.; Zhao, S.; Zhang, W.; Du, H.; Deng, Z.; Zhang, S. *Chromatographia* **2016**, *79*, 243-254.

(37) Qu, Q.; Xuan, H.; Zhang, K.; Ding, Y.; Xu, Q. *Electrophoresis* **2016**, *37*, 1367-1375.

(38) Dong, S.; Sun, Y.; Zhang, X.; Li, H.; Luo, G.; Zhao, L. *Carbohydr Polym* **2017**, *165*, 359-367.

(39) Guo, H.; Niu, X.; Pan, C.; Yi, T.; Chen, H.; Chen, X. *J Sep Sci* **2017**, *40*, 2645-2653.

(40) Zhang, Y.; Wang, W.; Xiao, X.; Jia, L. *J Chromatogr A* **2016**, *1466*, 180-188.

(41) Xiao, X.; Wang, W.; Zhang, Y.; Jia, L. *J Pharm Biomed Anal* **2017**, *140*, 377-383.

(42) Fu, Q.; Zhang, K.; Gao, D.; Wang, L.; Yang, F.; Liu, Y.; Xia, Z. *Anal Chim Acta* **2017**, *969*, 63-71.

(43) Wang, F. Q.; Zhang, Q.; Li, C. H.; Wang, Y. Z.; Hu, Y. J.; Zhang, Q. H.; Xia, Z. N.; Yang, F. Q. *Electrophoresis* **2016**, *37*, 736-743.

(44) D'Ulivo, L.; Feng, Y. L. *PLoS One* **2016**, *11*, e0153081.

(45) Kong, D.; Chen, Z. *J Sep Sci* **2017**, *40*, 2030-2036.

(46) Lee, H.; Dellatore, S. M.; Miller, W. M.; Messersmith, P. B. *Science* **2007**, *318*, 426-430.

(47) Decher, G. *Science* **1997**, *277*, 1232-1237.

(48) Borges, J.; Mano, J. F. *Chem Rev* **2014**, *114*, 8883-8942.

(49) Richardson, J. J.; Bjornmalm, M.; Caruso, F. *Science* **2015**, *348*, aaa2491.

(50) Pédehontaa-Hiaa, G.; Guerrouache, M.; Carbonnier, B.; Le Derf, F.; Morin, C. J. *Chromatographia* **2015**, *78*, 533-541.

(51) Pan, C.; Wang, W.; Zhang, H.; Xu, L.; Chen, X. *J Chromatogr A* **2015**, *1388*, 207-216.

(52) Bao, T.; Zhang, J.; Zhang, W.; Chen, Z. *J Chromatogr A* **2015**, *1381*, 239-246.

(53) Xu, Y.; Xu, L.; Qi, S.; Dong, Y.; ur Rahman, Z.; Chen, H.; Chen, X. *Anal Chem* **2013**, *85*, 11369-11375.

(54) Zhu, Y.; Zhou, C.; Qin, S.; Ren, Z.; Zhang, L.; Fu, H.; Zhang, W. *Electrophoresis* **2012**, *33*, 340-347.

(55) Zhu, Y.; Zhang, L.; Qian, J.; Zhang, W. *Talanta* **2013**, *104*, 173-179.

(56) Zhang, L. Y.; Zhu, Y. X.; Zhang, W. B. *Acta Chimica Sinica* **2013**, *71*, 62-68.

(57) Wang, X. N.; Liang, R. P.; Meng, X. Y.; Qiu, J. D. *J Chromatogr A* **2014**, *1362*, 301-308.

(58) Jinno, K.; Sawada, H. *TrAC, Trends Anal Chem* **2000**, *19*, 664-675.

(59) Guihen, E.; Glennon, J. D. *J Chromatogr A* **2004**, *1044*, 67-81.

(60) Cheong, W. J.; Yang, S. H.; Ali, F. *J Sep Sci* **2013**, *36*, 609-628.

(61) Knob, R.; Kulsing, C.; Boysen, R. I.; Macka, M.; Hearn, M. T. W. *TrAC, Trends Anal Chem* **2015**, *67*, 16-25.

(62) Xue, Y.; Gu, X.; Wang, Y.; Yan, C. *Electrophoresis* **2015**, *36*, 124-134.

(63) Cheong, W. J.; Ali, F.; Kim, Y. S.; Lee, J. W. *J Chromatogr A* **2013**, *1308*, 1-24.

(64) D'Orazio, G.; Asensio-Ramos, M.; Fanali, C.; Hernandez-Borges, J.; Fanali, S. *TrAC, Trends Anal Chem* **2016**, *82*, 250-267.

(65) Kapnissi-Christodoulou, C. P.; Nicolaou, A. G.; Stavrou, I. J. *J Chromatogr A* **2016**, *1467*, 145-154.

(66) Kasicka, V. *Electrophoresis* **2016**, *37*, 162-188.

(67) Miksik, I. *J Sep Sci* **2017**, *40*, 251-271.

(68) Hajba, L.; Guttman, A. *TrAC, Trends Anal Chem* **2017**, *90*, 38-44.

(69) Liu, X. X.; Yang, J. Q.; Yang, L. *Rev Anal Chem* **2016**, *35*, 115-131.

Chapter 1 Appendix

Table A1.1 New polymer-based SP materials developed for OT-CEC

	Material used	Electrolyte/ BG solution	Samples used	Separation mechanism	Ref.
1	N-phenylacrylamide-styrene-methacrylic acid (MAA) copolymer layer	60:40 (v/v) ACN/50 mM ammonium formate, pH 6.5	a synthetic mixture of five peptides	assemblage of a nonpolar monomer still capable of some interaction with peptides (styrene), a polar monomer for EOF generation (MAA), and a monomer (N-phenylacrylamide) capable of good interaction with peptides	[4]
2	tri-copolymer of styrene, MAA, N-phenylacrylamide	60:40 (v/v) ACN/ 25 mM sodium phosphate, pH 6.8	tryptic digest sample of cytochrome C, synthetic mixture of five standard peptides	(see 1)	[5]
3	poly(2-dimethylaminoethyl-methacrylate)-block-poly(acrylic acid)	20 mM sodium phosphate buffer, pH 3.2 (acidic compounds) and pH 5.0 (basic compounds)	*acidic compounds*: 2-nitrobenzoic acid, 2- fluorobenzoic acid, benzoic acid and 4-hydroxybenzoic acid *basic compounds*: benzyltriethylammonium chloride, benzylamine, amitriptyline and diphenhydramine	zwitterionic polymeric surface coating altering the EOF direction affecting migration of analytes; hydrophilicities of both polymer segments change with pH for selectivity and resolution control	[6]
4	MIPs based on polyhedral oligomeric silsesquioxanes (POSS) with the formula $(RSiO_{1.5})_n$	80:20 (v/v) ACN/ 50 mM acetate, pH 4.2	S-amlodipine and racemic amlodipine; S-Naproxen and racemic naproxen, d-Zopiclone and racemic zopiclone	Introduced POSS core as a host for encapsulating various kinds of hydrophobic molecules	[7]

5	MIP from S-(–)-propranolol (template), MAA (functional monomer), 3-(trimethoxysilyl)propyl methacrylate (cross-linking monomer) and AIBN (radical initiator)	70% ACN/ 20 mM boric acid salt, pH 6.9	S-(–)-propranolol and R-(+)-propranolol	chiral recognition determined by the steric arrangement of the interacting groups of the enantiomers and the polymer	[8]
6	MIP porous layer open tubular capillaries using MAA and 4-vinylpyridine as functional monomers, with Z-L-Asp-OH as the template	60% (v/v) ACN/ 20 mM $HCOONH_4$, pH 4.74	Z-Asp-OH racemates	nano-cavities of predetermined shape and appropriate orientation of functional groups employed as molecular recognition sites for selectivity towards a particular chiral compound	[9]
7	polystyrene-*co*-divinylbenzene polyHIPE	40% ACN/ 5 mM $Na_2B_4O_7 \cdot 10H_2O$ and 2.5 mM NaH_2PO_4, pH 9	ethylbenzene and pentylbenzene.	none described	[11]

Table A1.2 New framework-based SP materials developed for OT-CEC

	Material used	Electrolyte/ BG solution	Samples used	Separation mechanism	Ref.
1	MOF-180, an octahedral $Zn_4O(CO_2)_6$ with 4,4',4" -[benzene-1,3,5-triyl-tris(ethyne-2,1-diyl)] tribenzoate as organic ligands	10 mM phosphate buffer with 10% methanol, pH 3 for acids, and pH 5 for bases, pH 9 for neutrals	*acids*: benzoic acid; aspirin; phthalic acid *bases*: β-phenylethylamine, *N, N*-dimethylaniline, aniline	hydrophobic effect due to specific sites like ethyne groups and substantial number of benzene rings in the structure; larger pores size with cage size of 15 × 23 Å allowing small molecules entering the cages preferentially and eluted primarily in separation	[13]
2	MOF-5, based on reticulating organic dicarboxylate and octahedral Zn-O-C, also named IRMOF-1	10 mM Na_2HPO_4 buffer at pH 9.0	substituted benzenes: methylbenzene, styrene, ethylbenzene aromatic acids: 1,3,5-dimethylbenzoic acid, 2,4-aminobenzoic acid, benzoic acid aromatic bases: 2-phenylethylamine, *N, N*-dimethylbenzenamine, phenylamine	π-π and hydrophobic interaction between the benzene rings of the substituted benzenes and the benzene rings of dicarboxylate benzene struts linking octahedral Zn-O-C clusters of MOF-5; the higher pH value increased cation-π interactions between Zn^{2+} and substituted benzenes	[14]
3	homochiral MOF $[Zn(s\text{-}nip)_2]_n$	15% (v/v) methanol, 10 mM borate, pH 9.3 for isoprenaline pH 9.8 for synephrine, pH 8.8 for epinephrine, pH 9.3 for ephedrine and pseudoephedrine	monoamine neurotransmitters enantiomers of epinephrine, isoprenaline and synephrine; diastereoisomers of ephedrine and pseudoephedrine, the isomers of nitrophenols and analogues of bisphenols	enantioseparation recognition ability of the homochiral $[Zn(s\text{-}nip)_2]_n$ depend on chiral microenvironment and the hydrophobic and π–π interaction between the analytes and the aromatic and imidazole rings on the ligand of MOF	[15]
4	zeolite imidazolate framework-8 (ZIF-8) nanocrystals	9 mM sodium borate solution, pH 9.5	p-methoxyphenol, o-methoxyphenol, m-methoxyphenol, phenol, p-benzenediol, m-benzenediol, o-benzenediol, m-nitrophenol, p-nitrophenol, o-nitrophenol	main interaction between ZIF-8 and phenols was of unsaturated Zn sites with ionized phenols	[19]

5	zeolitic imidazolate framework-8	20:80 (v/v) ACN/20 mM Na_2HPO_4, pH 9.0	diphenol isomers: hydroquinone, resorcinol, catechol benzene series: n-butylbenzene, n-propylbenzene, ethylbenzene, methylbenzene PAHs: chlorobenzene, o-dichlorobenzene, 1,2,4-trichlorobenzene basic compounds: aniline, paratoluidine, and *N, N*-dimethylaniline	the π–π stacking interactions and hydrophobic interactions with diphenol isomers; the metal ions in the crystals enhancing interaction to the phenolic hydroxyl group; different positions of phenolic hydroxyl group determining the different interaction with stationary phase; charge induced dipole–dipole interaction and the cation–π interactions between the positively charged Zn^{2+} on ZIF-8 and the electron-rich π-system of four substituted benzenes	[20]
6	zeolitic imidazolate framework ZIF-8	15% (v/v) methanol, 20 mM NaAc-HAc buffer, pH 5.5	monoamine neurotransmitters (cationic): dopamine, epinephrine, isoprenaline, synephrine, norepinephrine and terbutaline flavonoids (neutral): praziquantel, flavanone, 6-methoxyflavanone and 4 ,5,6,7,8-pentamethoxy-flavanone simultaneous separation and detection of the six cationic and four neutral analytes in urine matrix	hydrogen bonding between the functional groups – NH_2 and –OH of cationic analytes and the imidazolium in the ZIF-8 framework, difference of the analytes' charge-to-mass ratio; the interaction between the neutral analytes and the microporous framework of the coating material ZIF-8 (i.e., hydrophobic and π - π interaction)	[21]
7	covalent organic frameworks-LZU1	25% (v/v) ACN/10 mM borate with, pH 9.5	alkylbenzenes: benzene, methylbenzene, ethylbenzene, propylbenzene, butylbenzene anilines:	with pore windows and multiple benzene rings, size selectivity and hydrophobic interactions affecting separation; eclipsed layered-sheet arrangement as a crucial factor	[24]

			p-phenylenediamine, m-iodoaniline, m-chloroaniline, and p-chloroaniline polycyclic aromatic hydrocarbons (PAHs): naphthalene, acenaphthene, and phenanthrene		
8	covalent organic framework LZU1	10% (v/v) MeOH/ 10mM phosphate buffer, pH 5.0 (alkylbenzenes); 20% (v/v) ACN/ 20 mM phosphate buffer, pH 8.5 (PAHs); 50% (v/v) MeOH/ 30 mM phosphate buffer, pH 8.5 (amino acids); 45% (v/v) MeOH/ 20 mM phosphate buffer (NSAIDs)	neutral analytes: methylbenzene, ethylbenzene, n-propylbenzene, chlorobenzene, 1,2-dichlorobenzene and 1,2,4-trichlorobenzene, naphthalene, 4-phenyltoluene and phenanthrene amino acids: L-phenylalanine, L-tryptophan, L-tyrosine nonsteroidal anti-inflammatory drugs (NSAIDs): ketoprofen, ibuprofen, flurbiprofen	hydrophobic interaction and π-interaction between neutral analytes and COF-LZU1; π-interaction of the amino acids with the COF-LZU1 layer, imine and primary amino groups of COF-LZU1 form hydrogen bond with the amino acids	[25]
9	boron COF-5	40% (v/v) MeOH/ 10 mM phosphate buffer, pH 7.0 (neutrals); 10 mM phosphate buffer, pH 8.0 (acids); 10 mM phosphate buffer pH 7.0. (bases); 20% (v/v) MeOH/ 10 mM phosphate buffer, pH 9.0 (alkylbenzenes)	***neutrals***: methylbenzene, ethylbenzene, n-propylbenzene n-butylbenzene, 4-methylbiphenyl, 1,3,5-trimethylbenzene ***acidic***: 4-aminobenzoic acid, benzoic acid, 3,5-dimethylbenzoic acid ***basic***: *N, N*-dimethylbenzenamine, phenylamine, 2-phenylethylamine	the π-π interaction between aromatics and aromatic framework in COF-5; hydrophobic interaction between alkylbenzenes and COF-5 layer; adsorption effect of porous COF-5 and benzene rings in its framework	[26]

Table A1.3 New nanoparticle and graphene-based SP materials developed for OT-CEC

	Material used	Electrolyte/ BG solution	Samples used	Separation mechanism	Ref.
1	GNPs functionalised with thiols β-cyclodextrin	5 mM Tris-H_3PO_4 buffer solution with 5% ACN, pH 5.0	meptazinol and its three intermediate enantiomers (intermediates II, III and IV) meptazinol in spiked urine samples	enantioselectivity of β-cyclodextrin; the phenol ring connected to the chiral carbon results in good inclusion and chiral differentiation of meptazinol, intermediate III and intermediate IV	[30]
2	β-cyclodextrin modified gold nanoparticles	5 mM β-CD, pH 2.5 (except for sibutramine hydrochloride, pH 2.0), 25 mM Tris-H_3PO_4)	basic drugs: zopiclone, chlorphenamine maleate, brompheniramine maleate, dioxopromethazine hydrochloride, carvedilol, homatropine hydrobromide, homatropine methylbromide, venlafaxine, sibutramine hydrochloride, terbutaline sulfate	synergistic effect between β-CD in BGE and on the OT-CEC column for the enantioseparation	[31]
3	titanium oxide (TiO_2) nanoparticles	40 mM phosphate buffer, pH 9.0	conalbumin, α- lactalbumin, β-lactoglobulin, and BSA; two variants of β-lactoglobulin and eight glycoisoforms of ovalbumin proteins in egg white from commercial chicken eggs	the difference in the electrophoretic mobilities of proteins; the interactions between these proteins and the TiO_2 coating via the ligand exchange of the analytes with the phosphate ions adsorbed onto the TiO_2 film	[32]
4	fibrous mesoporous silica nanoparticles	50:50 (v/v) MeOH/ 50 mM phosphate for neutral samples	neutrals: thiourea, naphthalene, biphenyl proteins: Lysozyme, ocytochrome C and α-chymotrypsinogen A egg white proteins: ovotransferrin, ovalbumin, ovomucoid chicken egg white proteins	retention mechanism basically a reversed-phase; both the electrophoretic mobility and the interaction between proteins and the C18 coating play important roles separation	[34]

5	methyldiethanolamine amination polychloromethyl styrene nanolatex	30% (v/v) ACN/ 30 mM Tris–24 mM $HClO_4$, pH 7.24	phytohormones: indole-3-acetic acid (IAA) and beta-indolebutyric acid (IBA) of different plant parts IAA and IBA measured in the different wheat plant part samples; sample pre-treatment using tetraazacalix[2] arene[2]triazine-modified silica gel as SPE sorbent	ion-exchange interaction	[36]
6	GO and silica nanoparticles hybrid nanostructures	30:70 (v/v) MeOH/ 5 mM Na_2HPO_4	Thiourea, mesitylene,, toluene, naphthalene, 2-methylnaphthalene, acenaphthene, fluorene chicken egg white acidic and basic proteins and three glycoisoforms of ovalbumin	π-π stacking, hydrophilic effect, π-π electron-donor-acceptor, and hydrogen bonding (GO and the analytes); improved peak shape due to weakened interactions with GO from increased SiO_2 NP coverage; enhanced interactions between C18 modified SiO_2 NPs and the analytes; reversed-phase retention mechanism	[37]

Table A1.4 New biomaterial-based SP materials developed for OT-CEC

	Material used	Electrolyte/ BG solution	Samples used	Separation mechanism	Ref.
1	nanocellulose crystals (NCCs) derivatised with 3,5-dimethylphenyl isocynate (DMPC)	pH 3.5 to 9, using acetic acid - sodium acetate and borate-phosphate at concentration range of 0.10 to 0.40 M (see reference)	amino acids: phenylalanine, tryptophan, tyrosine chiral drugs: ibuprofen, repaglinide, pazufloxaci chiral phenylethanol compounds: phenethyl alcohol, mandelonitrile, 1-phenyl-1-propanol pesticide residues; fluazifop-P, biphenyl triadimefon, deltamethrin, bifenthrin	chiral selectivity of DMPC/NCCs, small physical dimensions and high homogeneity of coating material, increased layer density and phase ratio improved enantioseparation performance	[38]
2	β-cyclodextrin/ polydopamine (PDA) composite	10 mM borate, pH 8 - 9.75 with 20-25% MeOH	epinephrine, norepinephrine, isoprenaline, terbutaline, verapamil, tryptophan, carvedilol	the chiral recognition capacity of β-CD, the benzene rings, amino, and phenolic hydroxyl groups of PDA may favor the enantiomeric separation or selectivity; affected by hydrophobic interactions, weak hydrogen bonding, and π–π interaction	[39]
3	bovine serum albumin (BSA)	cetuximab and rituximab - 40 mM phosphate buffer (pH 6.0); trastuximab - 40 mM phosphate buffer (pH 5.5) proteins: 40 mM phosphate buffer (pH 7.0)	monoclonal antibodies (mAbs): cetuximab, rituximab, trastuximab basic proteins: lysine, cytosine and ribonuclease A	electrostatic interaction between the BSA coating and basic proteins; electrophoretic mechanism in the separation of basic proteins; BSA coating showed special separation ability for the charge state profiles of the tested mAbs and effectively reduced the adsorption of mAbs to the capillary wall.	[40]

4	fibrin from in situ polymerization of fibrin in the presence of thrombin as a catalyst	cetuximab - 50 mM phosphate buffer (pH 6.0); trastuzumab - 50 mM phosphate buffer (pH 6.5); rituximab - 40 mM phosphate buffer (pH 7.5)	mAbs: cetuximab, rituximab, trastuximab	migration times in the order of rituximab, trastuzumab and cetuximab, in agreement with the decrease of their pI values; electrostatic interaction between the negatively charged fibrin coating and the positively charged mAbs; electrophoretic mechanism in the separation of mAbs and non-specific interactions between the mAbs and the stationary phase (hydrophobic, van der Waals forces and electrostatic attractions)	[41]
5	Escherichia coli (E. coli) DH5a	50 mM phosphate buffer, pH 6.0	S-(-)- ofloxacin, R-(+)-ofloxacin ofloxacin enantiomers in the commercial ofloxacin tablets	enantioseparation by the intrinsic chiral microenvironment of E. coli cells with chiral recognition behaviors	[42]
6	rabbit platelets	5 mM trisodium citrate with 5% (v/v) acetone, pH = 7.40	adenosine diphosphate (positive control), protocatechuic acid (negative control), salvianolic acid B, salvianic acid A sodium, hydroxysafflor yellow A, ferulic acid, chlorogenic acid, sinapic acid and caffeic acid evaluation of interactions between small molecules from natural products	The interactions evaluated by their retention factors and binding constants obtained based on peak-shift assay.	[43]
7	20-mer single-stranded (20-mer, 5-HTT and 20-mer, RC-5-HTT) and 20-bp double-stranded DNA oligonucleotides	10 mM triethylammonium acetate, pH 7	1,4-phenylenediamine, pyridine and 2,4-diaminotoluene	molecular structure and amino group positions influence the interaction affinity; aromatic amines have intercalative properties in the interaction with the DNA coating	[44]
8	Hydroxyapatite (HAP)	20 mM ammonium acetate ammonium hydroxide buffer solution, pH 7.4	Zoledronate, a third-generation bisphosphonate drug; 1-(2-hydroxyethyl) imidazole	P–C–P structure of zoledronate is structural basis for interaction with HAP	[45]

Chapter 2

Characterisation of surfactant adsorption by capillary electrophoresis

2.1 Abstract

Solid surface adsorption behaviour of surfactant aggregates was characterised using capillary electrophoresis by monitoring surface charge effects on dynamically introduced surfactants. Different concentrations of the surfactants CTAB and SDS were prepared with the buffer and the EOF mobility of a marker compound (acetone) was measured electrophoretically at the given variations of surfactant concentrations. The critical surface adsorption concentration (csac) was determined based on the surfactant concentration at the reversal of the EOF polarity, while the critical micelle concentration (cmc) was based on the concentration when the EOF magnitude became constant or at minimum (positively charged surface resulting in reverse or anodic EOF polarity). A cmc of 0.20 mM and csac of 0.042 mM were obtained with CTAB at 50 mM sodium tetraborate of pH 9.5 buffer, and 0.50 mM (cmc) and 0.10 mM (csac) for CTAB in 100 mM ammonium bicarbonate buffer (pH 8.5).

2.2 Introduction

A behaviour resulting from the amphiphilic structure of surfactants is their ability to orient themselves on the water surface (air-liquid interface) (thus the term surface-active agent or surfactant), or to cluster and aggregate into microstructures called micelles while in solution. In aqueous bulk solution at a concentration above the cmc, surfactant monomers orient due to hydrophobic interactions of the nonpolar carbon-chain tails and cluster around to assume a spherical form, the hydrophobic tails inside the core, while the hydrophilic or polar heads are directed outward to interact with water. Depending on the type of surfactant, type of solution media and conditions, other micellar forms are generated which have been characterised (Figure 2.1A).

Surfactants have also been known to demonstrate a similar behaviour onto solid surfaces, where surfactant molecules (as monomers) adsorb onto the surface, particularly on mineral oxide surfaces like silica and alumina. This phenomenon has been investigated extensively[2-5] through adsorption isotherms (a plot of amount of surfactant adsorbed with increasing surfactant concentration) that were depicted by either a two-step model[6] or a four region model[7] (Figure 2.2). The four-region model developed by Somasundaran and Fuerstenau[8] from a log – log scale plotted adsorption isotherm describes the mechanism of adsorption of surfactants on solid surfaces through four stages (or regions in the isotherm). In region I, surfactant monomers are electrostatically adsorbed to the surface or substrate with head groups in contact with the surface (ionic head groups attracted to the oppositely-charged surface) with the hydrophobic tails protruding into the solution; in region II, there is a notable increase in adsorption contributed by lateral hydrophobic interactions between hydrocarbon tail groups of adsorbed monomers, enabling

them to build primary aggregates called hemimicelles (Figure 2.1B). Surface coverage by hemimicelles is then observed by a reversal of the surface charge as all possible charged sites have been adsorbed with surfactant monomers and resulting aggregates. The hydrophobic interactions of tail groups predominate the adsorption forces over electrostatic ones, allowing further increase in adsorption in region III, forming another aggregate structure with a bilayer formation of interacting tails with head groups of the second layer directed towards the solution. These aggregate forms are called admicelles (Figure 2.1B).[9] The transition from region II to region III is marked by a significant change in surface charge density, enabling the monolayer structure (hemimicelle) to favour the formation of the second layer (admicelle).[4] Region IV is therefore depicted with surface morphology of fully formed bilayers and any further increase in surfactant concentration does not produce further adsorption.

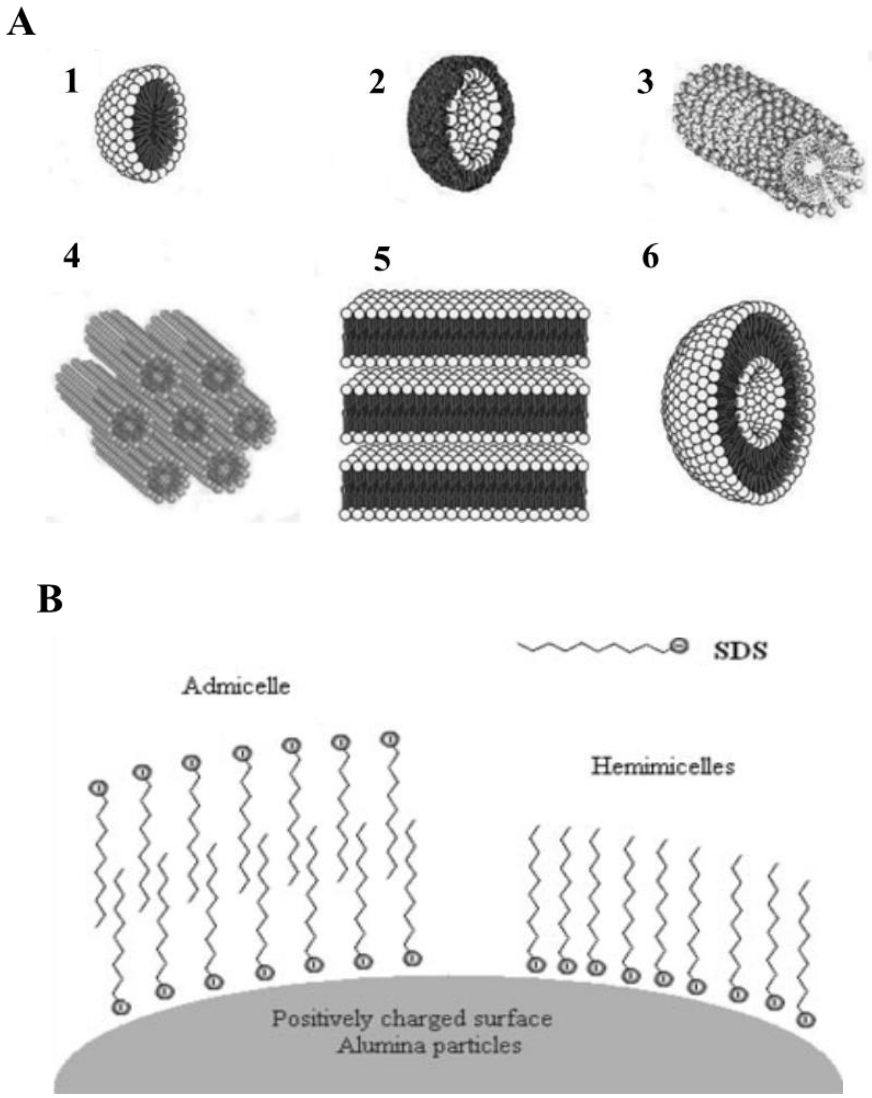

Figure 2.1. (A) Different forms of surfactant aggregation: micelles in water (1), reverse micelle in organic solvent (2), lyotropic liquid crystals (3 to 6) — elongated or rod-like micelle (3), the middle phase or hexagonal phase (4), the neat phase or lamellar phase (5), and liposomes (6). Reproduced from ref 1. (B) Aggregate structures formed by adsorbing anionic surfactant SDS on a positive gamma-alumina surface. Reproduced from ref 1.

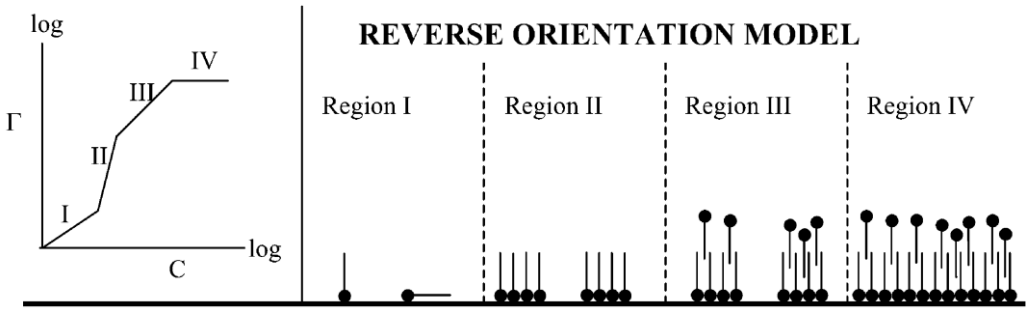

Figure 2.2 The four-region or reverse orientation model of adsorption. Proposed adsorption isotherm and surfactant aggregates on solid substrates. More discussion in the text. Adapted from ref 7.

Adsorption isotherms generated from traditional investigations involving solution depletion experiments (where adsorbed surfactants are measured from the concentration loss after adsorption equilibriation) have contributed valuable information on the mechanism of surfactant adsorption and have been summarised in a number of past reviews.[3,5] Newer techniques have been developed and utilised, such as atomic force microscopy (AFM),[2,10-12] fluorescence quenching experiments,[13-16] more sophisticated reflectance techniques like neutron reflectivity,[17-20] ellipsometry,[21,22] optical reflectometry,[12,23-25] dynamic light scattering[26-28] and contact angle[29-31] whereby further structural information has been obtained to closely describe actual surfactant aggregate morphologies and structures. The employment of a combination of such techniques was found useful in adsorption kinetics and equilibrium studies and insights from various data have further refined understanding of adsorption mechanism. Atkins, *et al.*[32] have proposed a reinforced four-span mechanism of cationic adsorption on mineral oxide surfaces derived from the consolidation of past and recent kinetic and structural data using newer techniques mentioned.

Hexadecyl- or cetyltrimethylammonium bromide (CTAB) and sodium dodecyl sulfate (SDS), both ionic surfactants, are well-studied surfactants that have been investigated for adsorption mechanisms and kinetics.[32] Their aggregates can form certain geometries on the adsorbed surface depending on the surfactant concentration, pH of the solution, presence of salt or electrolytes, as well as the properties of the surfactant and that of the solid surface in terms of roughness, chemistry and porosity. These geometries have been investigated and characterised using modern techniques like AFM,[24,33] fluorescence spectroscopy,[34] neutron reflectivity,[17] and ellipsometry.[35]

Understanding adsorption behaviour of surfactants is essential to tap into applications of surfactants in industry and particularly in separation science. An important stage is the characterisation of the point of equilibrium of surfactant monomerisation and micellisation which is marked at the critical micelle concentration (cmc). Micellisation phenomena are exploited in separation techniques like micellar electrokinetic chromatography (MEKC) where separations utilise surfactant concentrations above the cmc and requires optimisation of operational conditions such as type of surfactants usable, pH, type and ionic strength of buffer solution or background electrolyte and use of organic modifiers. Therefore, it is always a primary and essential consideration to determine the cmc of the surfactant system employed given the solution environment it is in. In the present study, the determination of the cmc is essential to differentiate retention behaviour of adsorbed surfactants and solution micelles, especially at conditions below the cmc but above the critical surface aggregation concentration (csac) and also conditions above the cmc to explore conditions suitable for chromatography (and may include electrochromatography) in open-tubular capillary columns.

A number of techniques have been employed to determine the cmc of selected surfactants, both ionic and nonionic ones, and have been adequately summarised in previous reviews.[36-38] Capillary electrophoresis-based techniques have been developed for cmc determinations[39-46] and have been shown to be convenient and useful under given operating conditions. Lin[47] elaborated these techniques by categorising them as the retention model – MEKC method,[39,40] the mobility model – CE (mobility) method,[41-44] electric current measurements by CE instrumentation[46] and other methods based on electroosmotic mobility[45] and ligand-exchange MEKC.[48,49]

The employment of surfactants in CE was to introduce surfactants as dynamic coatings on the inner fused-silica capillary wall as control for electroosmotic flow (EOF) in order to improve separation of highly mobile analytes either by EOF suppression or EOF reversal.[50,51] In MEKC, which is a mode of CE, surfactants are used further as pseudostationary phases to facilitate separation of neutral hydrophobic solutes that do not separate in CE because they are uncharged species.[52] The advantage of EOF reversal by the use of cationic surfactants like CTAB has been pointed out first by Tsuda[53] and has been well-acknowledged in CE.[50,54-56] The occurrence of such EOF reversal by cationic surfactants like CTAB had been attributed to the phenomenon of surface adsorption.

This chapter aims to describe characteristic molecular aggregation occurring in open-tubular fused-silica capillaries using CE techniques by monitoring surface charge changes indicated by the EOF mobility. This will enable the determination of the cmc and the csac as encompassing parameters of interest to define the admicellar and micellar regions. The csac and cmc obtained from the background solutions elaborate any chromatographic retention or behaviour of

surfactants used as stationary pseudophase surface coatings that will be investigated in the succeeding chapters.

2.3 Materials and methods

2.3.1 Reagents and general instrumentation

All chemicals and reagents not listed below were obtained from Sigma-Aldrich (New South Wales, Australia) or Fluka Analytical (St. Louis, MO, USA) and were used as delivered. Hexadecyltrimethylammonium bromide (or cetyltrimethyl-ammonium bromide, CTAB) was obtained from bioWORLD (Dublin, OH, USA). Purified water was from a Milli-Q system (Millipore, MA, USA). The pH and conductivity of solutions were measured using a bench top meter (Sper Scientific, Australia). Stock solutions of buffers (0.2 M ammonium formate pH 4.5, 0.2 M ammonium acetate pH 8.5 and phosphate buffers pH 2-10), surfactant stock solutions (0.2 mM SDS and 0.2 mM CTAB) and 3.5 M sodium chloride (NaCl) were sonicated and filtered using a 0.45 μm filter prior to use. Mobile phases were prepared by mixing appropriate volumes of buffer, surfactant solution stock, methanol (MeOH), acetonitrile (ACN) with purified water. 10% poly(diallyldimethylammonium chloride (PDADMAC) with average molecular weight of 400-500k was prepared in purified water. This was used to modify the capillary wall in the SDS experiments.

2.3.2 Determination of cmc and csac by electrophoretic measurements

Electrophoretic measurements were carried out using a Beckman P/ACE MDQ Capillary Electrophoresis instrument (employed with 210-nm wavelength UV detection) and Proteomelab 800 (at 200-nm wavelength UV detection)

(Beckman-Coulter, Brea, CA USA). The fused-silica capillaries used (Polymicro, Phoenix, AZ, USA) were 50 μm i.d. with 60-cm in total length with 50-cm length to detection window. Determination of cmc and csac were based on EOF measurements of background solutions (BGS) of different surfactant concentrations with respective buffer solutions. 50 mM sodium tetraborate ($Na_2B_4O_7.10H_2O$) at pH 9.5 was used with varying CTAB concentrations while 100 mM ammonium bicarbonate (NH_4HCO_3) at pH 8.5 was used for varying CTAB and SDS concentrations.

New capillaries were conditioned with 1M NaOH for 30 min, followed by water rinsing (MilliQ water) for 20 min. Daily preconditioning with 1M NaOH and purified water was done for 10 min each and post-conditioning at 5 min each was performed at end-of-day operation. Conditioning with base generated the necessary negative charge on the inner capillary wall. BGS was then flushed for 6 min (10 min for new capillaries). All preconditioning and rinses were carried at 1200 mbar pressure (or equivalent of 1.5x capillary volume being replaced within 60 s). For the SDS experiments, the capillary required pretreatment with the cationic polyelectrolyte poly(diallyldimethylammonium chloride) (PDADMAC) to establish a reversed charge (positive) on the inner wall to enable anionic SDS to adsorb. A diluted PDADMAC solution (1%) was flushed for 3 capillary volumes, followed by a one capillary volume rinse with purified water and BGS conditioning thereafter. Sample injection was 250 mbar-s (~3 mm injection plug length) and temperature was controlled at 20°C. Applied voltage used for bicarbonate buffer was + 20 kV (reversed for PDADMAC-coated capillary) and +25 kV for the borate buffer.

For every run, capillaries were reconditioned by a water-methanol-water flush (2-3 capillary-length rinses) to flush out any pre-existing surfactant coating, followed by a NaOH rinse (to recover surface negative charge) and BGS conditioning. A PDADMAC rinse was also performed after the NaOH and water rinses and before BGS conditioning with SDS.

2.4 Results and discussion

2.4.1 cmc and csac for CTAB

The EOF in CE is generated by the movement of hydrated cations as they migrate to the negative electrode (cathode) when an electric potential is applied to an ionised (buffer) solution along a column, usually a fused-silica capillary. This migration results from the creation of an electrical double-layer when cations in the solution interact electrostatically with the inner capillary wall rendered negative due to ionised silanol groups resulting from pH influence of the buffer or background electrolyte solution (silanol ionisation occurring at pH > 3).

Establishing a pH of 8.5 or 9.5 in the BGS of ammonium bicarbonate or sodium tetraborate, respectively, enabled a normally oriented EOF to flow towards the cathode as the surface charge of the inner wall was kept negative after preconditioning with NaOH. This allowed monomers of surfactant CTAB to interact with the wall with the cationic polar head group adhering to the negatively charged wall and the hydrophobic chain tails oriented away and towards the bulk solution. The plot of EOF mobility (μ_{EOF}) versus CTAB concentration [CTAB] in two basic buffers in Figure 2.3 (A) and (B) showed the following: at 0 mM CTAB, the EOF is cathodic from the negative charge at the surface due to the ionization of

the silanol groups at the pH used. As the CTAB concentration increases, the charged surface will gradually be populated by surfactant monomers, thus causing a change in the net surface charge or the zeta potential (ζ). The decrease in the electroosmotic mobility (μ_{EOF}) (Figure 2.3) indicates a decrease in the negativity of the surface charge as the surface is gradually saturated with surfactant monomers, with the cationic charge of the polar heads electrostatically neutralising the negative charged areas. This therefore reflects the gradual self-assembly of CTAB monomers into the hemimicelle aggregation when the number of adsorbed surfactant monomers increases, and the nearby hydrophobic tail chains start to associate strongly with each other. It was postulated that at a latter part of this stage, bilayer aggregates are also being formed alongside hemimicelles, although it was generally accepted that hemimicelles formation was more predominant.[4] The stronger tendency for electrostatic interaction of surfactant head groups with the charged wall over the competing interaction amongst hydrophobic chains favours the hemimicelle formation.

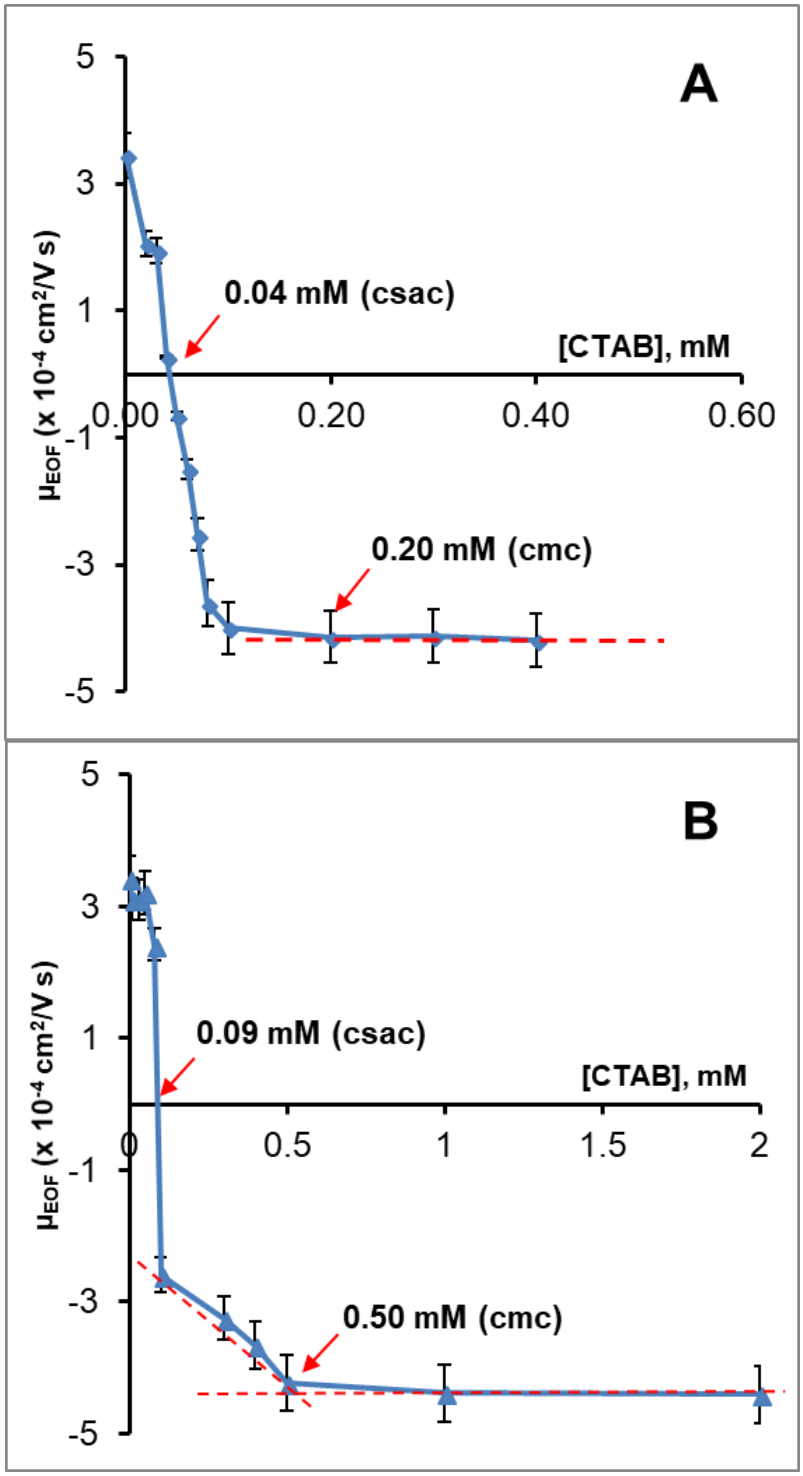

Figure 2.3. EOF mobilities (μ_{EOF}) obtained from varying CTAB concentrations in background electrolytes 50 mM sodium tetraborate in pH 9.5 (A) and 100 mM ammonium bicarbonate in pH 8.5 (B). Conditions as described in the methodology. EOF was detected using acetone (2%) as marker.

Figure 2.4 shows a schematic of the molecular organization of cationic CTAB at the interface between the bulk solution inside the capillary and the anionic inner capillary wall surface. There is adsorption and aggregation with increasing concentration of CTAB (from left to right).

The continued decrease in μ_{EOF} to zero would reflect saturation of negatively charged surface sites by hemimicelles and a transition followed thereafter where the mobility changed to a negative value and further magnified. This indicated that the surface progressively acquired a positive charge generated from the formation of the bilayer surfactant aggregation referred to as admicelles. In admicelles, a second layer of monomers builds up on the hemimicelle layer whereby hydrophobic chains of solution surfactants establish interaction with those of the adsorbed hemimicelles, and repulsion of hydrophilic head groups orient them towards the aqueous phase. The accumulation of polar or charged headgroups from the resulting admicelle renders the change in the surface charge characteristics, thus for CTAB, the prior negatively charged silica surface depletes to neutral as CTAB hemimicelles populate the surface, and then acquires a reversed charge (positive) due to the build-up of the cationic head groups of CTAB oriented towards the solution in the formation of admicelle aggregates (Figure 2.4).

The point at which the surface charge reverses in polarity, as indicated by the reversal of the sign of the $\mu_{EOF,}$ designates the significant transition of surfactant aggregation from hemimicelle to admicelles and is referred to as the csac of the surfactant. This refers to the amount of surfactant monomers in the solution that can effectively create the admicellar aggregation on the surface. The determination of the csac is necessary to determine the admicellar concentration range for subsequent investigations of separations employing admicelle structures. The csac

of CTAB in 50 mM sodium tetraborate in pH 9.5 and 100 mM ammonium bicarbonate in pH 8.5 were 0.04 mM and 0.09 mM respectively.

At surfactant concentrations above the csac, the μ_{EOF} continues to decrease rapidly, i.e. the EOF continues to speed up in the reverse direction, and this marks the surfactant solution equilibria to favour further admicellar assembly. The favourability of admicelle aggregation has been characterised on conditions of strong binding of the surfactant headgroup with buffer counterions on the surface, high surface charge densities, and high dielectric constants.[4] The buffer conditions, with the pH used (8.5 and 9.5), easily facilitated high surface charge densities due to better ionisation of surface silanols and minimised electrostatic repulsion among the ionic headgroups resulting from the screening or decrease of headgroup charge.

Above the csac, more and more surfactant monomers in solution establish the fast build-up of bilayer aggregates (admicelles), which further increases the positivity of the surface charge in the case of CTAB monomers. As the CTAB concentration in the BGS is increased, the number of CTAB monomers remaining in solution remains constant as the rest of the CTAB monomers incorporate into the surface self-assembly (Figure 2.4).

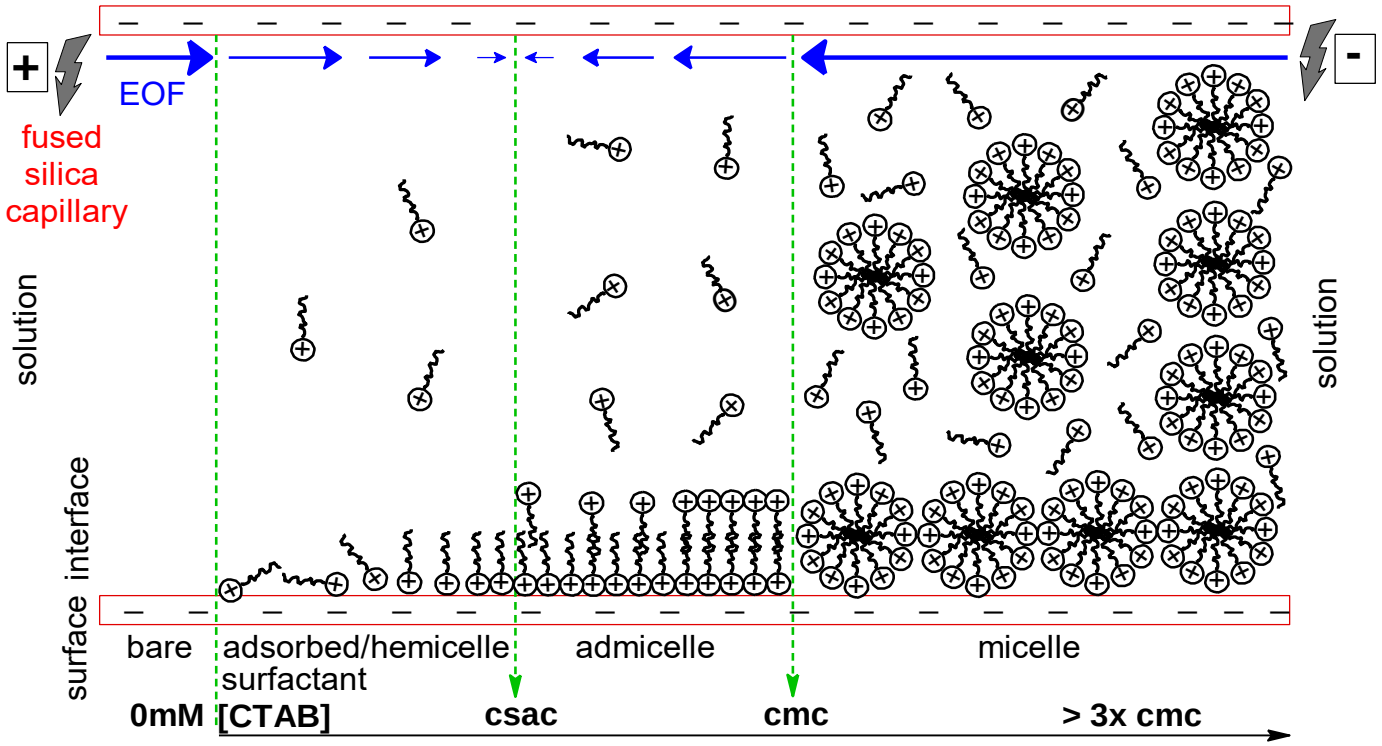

Figure 2.4 Schematic representation of the molecular organization of a long chain cationic surfactant on a fused-silica capillary surface. The resulting EOF from the applied electric field (voltage) is depicted according to the directionality of the EOF mobility (direction of arrows) and magnitude (arrow line length and thickness) due to surface charge effects brought about by changes in CTAB concentration in the background solution.

Further propagation of admicellar structures progresses very quickly to about more than twice the csac, but then slows down thereafter, which indicates the onset of saturation of the monolayer layer (hemimicelle) as fewer free surfactant monomers can infuse into the admicelle layer. A reduced rate of change in surface charge therefore results, leading to a diminishing decrease in μ_{EOF}. This trend leads to the transition point thereafter the μ_{EOF} becomes constant even as CTAB concentration is increased. This transition point can be ascribed as the cmc of the surfactant, which is the lowest concentration possible for a surfactant before micelles begin to form in the solution. Studies[57,58] have attributed this region as a micellisation region where adsorption is regarded as nearly constant due to the absence of increased activity of the surfactant even when concentration is increased. The adsorption appears to be constant but dynamic due to the adsorption-desorption process of surfactant monomers on the adsorbed layer at equilibrium with the micellisation process.

Admicelles are depicted to assume bilayer structure up to the cmc. As admicelles are fully formed when second layer sites have been saturated, the surface charge achieves its maximum possible magnitude and becomes constant, making the EOF move at a constant rate. Adsorbed aggregations of spherical micelles are then formed above the cmc[2,59,60] while free monomers self-assemble into solution micelles that build up in aggregation number when surfactant concentration is further increased (Figure 2.4). The establishment of a constant reversed electroosmotic flow as a feature to characterise the surfactant cmc, in this case that of CTAB, has already been demonstrated.[45,60]

For CTAB in the given buffer solutions, the cmc values are 0.20 mM and 0.50 mM respectively. The CTAB cmc in the literature in simple aqueous solution

of pH 7 is known to be 0.90 to 1.0 mM. Surfactant cmc values vary largely depending on the nature of the surfactant based on the hydrophobicity of the hydrocarbon chain (tail), net charge on the surfactant and the nature of the polar head and counterion,[61] background electrolyte composition with regards to pH,[62] ionic strength,[63] solution counterions,[64] additives,[65] including organic solvents, and temperature.[63,66] The lowering of the cmc of CTAB in buffered solutions demonstrates how addition of salts or electrolytes significantly decrease the cmc of surfactant due to the partial screening of electrostatic repulsion between charged headgroups of the surfactant. The decreased repulsion helps micelles to form at lower monomer concentrations. The differences in the cmc values of CTAB in different buffer solutions can generally be attributed to the effects of differences in ionic strength or concentration of added electrolyte.[66-69] Increase in ionic strength is directly related to further decrease in surfactant cmc.[67,70] The nature of the cations and anions of the added electrolyte can also exert an influence on the extent of lowering the cmc.[66,69]

Finally, above the cmc to >3x cmc, the reversed μ_{EOF} was almost unchanged, suggesting the formation of spherical micelles[2,59,60] which were closely arranged at the interface. The arrangement of micelles prevented the further addition of surfactant monomers into the micelle structure. The larger surface area formed from the surface of spherical micelles (convex shaped) in contact with the solution also provided a higher interfacial charge and stronger EOF. This was compared to the flat bilayer existing just below the cmc.

Some dispute exists on the validity of the use of electroosmotic mobility in the determination of cmc of surfactants.[43] As observed, the transition from pre-micellar to micellar conditions is not marked by a sharp change in the mobility

curve and the establishment of constant reversed μ_{EOF} is sometimes limited by the measurement errors. This makes it difficult to define the precise onset of micelle formation to mark the cmc. This could reflect the fact that cmc is acknowledged to be not a sharp transition point but more of a concentration range wherein negligible number of micelles may have formed below this range while they become predominant in number above the range.[67]

2.4.2 cmc and csac for sodium dodecyl sulfate (SDS)

Sodium dodecyl sulfate has been an extensively studied surfactant for its properties, aggregation behaviour and applications. Micellisation of SDS has been investigated using electrokinetic studies in particular to characterise its cmc.[41,42,62,72-74] The mobility method, introduced by Jacquier and Desbene,[41] involves micellar solubilisation of a neutral marker analyte and the electrophoretic mobility of the marker is monitored as a function of surfactant concentration.[47,75] Markers like naphthalene,[41] 2-naphthalenemethanol[42] or use of other test solutes[73] have been employed for the determination of cmc of SDS.

The use of electrokinetic techniques for cmc determination is also useful for characterisation of surfactant adsorption, as was demonstrated already for CTAB. With SDS as an anionic surfactant, the adsorption profile needed to be measured using a positively charged surface. For the electroosmotic mobility method to be realised successfully on fused-silica capillaries, the silica surface rendered negatively charged from NaOH conditioning had to be suitably coated with a cationic polyelectrolyte to provide a positively charged surface, thus the use of PDADMAC. This polyelectrolyte is considered to provide a stable coating with a stable charge.

Figure 2.5 shows the EOF mobilities as a function of SDS concentration. To provide the oppositely-charged surface (positive) for the adsorption of anionic SDS, the capillary had to be coated with the cationic polyelectrolyte PDADMAC. As a polyelectrolyte, PDADMAC provides a stable and reproducible oppositely-charged thin surface layer and has been used as a cationic coating for CE,[74] in polyelectrolyte multilayers as coatings for OT-CEC,[77,78] as a cationic layer on which other substrates can adsorb[79,80] or as ionic linkers.[81] The positively charged surface therefore produced negative μ_{EOF} of anodic directionality where the magnitude decreased when the SDS concentration was increased. The decrease in the negativity of μ_{EOF} reveals again the build-up of SDS hemicelle aggregation on the surface. The negatively charged ionic head groups of SDS are electrostatically attracted to the positive surface while the hydrophobic chain tails protrude, facing the solution. The surface slowly gets populated with adsorbing SDS monomers, forming hemimicelle aggregates, which therefore shield the positive surface and slow down the anodic EOF.

From 0 mM surfactant up to the csac (0.16 mM in Figure 2.5), the μ_{EOF} magnitude decreased, suggesting the adsorption of SDS monomers that neutralised the surface charge. Similar to cationic surfactant adsorption, the surface becomes saturated with hemimicelles as the surface charge is progressively neutralised, and μ_{EOF} approaches a zero value. Complete surface coverage by hemimicelles near the csac must have resulted in a neutral interface but was not observed.

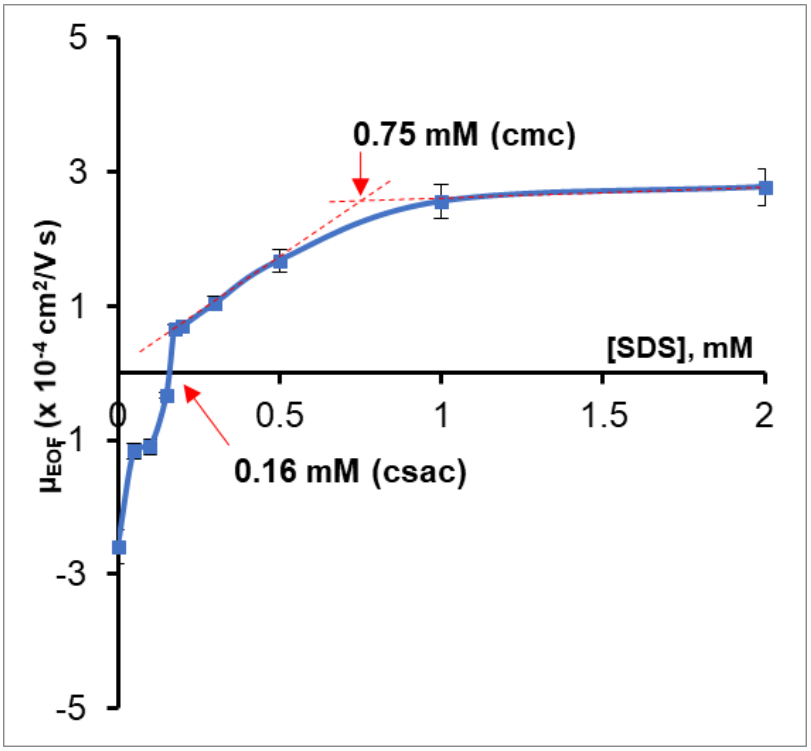

Figure 2.5. EOF mobilities (μ_{EOF}) obtained from varying SDS concentrations in background electrolyte of 100 mM ammonium bicarbonate in pH 8.5. Conditions as described in the methodology. EOF was detected using acetone (2%) as marker.

At surfactant concentrations above the csac, the μ_{EOF} direction was reversed (from anodic -μ_{EOF} to cathodic +μ_{EOF}), showing again the formation of a bilayer (admicelle) at the interface with the charged head group of the surfactants pointing at the solution. This was consistent with EOF reversal in aqueous solutions of CTAB at a fraction below the cmc[40]. Further SDS addition shifts the aggregation pattern to form bilayers as conditions allow favoured hydrophobic interactions of the hydrocarbon chain tails. For surfactant concentrations from the csac to the cmc (~0.75 mM in Figure 2.5), the reversed (cathodic) μ_{EOF} magnitude increased, implying an increase in interfacial charge and internal density due to the insertion of surfactant monomers into the bilayer. In this case, however, there was no established sharp transition to a constant μ_{EOF} to mark the cmc of SDS but rather a smooth curve of decreasing increments of μ_{EOF} before achieving a plateau. The cmc is estimated from the intersection of the slopes of the ascending and the horizontal curves (Figure 2.5). The low observed cmc value of 0.75 mM (compared to literature of ~ 8.1–8.4 mM[46,71] at 25°C in plain aqueous solution, pH 7, 3.50 mM in phosphate buffer, pH 7[42], or even at 7–10 mM range) is also a result of ionic strength effects or the effect of added electrolyte (buffer). Capillary electrophoresis (MEKC) measurements of cmc of SDS at 20 mM phosphate solutions using different neutral probes gave cmc values from 2.87 – 3.10 mM.[37] However, since these measurements related the micellisation of the probes to retention, retention may not be readily determinable as this might not occur even in the presence of micelles in solution. Further validation of the cmc value for SDS in the given experimental conditions may be needed to confirm whether the constant reversed EOF coincides well with the onset of cmc as observed in cationic surfactants. A simple method devised to confirm cmc values based on OT-MLC retention may

also be employed where cmc values coincided with the surfactant concentration yielding the highest retention of model neutral analytes, thereby showing consistency with EOF measurements (see Chapter 3 and 4).

2.5 Conclusion

The csac and cmc values for CTAB and SDS in their respective BGS conditions were determined using electrophoretic techniques whereby the EOF mobility is related to the surfactant concentration. The μ_{EOF} variation as a function of surfactant concentration was rationalised by the molecular aggregation of surfactants on the solid-solution interface. The csac values for CTAB (0.04 and 0.09 mM in sodium borate and ammonium bicarbonate BGS respectively) and for SDS (0.16 mM in ammonium bicarbonate) indicate the onset of admicelle aggregation reflected in the reversal of surface charge. The cmc of CTAB (0.20 and 0.50 mM in sodium borate and ammonium bicarbonate BGS, respectively) and of SDS (0.75 mM in ammonium bicarbonate) also indicate saturation of the admicelle layer and the onset of the formation of interfacial and solution micelles. The csac and cmc values also reflect the effects of ionic strength and added electrolyte when compared to unbuffered solutions. The main significance of the determination of csac and cmc is to define the concentration range of admicelle aggregation and interfacial and solution micelle formation. Determination of when these admicelles and micelles form enables us to employ them as soft stationary pseudophases for chromatographic separation. Their separation abilities will therefore be investigated and rationalised in the succeeding chapters. The buffer conditions to be employed will be based on the same csac and cmc ranges determined here.

2.6 References

(1) Moradi, M.; Yamini, Y. *J Sep Sci* **2012**, *35*, 2319-2340.

(2) Manne, S.; Gaub, H. E. *Science* **1995**, *270*, 1480-1482.

(3) Zhang, R.; Somasundaran, P. *Adv Colloid Interface Sci* **2006**, *123-126*, 213-229.

(4) Yeskie, M. A.; Harwell, J. H. *J. Phys. Chem.* **1988**, *92*, 2346-2352.

(5) Paria, S.; Khilar, K. C. *Adv Colloid Interface Sci* **2004**, *110*, 75-95.

(6) Gao, Y. Y.; Du, J. H.; Gu, T. R. *J Chem Soc Faraday Trans I* **1987**, *83*, 2671-2679.

(7) Fan, A. X.; Somasundaran, P.; Turro, N. J. *Langmuir* **1997**, *13*, 506-510.

(8) Somasundaran, P.; Fuerstenau, D. W. *J Phys Chem* **1966**, *70*, 90-96.

(9) Harwell, J. H.; Hoskins, J. C.; Schechter, R. S.; Wade, W. H. *Langmuir* **1985**, *1*, 251-262.

(10) Fujii, M. In *Structure-Performance Relationships in Surfactants*; CRC Press, 2003.

(11) Hu, K.; Bard, A. J. *Langmuir* **1997**, *13*, 5418-5425.

(12) Fleming, B. D.; Biggs, S.; Wanless, E. J. *J Phys Chem B* **2001**, *105*, 9537-9540.

(13) Chandar, P.; Somasundaran, P.; Turro, N. J. *J Colloid Interface Sci* **1987**, *117*, 31-46.

(14) Sivakumar, A.; Somasundaran, P. *Langmuir* **1994**, *10*, 131-134.

(15) Ström, C.; Hansson, P.; Jönsson, B.; Söderman, O. *Langmuir* **2000**, *16*, 2469-2474.

(16) Benrraou, M.; Bales, B. L.; Zana, R. *J Phys Chem B* **2003**, *107*, 13432-13440.

(17) Rennie, A. R.; Lee, E. M.; Simister, E. A.; Thomas, R. K. *Langmuir* **1990**, *6*, 1031-1034.

(18) Fragneto, G.; Thomas, R. K.; Rennie, A. R.; Penfold, J. *Langmuir* **1996**, *12*, 6036-6043.

(19) McDermott, D. C.; Lu, J. R.; Lee, E. M.; Thomas, R. K.; Rennie, A. R. *Langmuir* **1992**, *8*, 1204-1210.

(20) Hines, J. D.; Fragneto, G.; Thomas, R. K.; Garrett, P. R.; Rennie, G. K.; Rennie, A. R. *J Colloid Interface Sci* **1997**, *189*, 259-267.

(21) Eskilsson, K.; Yaminsky, V. V. *Langmuir* **1998**, *14*, 2444-2450.

(22) Wängnerud, P.; Olofsson, G. *J Colloid Interface Sci* **1992**, *153*, 392-398.

(23) Pagac, E. S.; Prieve, D. C.; Tilton, R. D. *Langmuir* **1998**, *14*, 2333-2342.

(24) Velegol, S. B.; Fleming, B. D.; Biggs, S.; Wanless, E. J.; Tilton, R. D. *Langmuir* **2000**, *16*, 2548-2556.

(25) Atkin, R.; Craig, V. S. J.; Biggs, S. *Langmuir* **2000**, *16*, 9374-9380.

(26) Anderson, M. T.; Martin, J. E.; Odinek, J. G.; Newcomer, P. P. *Chem Mater* **1998**, *10*, 1490-1500.

(27) Bellmann, C.; Synytska, A.; Caspari, A.; Drechsler, A.; Grundke, K. *J Colloid Interface Sci* **2007**, *309*, 225-230.

(28) Patel, V.; Dharaiya, N.; Ray, D.; Aswal, V. K.; Bahadur, P. *Colloids Surf, A* **2014**, *455*, 67-75.

(29) Fuerstenau, D. W *J Colloid Interface Sci* **2002**, *256*, 79-90.

(30) Onaizi, S. A.; Nasser, M. S.; Al-Lagtah, N. M. A. *Colloid Polym Sci* **2015**, *293*, 2891-2899.

(31) Grant, L. M.; Ederth, T.; Tiberg, F. *Langmuir* **2000**, *16*, 2285-2291.

(32) Atkin, R.; Craig, V. S. J.; Wanless, E. J.; Biggs, S. *Adv. Colloid Interface Sci* **2003**, *103*, 219-304.

(33) Schulz, J. C.; Warr, G. G. *Langmuir* **2002**, *18*, 3191-3197.

(34) Ström, C.; Hansson, P.; Jönsson, B.; Söderman, O. *Langmuir* **2000**, *16*, 2469-2474.

(35) Eskilsson, K.; Yaminsky, V. V. *Langmuir* **1998**, *14*, 2444-2450.

(36) Dominguez, A.; Fernandez, A.; Gonzalez, N.; Iglesias, E.; Montenegro, L. *J Chem Educ* **1997**, *74*, 1227-1231.

(37) Fuguet, E.; Ràfols, C.; Rosés, M.; Bosch, E. *Anal Chim Acta* **2005**, *548*, 95-100.

(38) Chakraborty, T.; Chakraborty, I.; Ghosh, S. *Arab J Chem* **2011**, *4*, 265-270.

(39) Terabe, S.; Otsuka, K.; Ichikawa, K.; Tsuchiya, A.; Ando, T. *Anal Chem* **1984**, *56*, 111-113.

(40) Khaledi, M. G.; Smith, S. C.; Strasters, J. K. *Anal Chem* **1991**, *63*, 1820-1830.

(41) Jacquier, J. C.; Desbene, P. L. *J Chromatogr A* **1995**, *718*, 167-175.

(42) Nakamura, H.; Sano, A.; Matsuura, K. *Anal Sci* **1998**, *14*, 379-382.

(43) Lin, C. E.; Wang, T. Z.; Chiu, T. C.; Hsueh, C. C. *J High Res Chrom* **1999**, *22*, 265-270.

(44) Lin, C.-E.; Lin, K.-S. *J Chromatogr A* **2000**, *868*, 313-316.

(45) Lucy, C. A.; Underhill, R. S. *Anal Chem* **1996**, *68*, 300-305.

(46) Cifuentes, A.; Bernal, J. L.; DiezMasa, J. C. *Anal Chem* **1997**, *69*, 4271-4274.

(47) Lin, C.-E. *J Chromatogr A* **2004**, *1037*, 467-478.

(48) Chen, Z.; Lin, J.-M.; Uchiyama, K.; Hobo, T. *Anal Chim Acta* **2000**, *403*, 173-178.

(49) Chen, Z.; Yamada, K.; Niitsuma, M.; Uchiyama, K.; Hobo, T. *Chromatographia* **2001**, *54*, 629-633.

(50) Melanson, J. E.; Baryla, N. E.; Lucy, C. A. *TrAC, Trends Anal Chem* **2001**, *20*, 365-374.

(51) Znaleziona, J.; Petr, J.; Knob, R.; Maier, V.; Ševčík, J. *Chromatographia* **2008**, *67*, 5-12.

(52) Terabe, S.; Otsuka, K.; Ando, T. *Anal Chem* **1985**, *57*, 834-841.

(53) Tsuda, T. *J High Resolut Chromatogr Chromatogr Commun* **1987**, *10*, 622-624.

(54) Diress, A. G.; Lucy, C. A. *J Chromatogr A* **2004**, *1027*, 185-191.

(55) Baryla, N. E.; Lucy, C. A. *J Chromatogr A* **2002**, *956*, 271-277.

(56) Mora, M. F.; Felhofer, J.; Ayon, A.; Garcia, C. D. *Anal Lett* **2008**, *41*, 312-334.

(57) Somasundaran, P.; Middleton, R.; Viswanathan, K. V. *ACS Symposium Series* **1984**, *253*, 269-290.

(58) Bohmer, M. R.; Koopal, L. K. *Langmuir* **1992**, *8*, 2649-2659.

(59) Liu, J. F.; Ducker, W. A. *J Phys Chem B* **1999**, *103*, 8558-8567.

(60) Baryla, N. E.; Melanson, J. E.; McDermott, M. T.; Lucy, C. A. *Anal Chem* **2001**, *73*, 4558-4565.

(61) Huang, J. M.; DiStefano, J. *J Liq Chromatogr Relat Technol* **2011**, *34*, 1712-1728.

(62) Lin, J. M.; Nakagawa, M.; Uchiyama, K.; Hobo, T. *Chromatographia* **1999**, *50*, 739-744.

(63) Myers, D. In *Surfactant Science and Technology*; John Wiley, 2005, pp 107-159.

(64) Palladino, P.; Ragone, R. *Langmuir* **2011**, *27*, 14065-14070.

(65) Naskar, B.; Dey, A.; Moulik, S. P. *J Surfactants Deterg* **2013**, *16*, 785-794.

(66) Wan, L. S.; Poon, P. K. *J Pharm Sci* **1969**, *58*, 1562-1567.

(67) Baloch, M. K.; Hameed, G.; Bano, A. *J Chem Soc Pak* **2002**, *24*, 77-86.

(68) Corrin, M. L.; Harkins, W. D. *J Am Chem Soc* **1947**, *69*, 683-688.

(69) Rosen, M. J. *Surfactants and Interfacial Phenomena*, 3rd ed.; John Wiley and Sons: New Jersey, 2004.

(70) Palladino, P.; Ragone, R. *Langmuir* **2011**, *27*, 14065-14070.

(71) Mukerjee, P.; Mysels, K. J. *Critical micelle concentrations of aqueous surfactant systems*; U.S. National Bureau of Standards, U.S. Gov. Print. Office: Washington, D.C., 1971; Vol. 36.

(72) Rahman, A.; Brown, C. W. *J Appl Polym Sci* **1983**, *28*, 1331-1334.

(73) Lin, C.-E.; Chen, M.-J.; Huang, H.-C.; Chen, H.-W. *J Chromatogr A* **2001**, *924*, 83-91.

(74) Liu, H.; Gao, Y.; Hu, Z. *J Anal Chem* **2007**, *62*, 176-178.

(75) Saux, T. L.; Varenne, A.; Gareil, P. In *Electrokinetic Chromatography*, 2006, pp 33-54.

(76) Liu, Q. C.; Lin, F. M.; Hartwick, R. A. *J Chromatogr Sci* **1997**, *35*, 126-130.

(77) Pelcova, P.; Kuban, V.; Kiplagat, I. K.; Kuban, P. *J Chromatogr A* **2009**, *1216*, 9022-9026.

(78) Graul, T. W.; Schlenoff, J. B. *Anal Chem* **1999**, *71*, 4007-4013.

(79) Qu, Q.; Gu, C.; Gu, Z.; Shen, Y.; Wang, C.; Hu, X. *J Chromatogr A* **2013**, *1282*, 95-101.

(80) Qu, Q.; Liu, D.; Mangelings, D.; Yang, C.; Hu, X. *J Chromatogr A* **2010**, *1217*, 6588-6594.

(81) Lee, G. S.; Lee, Y. J.; Yoon, K. B. *J Am Chem Soc* **2001**, *123*, 9769-9779.

Chapter 3

Open-tubular admicellar liquid chromatography and electrochromatography

3.1 Abstract

Chromatographic separations of neutral and charged analytes in open-tubular fused-silica capillaries using soft stationary pseudophases or admicelles are introduced. The pseudophases are formed in-situ from buffered aqueous mobile phases with hexadecyltrimethylammonium bromide (CTAB) at concentrations between the critical surface aggregation concentration (csac) and critical micelle concentration (cmc), which were determined by electroosmotic mobility measurements. Pressure- and voltage-driven separation or open-tubular admicellar liquid chromatography (OT-AMLC) and electrochromatography (OT-AMEC) showed similar retention of neutral analytes, implying that the admicelles were indeed stationary even in the presence of an electric field in OT-AMEC. This is in contrast with electrokinetic chromatography with an electrophoretically moving pseudophase. In OT-AMLC, increased retention of neutral solutes was observed with an increase in surfactant concentration and at lower percentages of methanol in the mobile phase, suggesting a reversed-phase type separation with the CTAB pseudophase. The retention was also stronger with smaller i.d. capillaries, as expected in open-tubular chromatography. The formation of the pseudophase was affected by the salt content and pH of the separation medium, which in turn affected the csac and the charge of the capillary wall surface, respectively. With neutral pesticides and sulfonamides as test analytes, the analytical figures of merit were

found to be acceptable. Sample matrix effects on the separations were not significant from environmental water samples that were subjected to appropriate sample preparation procedures. The use of pseudophases at the solid-surface and liquid interface could be a viable solution to problems associated with the use of solid stationary or support materials in nano- and micro-liquid chromatography.

*All of the research contained in this chapter will be submitted for journal publication as Tarongoy, F. M., Jr.; Haddad, P. R.; Quirino, J. P., Open-tubular admicellar liquid chromatography and electrochromatography.

3.2 Introduction

The interest in open-tubular liquid chromatography (OT-LC) can be attributed to its obvious practical advantages over conventional LC (with packed columns), such as low column back-pressure and small sample size and mobile phase requirements. OT-LC is employed in narrow inner diameter (id) capillaries (preferably ≤10 □m id) with an ample layer of solid stationary phase embedded at the walls.[1-3] Over the last three years, research efforts have been directed primarily towards the development of stationary phase materials and procedures to attach these phases onto the OT-LC columns.[4-20] Similarly, the advantages of OT-CEC harnessing the strengths of capillary liquid chromatography and CE continue to stimulate interest in developing new materials for column stationary phases.[2,21,22] Stationary phases are typically prepared as a thick coating or porous layer. Novel phases based on metal-organic frameworks (MOFs) and covalent organic frameworks, nanoparticles, polymers, cyclodextrin, elongated pillars, silica monoliths and even biological ones (e.g. rabbit red blood cells) has been reported. These phases were attached to the capillary walls by chemically bonding, layer-by-layer assembly, polymerization, microfabrication, and physical adsorption.

Demonstrated here is the chromatographic retention of neutral and (anionic) charged solutes in OT-LC and OT-CEC with fused-silica capillaries and CTAB at concentrations <cmc and >csac in the separation medium. At >csac, the admicelles or bilayer that formed at the capillary wall and liquid interface acted as the stationary pseudophase.

The significance of employing admicelles as soft stationary pseudophases for OT-LC and OT-CEC comes from the structural attributes of their hydrophobic

core and hydrophilic exterior that can interact with a wide variety of substances by adsolubilisation. This process involves these aggregates incorporating hydrophobic substances or other chemical species that interact poorly with the aqueous environment and are partitioned in the interior of the admicelle. However, the adsolubilisation of various compounds has only been exploited for solid-phase extraction (SPE) using admicelles as extraction/preconcentration sorbents for organic analytes[23] such as polyaromatic hydrocarbons,[24] chlorophenols,[25] estrogens,[26] pesticide multiresidues,[27] and phthalate esters,[28] obtained mostly from environmental samples. An admicellar-based batch separation chromatography and concentration technique (termed "admicellar chromatography") has been developed for the separation of isomeric heptanols[29] where organic solutes are adsolubilised in admicelles and the surfactant recovered and solute concentrated by pH change (Figure 3.1). So far, the potential of surfactant admicelle aggregates as stationary pseudophases for standard flow- or electrodriven open-tubular capillary column chromatography has not been realised or investigated.

Pressure- and voltage-driven separations, appropriately named OT-admicellar LC (OT-AMLC) and OT-admicellar electrochromatography (OT-AMEC), respectively, are hereby proposed based on the retention of neutral solutes. Here, there are no micelles in the separation media, in contrast to micellar liquid chromatography (MLC). Fundamental studies on the pseudophase were performed with OT-AMLC using different inner diameter (i.d.) capillaries and mobile phase conditions, including CTAB concentration, pH, salt and methanol content. Analytical figures of merit and real sample matrix effects (environmental water samples) were conducted by studies on neutral pesticides and sulfonamides (as anions).

In this chapter, the conditions defined in the formation of admicelles, namely background electrolytes, ionic strength, and pH, have been reproduced based on the previous work and the surfactant concentration was chosen within the csac and cmc range as previously determined (see Chapter 2): namely 0.04 – 0.20 mM CTAB in 50 mM sodium tetraborate at pH 9.5 and 0.10 – 0.50 mM CTAB in 100 mM ammonium bicarbonate at pH 8.5. The scope of the current investigation focuses only on CTAB as the surfactant of interest for fundamental studies necessary to demonstrate the technique.

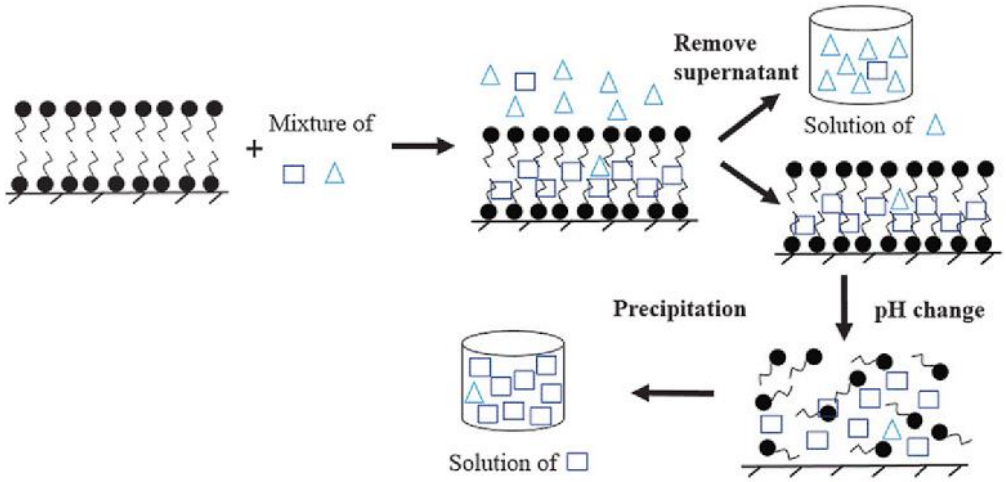

Figure 3.1. Schematic of an admicellar-based batch separation chromatography. Reproduced from ref. 30.

3.3 Materials and Methods

3.3.1 Reagents and general equipment

Chemicals (test analytes, buffer compounds, surfactants, polyelectrolyte, salts, and organic solvents) were obtained from Fluka Analytical (St. Louis, MO, USA) or Sigma-Aldrich (New South Wales, Australia). Hexadecyltrimethyl-ammonium bromide (or cetyltrimethylammonium bromide, CTAB) was obtained from bioWORLD (Dublin, OH, USA). Purified water was from a Milli-Q system (Millipore, MA, USA). The pH and conductivity of solutions were measured using a bench top meter (Sper Scientific, Australia). Stock solutions of buffers (0.2 M ammonium bicarbonate, pH 8.5; 0.2 M sodium borate, pH 9.5; and phosphate buffers pH 2 – 10), 0.2 M CTAB stock solution and 3.5 M sodium chloride (NaCl) were sonicated and filtered using a 0.45 μm filter prior to use. Mobile phases were prepared by mixing appropriate volumes of buffer, CTAB solution stock, and methanol (MeOH) with purified water. 10% poly(diallyldimethylammonium chloride (PDADMAC) with average molecular weight of 400-500k was prepared in purified water. Stock solutions of 0.5 – 1 mg/mL analytes (alkyl phenyl ketones or alkylphenones, sulfonamides, and pesticides) were prepared in water or 50% MeOH and were stored at 4ºC when not in use. Sample solutions were prepared by mixing appropriate amounts of analyte stock solutions with the mobile phase or as indicated in the text.

3.3.2 Separation instrumentation

OT-LC and capillary electrophoresis (CE) were conducted using a Beckman P/ACE MDQ system (Beckman-Coulter, Brea, CA USA) and 375 μm o.d. fused-silica capillaries (Polymicro, Phoenix, AZ, USA). The total capillary

length was 60 cm (50 cm to UV detector at 200 nm). The temperature of the capillary was controlled at 20°C. The samples prepared in the separation electrolyte were injected at 25 mbar for 10s (~1 mm plug). At least three determinations were made for each experimental condition.

3.3.3 OT-LC procedures

The capillary inner diameter (i.d.) used was 50 µm except as indicated in text. Sample injection and separation were accomplished by applying pressure with the sample and mobile phase at the inlet end of the column. New capillaries were conditioned by flushing (e.g., at 1500 mbar) with 0.1 M NaOH (10 capillary volumes) followed by purified water (5 capillary volumes). The pressure used for conditioning, injection and separation was dependent on the capillary i.d., with higher pressures being used for narrower i.d. capillaries. The capillary was conditioned with purified water (2 capillary volumes), 0.1 M NaOH (3 capillary volumes), purified water (2 capillary volumes) and then the mobile phase (4 capillary volumes) before each sample injection. Void time (t_0) was determined based on the retention time of the unretained solute, methyl phenyl ketone, as marker.

3.3.4 CE procedures

The initial steps for the CE separations were the same as in the OT-LC procedures. The separations were achieved by applying voltage with the mobile phase or background solution (BGS) at both ends of the capillary until all peaks were observed. For Figure 3.5(c), the capillary was treated with PDADMAC as described in Chapter 2. The EOF time (t_{EOF}) was based on the retention time of the unretained marker, methyl phenyl ketone.

3.4 Results and Discussion

3.4.1 Pressure and voltage driven separations of neutral analytes using [CTAB] ≥ csac

Pressure- and voltage-driven separations of neutral alkyl phenyl ketones were conducted using CTAB from 0 mM to 3x cmc in 50 mM sodium tetraborate pH 9.5. The relative retention time (RRT) of the most hydrophobic analyte (pentyl phenyl ketone) *versus* CTAB concentration is presented in Figure 3.2. In the pressure-driven separations (P, blue), RRT was calculated by dividing the retention time (t_R) of pentyl phenyl ketone by the void time (t_0). In the voltage-driven separations (V, red), RRT was obtained by dividing t_R by the detection time of the EOF (t_{EOF}).

Surfactant concentrations in the csac-cmc region: At 0.04 – 0.2 mM CTAB, corresponding to surfactant concentrations falling between the csac and the cmc (labelled here as csac-cmc), the RRT increased with increasing CTAB concentration (see Figure 3.2). Values of RRT > 1 suggested the chromatographic retention due to the bilayer. It can be noted that there was no retention (RRT = 1) observed with 0 mM CTAB, as expected. The observed increase in retention for csac-cmc can be explained by the phase ratio ((β).[31] Here, this is the ratio of the volume of the mobile phase or electrolyte (V_C) to that of the admicellar pseudophase (V_{AM}), see equation (3.1). In open-tubular chromatography, V_C is the geometric internal volume of the capillary.

$$\beta = {}^{V_C}/_{V_{AM}} \tag{3.1}$$

At above the csac, the V_{am} increases with an increase in the concentration of surfactant, where the excess surfactant monomers in solution are organised or

inserted into the bilayer structure (see Figure 2.4, schematic, csac to cmc). This results in a decrease in β and an increase in the retention.

Interestingly, similar RRT values for the two separation modes were observed. This suggested that the admicellar pseudophase did not move in the presence of an electric field. Therefore, the pressure and voltage separation are termed as OT-AMLC and OT-AMEC, respectively. OT-AMEC is electrochromatography and not electrokinetic chromatography, with the latter term being typically associated with an electrophoretically moving pseudophase.[32] A representative chromatogram and electrochromatogram for OT-AMLC and OT-AMEC, respectively, is shown in Figure 3.3. The $t_0 = t_{EOF}$, and thus the t_R for each alkyl phenyl ketone in OT-AMLC and OT-AMEC are almost identical.

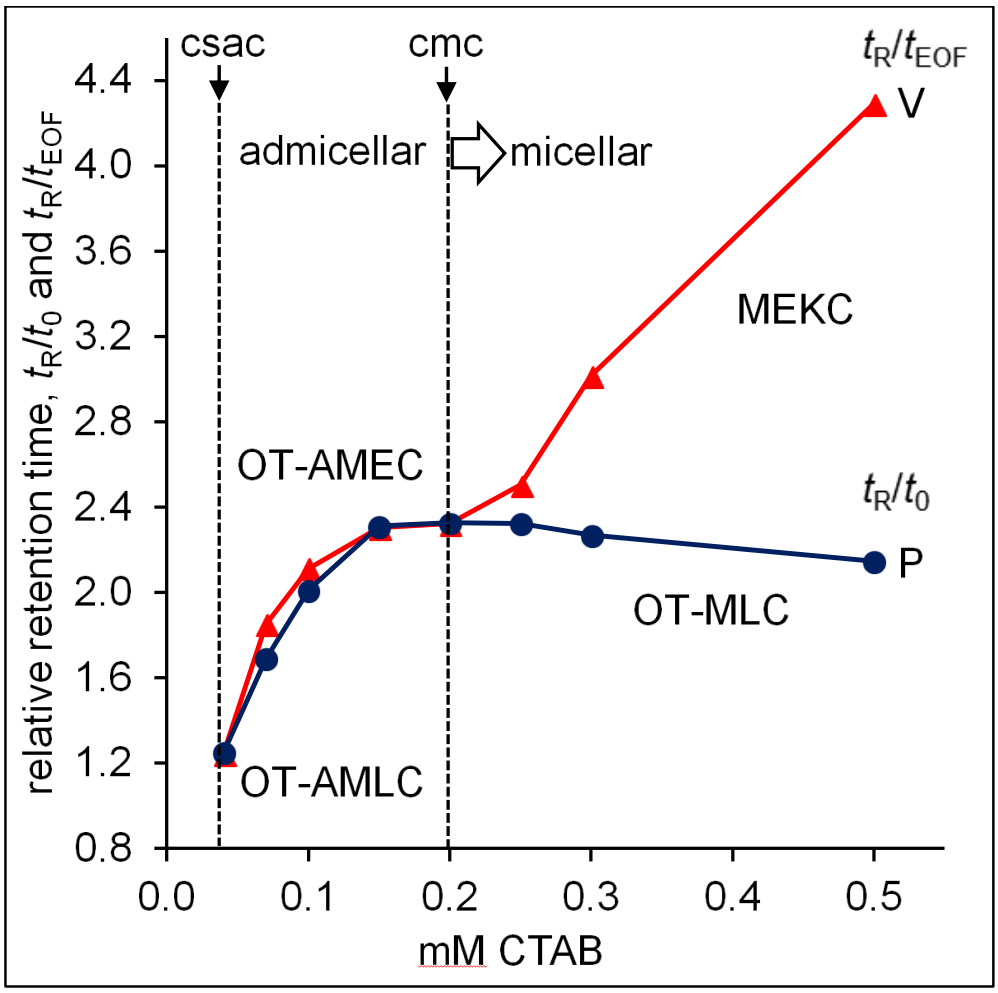

Figure 3.2 CTAB concentration (mM) versus RRT (t_R/t_0 and t_R/t_{EOF} for pressure (P) and voltage (V) driven separation, respectively). Mobile phase/BGS was 0.04 – 0.5 mM CTAB in 50 mM sodium tetraborate pH 9.5. Sample containing the probe (pentyl phenyl ketone) in the mobile phase/BGS was injected at 25 mbar for 10s. Separation pressure (P) was 150 mbar with the mobile phase at the inlet end of the capillary (blue plot, circles). Voltage (V) was 25 kV at negative (≥csac) or positive (0 mM CTAB) polarity with the BGS at both ends of the capillary (red plot, triangles). %RSD (n =3) was for each determination was <1.5% and <4.7% for P and V, respectively. More explanation in the text.

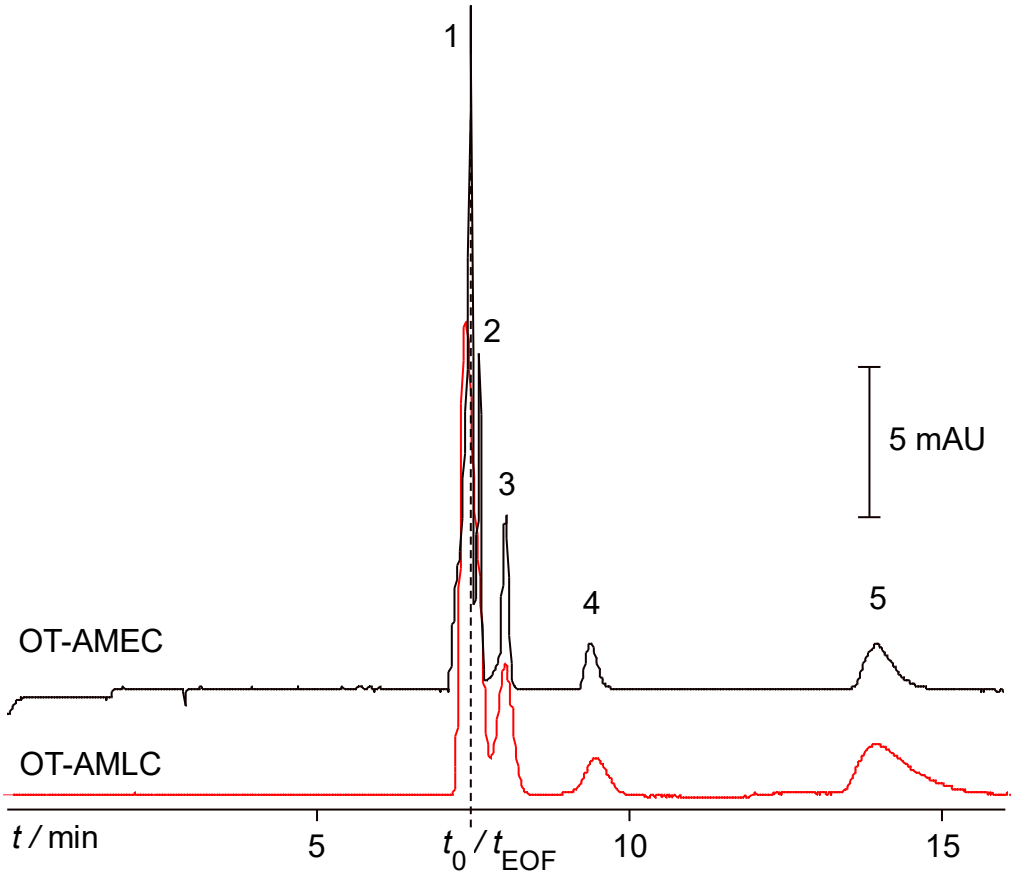

Figure 3.3 Representative OT-AMLC chromatogram and OT-AMEC electrochromatogram of alkyl phenyl ketones, where the t_0 was adjusted such that $t_0 = t_{EOF}$. Mobile phase (OT-AMLC) /BGS (OT-AMEC) was 0.1 mM CTAB in 50 mM sodium tetraborate pH 9.5. csac of CTAB in the buffer was ~0.04 mM. Sample in the mobile phase/BGS (10 – 50 µg/mL of each analyte) was injected. Separation pressure in OT-AMLC was 97 mbar with the mobile phase at the inlet end of the capillary. Separation voltage in OT-AMEC was 19 kV at negative polarity with the BGS at both ends of the capillary. Peak identity: methyl (1, t_0 marker), ethyl (2), propyl (3), butyl (4), and pentyl (5) phenyl ketone. More information and explanation in the main text.

The similar retentions were further verified using a different buffer (100 mM ammonium bicarbonate at pH 8.5) and a set of neutral analytes (pesticides). The results are shown in Figure 3.4, depicting again the similar t_R of analytes in OT-AMLC and OT-AMEC. The $t_{EOF} = t_0$ was achieved by adjusting the pressure separation in OT-AMLC. The peaks for the less retained analytes (peaks 1 and 2) were clearly sharper and for the more retained analytes (peaks 3-5) were slightly sharper in OT-AMEC (see also Figure 3.3). This is because of the well-known flat flow profile of the EOF in electrodriven separations.

Surfactant concentrations >cmc: At >0.2 mM CTAB or >cmc in the pressure-driven mode, the RRT decreased with increasing CTAB concentration and will be elucidated in the succeeding chapter as OT-MLC (see Figure 3.2). In the voltage-driven mode or MEKC, the RRT increased due to the CTAB micelles that migrated electrophoretically (to the cathode) and in the opposite direction of the EOF (to the anode or detector). The RRT further decreased and increased in OT-MLC and MEKC, respectively, at 0.6 mM CTAB (data not shown).

The decrease in RRT in OT-MLC can be explained by the micellar phase ratio (β_{mc}), see equation (3.2), as further discussed in the next chapter, where V_{sm} and V_{im} are the volume of the solution micelles and interfacial micelles, respectively.

$$\beta_{mc} = {}^{V_{sm}}/_{V_{im}} \tag{3.2}$$

The increase in the concentration of CTAB after the cmc leads to an increase in β_{mc} and a decrease in the retention due to an increase in the eluting power of the mobile phase that contained the solution micelles. On the other hand, the increase in RRT with an increase in the concentration of surfactant above the cmc in MEKC has

been explained by the phase ratio (β_{MEKC}), see equation (3.3), where V_{aq} is the volume of the remaining aqueous phase.[33]

$$\beta_{MEKC} = {}^{V_{sm}}\!/_{V_{aq}} \tag{3.3}$$

V_{aq} is also equivalent to V_C in equation (1). However, Equation (3.3) does not account for the effect of the interfacial micelles, since this equation was initially developed for sodium dodecyl sulfate (SDS). Anionic SDS will not molecularly organize to form such micelles at the negatively charged fused-silica capillary wall. The effect of interfacial micelles on MEKC retention could be an interesting future study.

Representative OT-MLC and MEKC separations of the pesticides are shown in Figure 3.4 where the $t_0 \sim t_{EOF}$. Retention times are longer in MEKC due to the solution micelles that are electrophoretically moving to the inlet. The solution micelles in OT-MLC, on the one hand promote the elution in the pressure-driven system, resulting in lower retention times for the analytes compared to MEKC, and under the experimental conditions used in Figure 3.4 also to OT-AMLC and OT-AMEC.

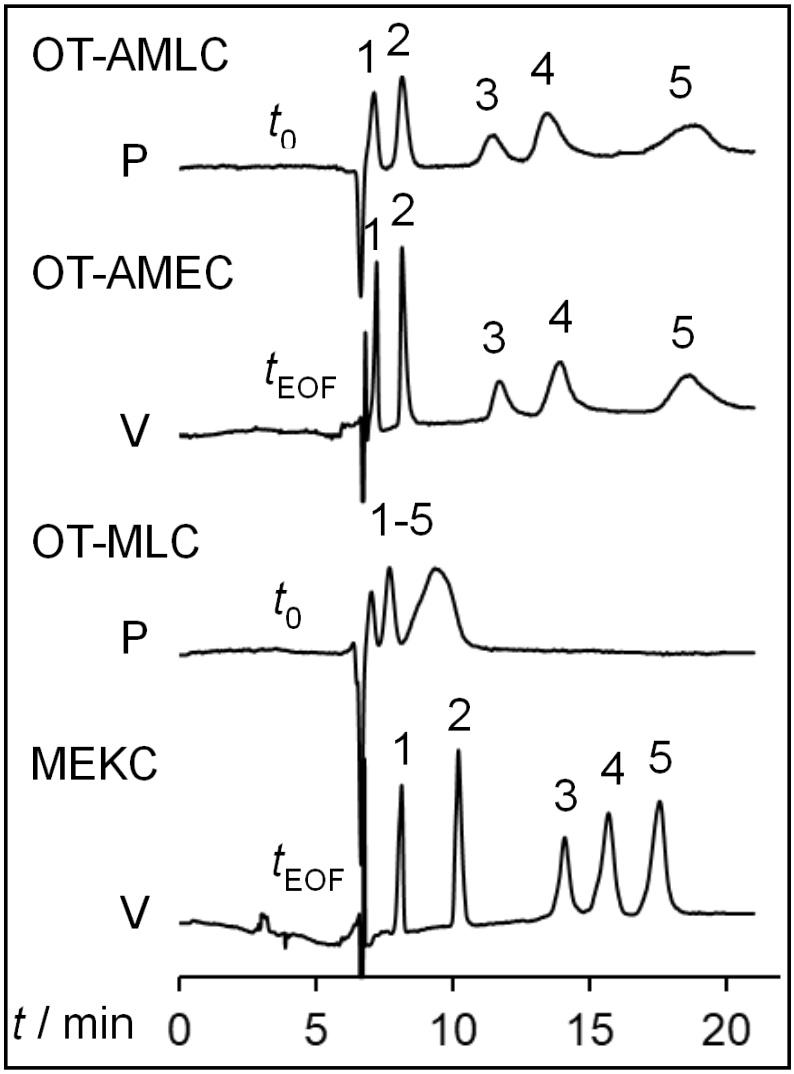

Figure 3.4 Representative chromatograms/electrochromatograms obtained from pressure/P (OT-AMLC and OT-MLC) or voltage/V (OT-AMEC and MEKC) driven separations of neutral analytes. The sample of pesticides atrazine (1), diuron (2), diazinon (3), fenitrothion (4), and parathion (5) were prepared in the mobile phase/BGS at 1.5 – 4 mM. Sample injection was the same as in Figure 3.2. For OT-AMLC and OT-AMEC, the mobile phase/BGS was 0.15 mM CTAB and 5% MeOH in 100 mM ammonium bicarbonate pH 8.5. Separation pressure was 117 mbar. For OT-MLC and MEKC, the mobile phase/BGS was 1.5 mM CTAB and 5% MeOH in 100 mM ammonium bicarbonate pH 8.5. Voltage was 21 and 19 kV at negative polarity for OT-AMEC and MEKC, respectively. More explanation in the text.

3.4.2 Pressure-driven OT-LC with surfactants –in different i.d. capillaries and a new method for determination of cmc

In Figure 3.2, the concentration of CTAB that gave the highest value for t_R/t_0 is consistent with the CTAB cmc of 0.2 mM from EOF measurements (see Figure 2.3 (A)). The strong retention in the vicinity of the cmc can be explained by the denser spherical interfacial micelles formed and the faster rate of micellisation-demicellisation that improved the mass transport of the analytes to the interfacial micelles. Similar pressure-driven experiments to those in Figure 3.2 were conducted using different i.d. (i.e., 50, 100, and 200 µm) capillaries and 0.1, 0.2, 0.3, and 0.4 mM CTAB (>csac and/or >cmc) in the mobile phase. The results are shown in Figure 3.5.

The highest retention for the probe analyte in all capillary i.d.s was consistently at 0.2 mM CTAB, or the approximated cmc. As expected in open-tubular chromatography, the retention decreased with an increase in capillary i.d. (e.g., very low but still observable retention in the wide 200 µm i.d. capillary). The retention due to nanosized admicelles and micelles at the interface is very surprising and may be probed by powerful microscopic techniques. Nevertheless, OT-LC could prove to be a potentially simple tool to estimate the cmc of surfactants.

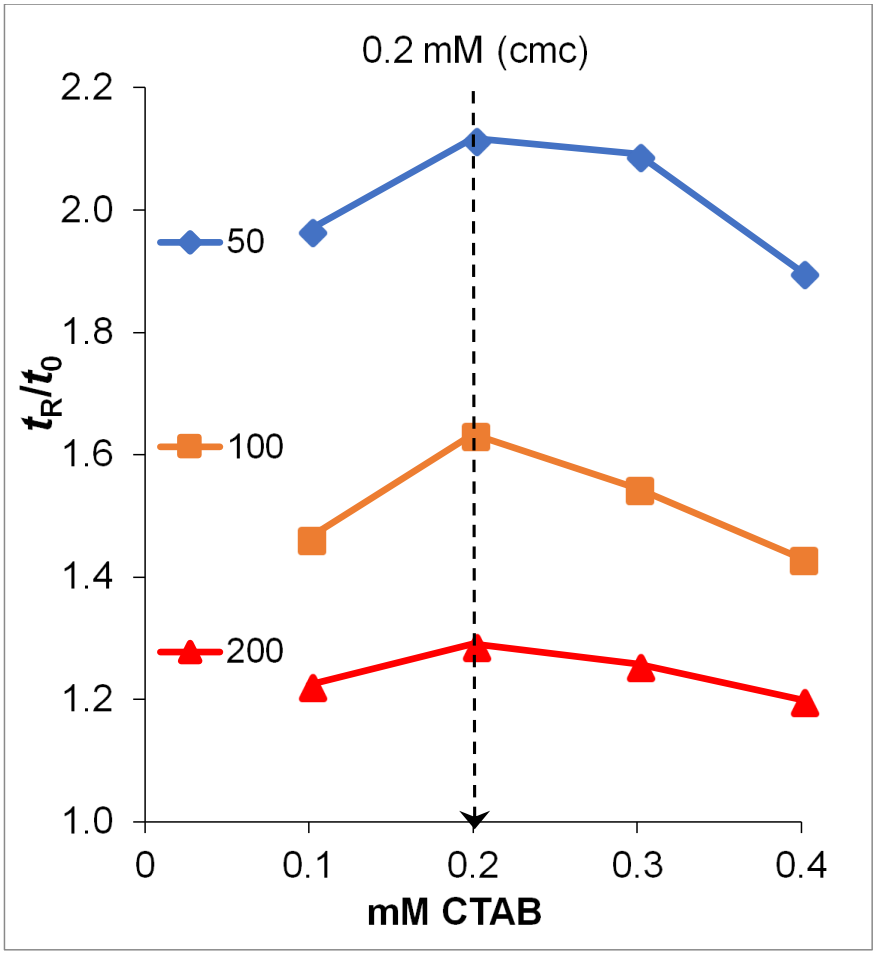

Figure 3.5 CTAB concentration (mM) versus relative retention time (t_R/t_0) in OT admicellar (below cmc) and micellar (above) LC. Mobile phase was 0.1 – 0.5 mM CTAB in 50 mM sodium tetraborate pH 9.5. Sample containing the probe (pentyl phenyl ketone) in the mobile phase was injected to make a ~1 mm plug. Capillary i.d.s were 50, 100, and 200 µm. Separation pressure was 145, 35, and 7 mbar, respectively with the mobile phase at the inlet end of the capillary. More explanation in the text.

3.4.3 Mobile phase parameters

Effects of mobile phase parameters, including salt (*i.e.*, NaCl) concentration, buffer pH, and MeOH content, were studied in OT-AMLC with 0.07 mM CTAB and the results are shown in Figure 3.6(b), (c), and (d), respectively. The RRT values for neutral analytes (*i.e.*, propyl, butyl, and pentyl phenyl ketone of increasing hydrophobicity and retention) were plotted *versus* each parameter. A more detailed study on the effect of CTAB (more concentrations between the csac and cmc) is also shown in Figure 3.6(a), verifying the increase in analyte retention with an increase in concentration of CTAB up to the cmc (0.2 mM) in the mobile phase. The above parameters were difficult to study by OT-AMEC (voltage-driven), due to excessively long analysis times caused by changes in the EOF with pH and high running currents resulting from the addition of salt to the separation solution.

The RRTs increased gradually as the concentration of salt in the mobile phase was increased (see Figure 3.6(b)). The increase in the ability of the admicelles to retain the analytes is explained by the inclusion of more surfactant monomers into the aggregates or a decrease in the csac forming more CTAB admicelles at the interface. This is similar to the well-known decrease in the cmc of surfactants (e.g., CTAB) with the addition of salts into the solution.[34] Measurements with >300 mM NaCl were hindered by the clogging of the capillary due to the crystallization of NaCl under the experimental conditions used. An increase in the RRT at higher concentrations of NaCl was not expected since the concentration of CTAB (0.07 mM) used was too low to reach the cmc and thus allow OT-MLC separations with micelles in solution. For the pH study, the retention of analytes (RRT > 1) was observed only at pH $\geq$6 (see Figure 3.6(c)). At

pH 6, there was sufficient ionization of the silanol groups at the capillary wall (pKa of silanol is ~4.9[35]) for CTAB to form admicelles. However, the retention was weak due to incomplete capillary wall surface coverage by the admicelles. The RRTs increased from pH 6 to 8 due to the increased surface coverage and charge of the silica surface with the increase in the pH. The RRTs were approximately constant at pH $\geq$ 8 due to the complete ionization of the silanol groups providing an unchanging surface for the CTAB molecules to aggregate. Figure 3.5(d) shows that the RRT values decreased with an increase in the concentration of MeOH in the mobile phase. This suggests a reversed-phase mechanism on the CTAB admicellar pseudophase, where the eluting strength of the mobile phase was increased by the addition of MeOH. The effect of solvent strength on reversed-phase retention is demonstrated by the linear relationship between log k' or log RRT against increasing volume percentage of methanol in water as shown in Figure A3.1. There was no retention with ≥30% MeOH, which could also be due to an increase in the csac of CTAB to above 0.04 mM (measured csac with the borate buffer) and thus no admicellar stationary pseudophase being formed at the interface.

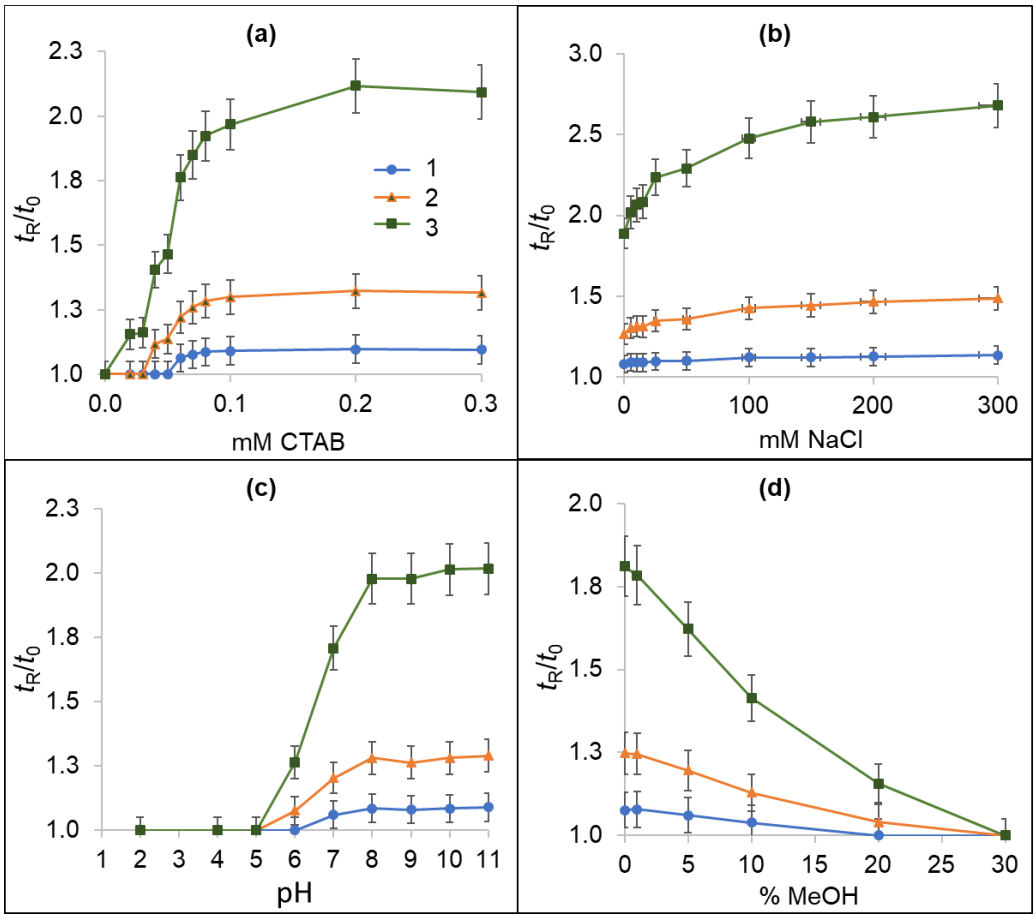

Figure 3.6 RRT (t_R/t_0) versus CTAB concentration from 0-0.3 mM (a), NaCl concentration from 0-300 mM (b), pH from 2-11 (c), and MeOH percentage from 0-30% in the mobile phase in OT-AMLC using a 50 µm i.d. capillary (d). In (a), CTAB >0.2 mM is OT-MLC. The mobile phases contained 50 mM sodium tetraborate pH 9.5 except for (c) and 0.07 mM CTAB except for (a). Separation pressure was 180 mbar except for (a) with 150 mbar. In (c), the conductivity of the mobile phases using phosphate buffers was controlled and equal to 6.0 $\pm$ 0.2 mS/cm. The analyte concentrations were 0.4-1 mM. The analytes were propyl (1), butyl (2), and pentyl (3) phenyl ketone. More explanation in the text.

3.4.4 OT-AMLC and OT-AMEC of anionic analytes

Separations of anionic sulfonamides by OT-AMLC and OT-AMEC at high pH are shown in Figure 3.7(a) and 3.7(b), respectively. In OT-AMLC, the elution time of the highly retained sulfonamides (peaks 3 and 4) was controlled to less than 14 min. by employing a pressure step gradient (higher pressure from 7 min for faster elution of peaks 2-4) and a high concentration of the buffer component (400 mM ammonium bicarbonate). 0.2 mM CTAB was confirmed to be below the cmc in Figure 3.7(a), from cmc determination results by OT-AMLC as described earlier. The retention or migration times of the sulfonamides were close to the EOF in OT-AMEC, and this was due to the affinity of the analytes to the admicellar pseudophase (see Figure 3.7(b)) as explained below.

In the OT-AMEC of a charged analyte (a'), the effective electrophoretic mobility ($\mu(a')_{eff}$) is given by equation (3.4), where $\mu(a')_{ep}$ and k are the electrophoretic mobility and retention factor, respectively.

$$\mu(a')_{eff} = \frac{1}{1+k}\mu(a')_{ep} \tag{3.4}$$

This equation is consistent with the expression for CEC retention factor worked out by Wei *et al.*[36] based on the proposed overall migration velocity of charged solutes in CEC by Knox and Grant[37] and the definition of CEC retention factor, *k'*, as defined by Rathore and Horvath.[38] The equation incorporates both the chromatographic retention factor and the electrophoretic velocity factor to explain charged solute retention in CEC. This equation is different from MEKC with a moving pseudophase, where in MEKC there is a contribution from the electrophoretic mobility of the pseudophase to the $\mu(a')_{eff}$. For electrochromatographic separations, when stronger retention brings about

decreased μ_{eff}, the observed mobility, i.e. the sum of the μ_{eff} and μ_{eof}, will fall close to the μ_{eof}. The decreased μ_{eff} of sulfonamides due to strong affinity with the admicelles slows down their migration at reverse polarity in the same direction of the EOF, and thus migrate closer to the EOF.

The migration of the tested sulfonamides was further investigated by running the same experiments described in Figure 3.7(b) in a capillary coated with a cationic polyelectrolyte (*i.e.*, PDADMAC), which prevented the formation of the admicelles (see Figure 3.7(c)). Note that positively charged CTAB only organizes to form admicelles at the interface between a negatively charged surface and bulk solution. The migration times of all peaks were far from the EOF because of the absence of admicelles. This confirms the contribution of the pseudophase to the analyte migration that was close to the EOF in Figure 3.6(b). However, peak 4 (sulfaquinoxaline) was separated from peak 1 (sulfamethoxazole), most likely due to the formation of ion-pairs between CTAB monomers and sulfaquinoxaline, thereby decreasing the anodic electrophoretic migration of sulfaquinoxaline but not sulfamethoxazole. Capillary zone electrophoresis with PDADMAC and using the same buffer in Figure 3.6(c) without CTAB was conducted (see Figure A3.2). Sulfamethoxazole and sulfaquinoxaline were not separated, verifying the ion-pair formation between sulfaquinoxaline with CTAB monomers in Figure 3.7(c).

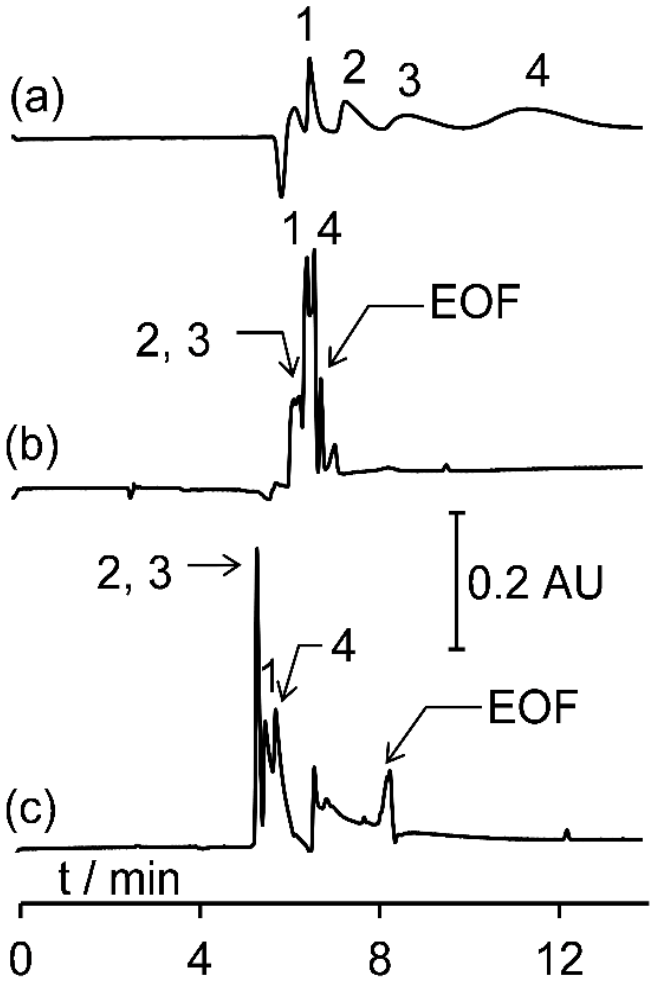

Figure 3.7 OT-AMLC (a), OT-MLC (b), and CZE (c) of anionic sulfonamides. Sulfamethoxazole (1), sulfadimethoxine (2), sulfamethizole (3), and sulfaquinoxaline (4) in the mobile phase/BGS at 0.2 - 0.6 mM. Sample injection was the same as in Fig. 3.4. In (a), the mobile phase in was 0.2 mM CTAB and 2% MeOH in 400 mM ammonium bicarbonate pH 8.5. Pressure separation was 150 mbar from 0 to 7 min, then 400 mbar from 7 to 14 min. In (b) and (c), BGS was 0.2 mM CTAB and 2% MeOH in 100 mM NH_4HCO_3 pH 8.5. Separation voltage was 20 kV at negative polarity. In (c), the capillary was coated with PDADMAC. More explanation in the text.

3.4.5 Analytical figures for merit and sample matrix effects studies for OT-AMLC of neutral and anionic analytes

Low EOF was encountered in OT-AMEC with CTAB, with higher electric field strengths being required for reasonable separation times. The high applied voltages also resulted in high running currents that could lead to Joule heating effects under the experimental conditions used. There is also the contribution of the charged analytes' electrophoretic mobility on OT-AMEC separations. A more substantial study on OT-AMEC is required and this will be conducted in the future, including the utility of other surfactants. In this section, the focus is therefore on the analytical figures of merit for OT-AMLC and its potential for real sample analysis.

The analytical figures of merit (linearity, limit of detection (LOD), intra- and inter-day repeatability of t_R and peak area) for the OT-AMLC analysis of neutral pesticides and anionic sulfonamides are shown in Table 3.1 and 3.2, respectively. The separation conditions used for the pesticides were similar to those in Figure 3.4(a) except the pressure during separation was increased to 300 mbar for faster analysis. The separation conditions used for the sulfonamides were the same as in Figure 3.7(a). The coefficients of variation, LODs, (intra and interday) repeatability of t_R, and repeatability of peak area were $\geq$ 0.98, 2.4 x10^{-6} M, -8.5 x 10^{-5} M, 0.2 – 1.9%, and 0.7 – 9.5%, respectively. Note that these values were obtained from equipment designed for CE separations and it can therefore be expected that these values could be improved by the development of equipment that is optimized for open tubular separations with surfactant solutions.

Studies on the effect of a real sample matrix were conducted and the results are shown in Figure 3.8. The tested model pesticides and sulfonamides were not detected in the water samples (Browns river and Dru Point estuary) collected from the pristine Tasmanian environment (see Figure 3.8(a) (i) and (iii) and Figure 3.8(b) (ii) and (iv)). The samples were subjected to sample preparation that was appropriate to the nature of the targeted analytes (see Chapter Appendix sample preparation procedures). The sample matrix did not show any negative effect on the chromatography as shown by the OT-AMLC of the prepared samples that were spiked with the standards (see Figure 3.8(a) (ii) and (iv) and Figure 3.8(b) (iii) and (v)).

Table 3.1 OT-AMLC of neutral pesticides. Analytical figures of merit.

	analyte				
	atrazine	diuron	diazinon	fenitrothion	parathion
Linearity					
concentration range, $x\ 10^{-4}$ M	1.2 – 9.3	1.1 – 8.6	1.5 – 12.0	1.8 – 14.0	2.1 – 17.0
equation of line (y = mx+b)					
slope (m)	25.0	26.6	13.7	14.4	16.4
y-intercept (b)	+ 753.6	+ 644.3	+ 174.9	+ 1130.1	+ 494.4
coefficient of variation (R^2)	0.990	0.994	1.000	0.979	0.992
limit of detection					
(S/N = 3), $x\ 10^{-4}$ M	0.19	0.20	0.85	0.57	0.73
Repeatability, RSD (%)					
retention time					
intraday (n=3)[1]	0.3 – 0.6	0.5 – 0.6	0.2 – 0.9	0.3 – 1.3	0.3 – 1.0
interday (n=12)[2]	0.4	0.5	1.0	1.0	1.4
peak area					
intraday (n=3)[1]	1.4 – 7.8	0.7 – 2.9	5.5 – 9.5	1.0 – 9.4	1.1 – 7.4
interday (n=12)[2]	4.2	2.3	4.6	4.2	3.1

Mobile phase was 100 mM NH_4HCO_3 pH 8.5 + 0.15 mM CTAB in 5% MeOH. Other conditions are in the Materials and Methods section.

Table 3.2 OT-AMLC of sulfonamides. Analytical figures of merit.

	analyte			
	sulfamethoxazole	sulfadimethoxine	sulfamethizole	sulfaquinoxaline
Linearity				
concentration range, $x\ 10^{-4}$ M	0.19 – 6.1	0.62 – 20.0	0.71 – 23.0	0.64 – 20.0
equation of line (y = mx+b)				
slope (m)	3358.1	340.5	274.0	1356.8
y-intercept (b)	- 7375.5	+ 1994.8	+ 139.6	- 6340.3
coefficient of variation (R^2)	0.995	0.999	0.997	0.999
limit of detection				
(S/N = 3), $x\ 10^{-4}$ M	0.02	0.15	0.34	0.19
Repeatability, RSD (%)				
retention time				
intraday (n=3)[1]	0.6 – 1.4	0.4 – 1.9	0.5 – 0.7	0.3 – 1.0
interday (n=12)[2]	0.7	0.7	1.3	1.5
peak area				
intraday (n=3)[1]	0.7 – 3.7	1.4 – 5.4	3.2 – 3.9	4.1 – 6.5
interday (n=12)[2]	7.2	4.7	5.4	6.2

OT-AMLC conditions as in Figure 3.7(a).

[1]RSD range taken within 4 days with three replicates (n=3) per day.
[2]Taken from 12 pooled peak areas (n=12) within 4 days.

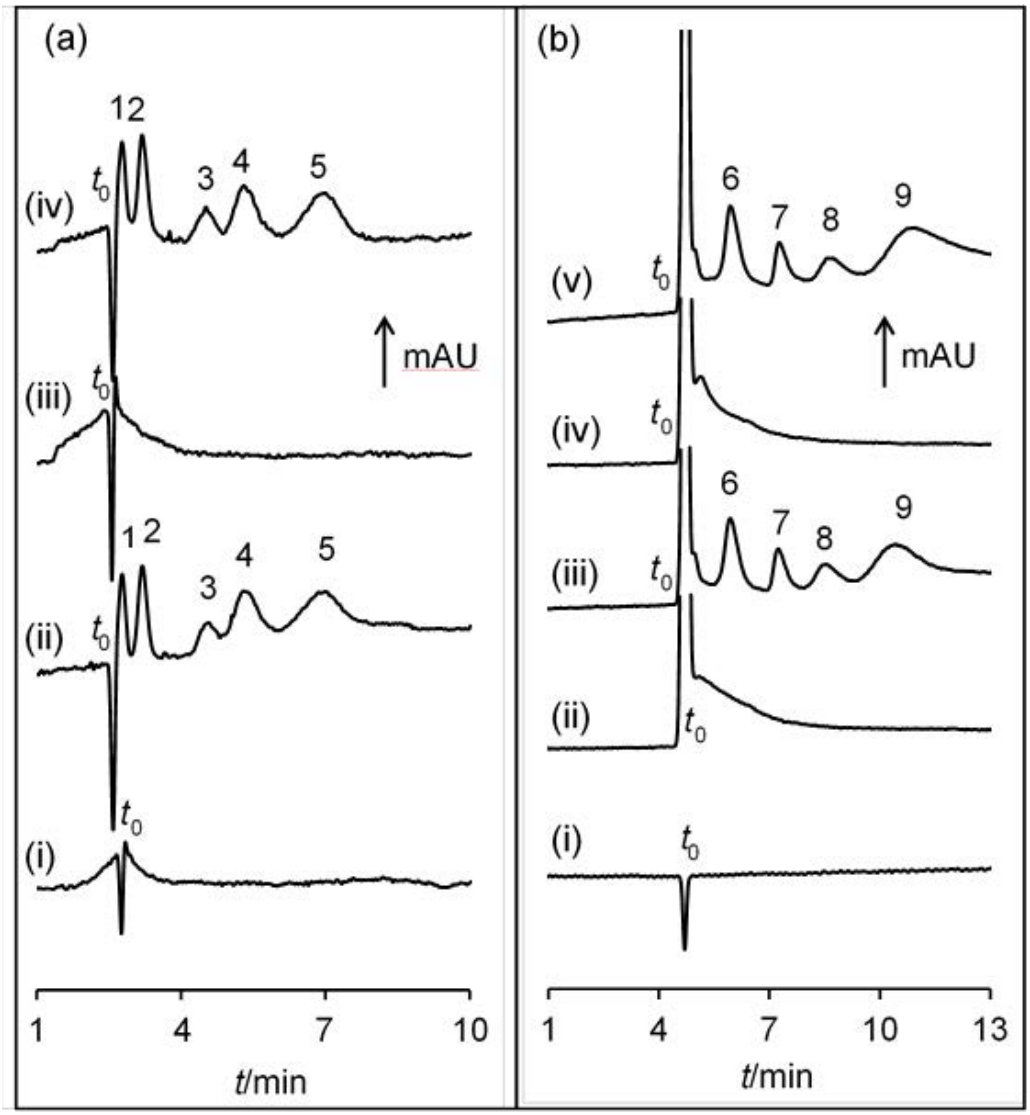

Figure 3.8 Evaluation of OT-AMLC with real sample matrices. Analysis of neutral pesticides (a) and sulfonamides (b). Mobile phase in (a) and (b) was the same as in Figure 3.3 OT-AMLC and Figure 3.6 (a), respectively. Pressure separation was 300 mbar in (a) and the same as in Figure 3.6 (a) in (b). Other conditions are in the Materials and Methods section of the main text. Pesticides at 0.3 – 0.5 mM were atrazine (1), diuron (2), diazinon (3), fenitrothion (4), and parathion (5). Sulfonamides at 0.2 – 0.6 mM were sulfamethoxazole (6), sulfadimethoxine (7), sulfamethizole (8), and sulfaquinoxaline (9). In (a), the (i), (ii), (iii), and (iv) was Browns River extract, spiked Browns River extract, Dru Point water extract, and spiked Dru Point water extract, respectively. In (b), the (i), (ii), (iii), (iv) and (v) was mobile phase without CTAB, Browns River extract, spiked Browns River extract, Dru Point water extract, and spiked Dru Point water extract, respectively. Sample processing is described in Chapter 3 Appendix Real sample preparation procedures.

3.5 Conclusion

Fundamental studies on the use of surfactant admicelles as soft stationary phase materials for open-tubular liquid chromatography (*i.e.*, OT-AMLC) and open-tubular electrochromatography (*i.e.*, OT-AMEC) applied to the separation of neutral and anionic analytes were presented. The preparation of a conventional solid stationary phase was not required for separation to be achieved. The working concentration range of the surfactant was between the csac and cmc which were determined using EOF measurements by CE. The characterization of the CTAB pseudophase was difficult by OT-AMEC due to complications involving electrokinetic separations regarding EOF changes or stability (e.g., effect of high MeOH content and loss of EOF at low pH) and Joule heating (high NaCl content). In OT-AMLC, retention was found to be stronger under alkaline conditions due to the effect of pH on the number of sites at the capillary wall for the CTAB to molecularly organise into admicelles. The retention of analytes increased with an increase in the CTAB concentration due a commensurate increase in the admicellar stationary phase which affected the chromatographic phase ratio. The effect of methanol on the retention suggested that a reversed-phase retention mechanism was applicable, which was expected due to the long alkyl chain of CTAB. The retention in OT-AMEC suggested that the use of CTAB as EOF modifier in the determination of electrophoretic mobility and binding constants by CE should be avoided because the presence of admicelles could affect the results. A simple method to determine cmc by OT-LC was also proposed, based on the increase in retention for surfactant concentrations between the csac to the cmc, followed by a decrease in the retention after the cmc. The limitations (e.g., low separation efficiencies and peak capacity) on the use of admicelles in OT-LC were the same

as those found with micelles[21]. The use of other surfactants as pseudophases, narrower i.d. capillaries, real sample applications, and side-by-side comparisons with related separation techniques will be the subjects of future investigations.

OT-LC using fused-silica capillaries and without the preparation of a solid stationary phase material or support has been demonstrated. Using CTAB added to the mobile phase at concentrations above the critical micelle concentration (cmc), the surfactants formed micelles in solution and at the capillary wall surface and bulk solution interface. The interaction of the analytes with the nanosized interfacial micelles caused unexpected retention of analytes in this new form of OT-LC, which is described as OT-micellar LC (OT-MLC) and is discussed further in the next chapter.

3.6 References

(1) Desmet, G.; Eeltink, S. *Anal. Chem.* **2013**, *85*, 543-556.

(2) Cheong, W. J.; Ali, F.; Kim, Y. S.; Lee, J. W. *J Chromatogr A* **2013**, *1308*, 1-24.

(3) Collins, D. A.; Nesterenko, E. P.; Paull, B. *Analyst* **2014**, *139*, 1292-1302.

(4) Qu, Q.; Liu, Y.; Shi, W.; Yan, C.; Tang, X. *J Chromatogr A* **2015**, *1399*, 25-31.

(5) Bao, T.; Zhang, J.; Zhang, W.; Chen, Z. *J Chromatogr A* **2015**, *1381*, 239-246.

(6) Knob, R.; Kulsing, C.; Boysen, R. I.; Macka, M.; Hearn, M. T. W. *TrAC, Trends Anal Chem* **2015**, *67*, 16-25.

(7) Desmet, G.; Callewaert, M.; Ottevaere, H.; De Malsche, W. *Anal. Chem.* **2015**, *87*, 7382-7388.

(8) Kazarian, A. A.; Sanz Rodriguez, E.; Deverell, J. A.; McCord, J.; Muddiman, D. C.; Paull, B. *Anal Chim Acta* **2016**, *905*, 1-7.

(9) Zhou, S. S.; Zhai, R.; Jiao, F. L.; Hao, F. R.; Ls, Y. Y.; Qian, X. H.; Zhang, Y. J. *Chin J Chromatogr* **2016**, *34*, 226-231.

(10) Zhang, F.; Zhao, X.; Xu, B.; Cheng, S.; Tang, C.; Duan, H.; Xiao, X.; Du, W.; Xu, L. *Anal Bioanal Chem* **2016**, *408*, 2441-2448.

(11) Peng, L.; Zhu, M.; Zhang, L.; Liu, H.; Zhang, W. *J Sep Sci* **2016**, *39*, 3736-3744.

(12) Vehus, T.; Roberg-Larsen, H.; Waaler, J.; Aslaksen, S.; Krauss, S.; Wilson, S. R.; Lundanes, E. *Sci Rep* **2016**, *6*, 37507.

(13) Schmarr, H. G.; Wacker, M.; Mathes, M. *J Chromatogr A* **2017**, *1481*, 111-115.

(14) Shao, X.; Zhang, X. *Proteomics* **2017**, *17*, 1600463.

(15) Ali, A.; Cheong, W. J. *J Sep Sci* **2017**, *40*, 2654-2661.

(16) Wang, H.; Yao, Y.; Li, Y.; Ma, S.; Peng, X.; Ou, J.; Ye, M. *Anal Chim Acta* **2017**, *979*, 58-65.

(17) da Silva, M. R.; Brandtzaeg, O. K.; Vehus, T.; Lancas, F. M.; Wilson, S. R.; Lundanes, E. *J Chromatogr A* **2017**, *1518*, 104-110.

(18) Chen, K.; Zhang, L.; Zhang, W. *J Sep Sci* **2018**, *0*.

(19) Skjaervo, O.; Brandtzaeg, O. K.; Lausund, K. B.; Pabst, O.; Martinsen, O. G.; Lundanes, E.; Wilson, S. R. *J Chromatogr A* **2018**, *1534*, 195-200.

(20) Zhu, M.; Zhang, L.; Chu, Z.; Wang, S.; Chen, K.; Zhang, W.; Liu, F. *Talanta* **2018**, *184*, 29-34.

(21) Tarongoy, F. M., Jr.; Haddad, P. R.; Quirino, J. P. *Electrophoresis* **2018**, *39*, 34-52.

(22) Tarongoy, F. M., Jr.; Haddad, P. R.; Boysen, R. I.; Hearn, M. T.; Quirino, J. P. *Electrophoresis* **2016**, *37*, 66-85.

(23) Nayyar, S. P.; Sabatini, D. A.; Harwell, J. H. *Environ Sci Technol* **1994**, *28*, 1874-1881.

(24) Saitoh, T.; Matsushima, S.; Hiraide, M. *J Chromatogr A* **2004**, *1040*, 185-191.

(25) Saitoh, T.; Nakayama, Y.; Hiraide, M. *J Chromatogr A* **2002**, *972*, 205-209.

(26) Garcia-Prieto, A.; Lunar, L.; Rubio, S.; Perez-Bendito, D. *Analyst* **2006**, *131*, 407-414.

(27) Luque, N.; Rubio, S. *J Chromatogr A* **2012**, *1248*, 74-83.

(28) Ezoddin, M.; Taghizadeh, T.; Abdi, K.; Jamali, M. R. *Desalin Water Treat* **2013**, *53*, 671-680.

(29) Barton, J. W.; Fitzgerald, T. P.; Lee, C.; O'Rear, E. A.; Harwell, J. H. *Sep Sci Technol* **1988**, *23*, 637-660.

(30) Shen, L.-C.; Hankins, N. P.; Singh, R. In *Emerging Membrane Technology for Sustainable Water Treatment*; Elsevier: Boston, **2016**, pp 249-276.

(31) IUPAC. Compendium of Chemical Terminology, 2nd ed. (the "Gold Book"). Compiled by A. D. McNaught and A. Wilkinson. Blackwell Scientific Publications, Oxford (1997). XML on-line corrected version: http://goldbook.iupac.org (2006-) created by M. Nic, J. Jirat, B. Kosata; updates compiled by A. Jenkins. ISBN 0-9678550-9-8. https://doi.org/10.1351/goldbook.

(32) Terabe, S.; Otsuka, K.; Ichikawa, K.; Tsuchiya, A.; Ando, T. *Anal. Chem.* **1984**, 56, 111-113.

(33) https://ls.beckmancoulter.co.jp/files/appli_note/CEPrimer3.pdf

(34) Ei-Aila, H.J.Y. *Tenside, Surfactants, Detergents,* **2011**, 48, 312-317.

(35) Fan, H.; Li, F.; Zare, R.N.; Lin. K. *Anal. Chem.* **2007**, 79, 3654-3661

(36) Wei, W.; Guoan, L.; Chao, Y. *J Sep Sci* **2001**, *24*, 203-207.

(37) Knox, J. H.; Grant, I. H. *Chromatographia* **1991**, *32*, 317-328.

(38) Rathore, A. S.; Horváth, C. *Electrophoresis* **2002**, *23*, 1211-1216.

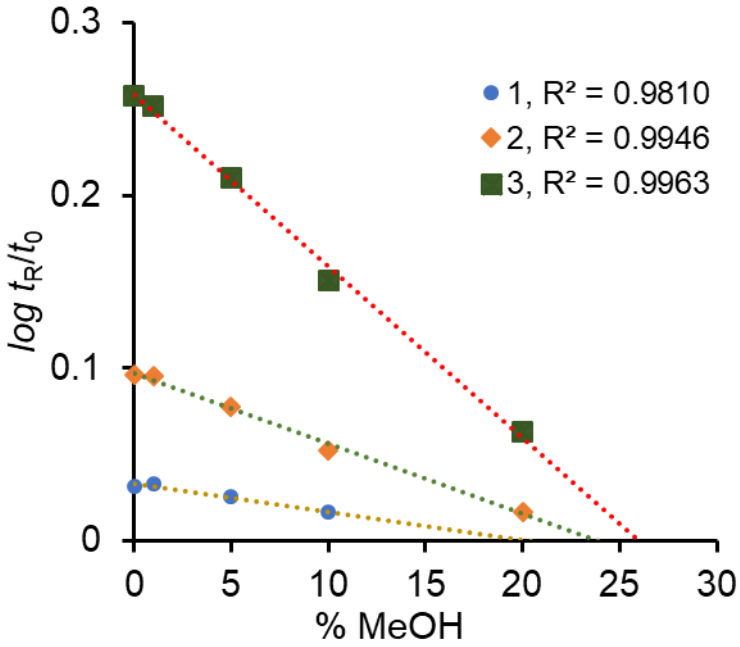

Figure A3.1 Log RRT (t_R/t_0) versus MeOH percentage from 0-30% in the mobile phase in OT-AMLC using a 50 µm i.d. capillary. Experimental conditions are described in Figure 3.6. The analytes were propyl (1), butyl (2), and pentyl (3) phenyl ketone.

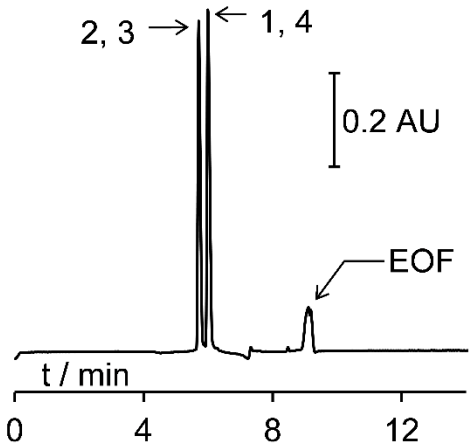

Figure A3.2 Capillary zone electrophoresis (CZE) of sulfonamides in Figure 3.7. BGS was 2% MeOH in 100 mM NH_4HCO_3 pH 8.5 (no CTAB). The capillary was coated with PDADMAC. Other conditions are the same as in Fig. 3.7. More explanation in the text.

Real sample preparation procedures. The environmental water samples were collected from Browns river (Kingston, Tasmania, Australia) and Dru Point estuary (Margate, Tasmania, Australia).

Figure 3.8(a). The procedure to prepare the sample was as follows. 15 mL water sample was extracted with 5.4 mL dichloromethane (DCM from Sigma Aldrich). The resulting mixture was centrifuged (5 min) to form 2 clear phases. 5 mL aliquot of the lower organic phase was collected and then vacuum-dried overnight. Dried extract was reconstituted with 150 μL of mobile phase to form the sample for analysis.

Figure 3.8(b). The procedure to prepare the sample was as follows. 100 mL sample was freeze dried (48 hr) and then dried to completeness in a vacuum oven (30^0C). The sample was reconstituted with 10 mL methanol, centrifuged (5 min), and the clear extract was collected. The methanol extract was vacuum dried and then reconstituted with 150 μL of mobile phase to form the sample for analysis.

Chapter 4

Open-tubular micellar liquid chromatography

4.1 Abstract

A new and green liquid chromatography approach in open-tubes is introduced here based on the molecular organisation of common long chain ionic surfactants (*i.e.*, CTAB and SDS) to form micelles in solution and at the solid surface-liquid interface. Open-tubular micellar liquid chromatography (OT-MLC) works by the differential solubilisation or distribution of solutes between interfacial and solution micelles. This approach has produced the unexpected separation and retention of various types of molecules, including aromatic hydrocarbons, anionic, cationic, and amphiphilic drugs, pesticides, peptides and a small protein. Chromatography was performed in 25-200 μm range inner diameter and 60 or 120 cm long fused-silica capillaries against a flow of predominantly aqueous surfactant solutions above the critical micelle concentration (CTAB or SDS added to ammonium bicarbonate and sodium tetraborate buffer solutions) as mobile phase. Distribution between these micelles was affected by the mobile phase conditions, such as surfactant concentration, pH, salt concentration and organic solvent content used, which were harnessed to demonstrate sample enrichment. Analytical performance was assessed in the separation of pesticides and antioxidants and in real sample matrices. This important fundamental behaviour of surfactant micelles might find use in the development of green extraction technologies, nano/micro separations and portable devices. With greening efforts in analytical chromatography mostly on the reduction of chemical waste and replacement of organic solvents used in the mobile phase, this new OT-MLC technique gives more

advantages and/or features including up to zero chemical waste, minimal use of reagents and samples, no preparation of a solid stationary phase, relatively fast separations and reproducible results.

*All of the research contained in this chapter has been published as Quirino, J. P.; Tarongoy, F. M., Liquid chromatography with micelles in open-tube capillaries. *Green Chemistry* **2018,** *20*(11), 2486-2493.

.

4.2 Introduction

Liquid chromatography (LC) is a mature and essential technique in the chemical, food and pharmaceutical industries as well as in academic and industry research.[1-10] A LC expert preferably uses a column with dimensions of 2 – 7.8 mm internal diameter (i.d.) and 10 – 25 cm length, and the organic solvent-rich mobile phase flows at a rate of 0.5 – 1.5 mL/min.[11] The total volume of solvent or chemical waste generated per day by LC instruments worldwide is significant and is a growing subject in green chemistry.[12-16] There are the three Rs (i.e., reduce, replace and recycle) on top of the well-known 12 principles of green chemistry[17] associated with the greening of analytical chromatography.[12] Most of the efforts have been on the replacement of solvents with greener alternatives (e.g., bio-derived alcohols and more recently with carbonated water) and on an overall reduction in the amount of solvents used and chemical waste created.[18-20] Solvent reduction had been achieved by performing fast chromatographic separations with existing LC instrumentation or reducing the overall size of the LC instrument. The scaling down of LC includes the use of narrow bore columns which are either fully packed with or coated with a thick layer of stationary solid phase materials, with the latter classified as open-tubular liquid chromatography (OT-LC). OT-LC must be performed in very narrow capillaries ($\leq$10 μm i.d.) with a suitable layer of stationary solid phase.[21-24]

In micellar LC[25] and electrokinetic chromatography (MEKC),[26] surfactants above the critical micelle concentration (cmc) are added into the mobile phase to create micelles or pseudophases. These micelles allow the use of chromatography with unique selectivities, lower costs and increased safety. In micellar LC, surfactant monomers adsorb at the stationary phase, but the selectivity is often from the solution micelles that provide diverse interactions (electrostatic, hydrophobic

and steric). In MEKC, the micelles act as the "pseudo" stationary phase where the distribution of solutes between the solution micelles and bulk phase facilitates the separation in the presence of an electric field. In surfactant mediated capillary electrochromatography (CEC),[27,28] surfactants are added to the mobile phase to alter the selectivity in the same manner as in micellar LC and the separation is driven by an electric field similar to MEKC.

In this work, a green chromatographic approach in an OT-LC format is presented using pseudophases from common long chain ionic surfactants and unusually wide i.d. capillaries. The construction of a solid stationary phase or support was not required. The simple OT-LC procedure involved conditioning a capillary with the surfactants above the cmc in the mobile phase. The surfactants form micelles at the solid surface-liquid interface and in the free solution.[29-31] The nanometer sized interfacial micelles were always expected to be similar to solution micelles,[31] but a surprising distribution of solutes between interfacial and solution micelles is shown here, which can be modulated by simple manipulation of micellar solution conditions. Thus, this distribution will affect chromatographic separations with the interfacial micelles as the stationary phase and the solution micelles, as well as bulk liquid as the mobile phase.

Due to the wide (25 to 200 μm) i.d. of the OT-LC capillaries used in this study, a mechanism is proposed for the unexpected retention of various neutral and charged compounds in the presence of solution and interfacial micelles. Proof of solute retention was shown with both a cationic and anionic surfactant, hexadecyltrimethylammonium bromide (CTAB) and sodium dodecyl sulfate (SDS), respectively. With CTAB as the pseudophase, fast separations of structurally similar solutes were demonstrated using high separation flow

velocities. The parameters such as surfactant concentration, pH, salt concentration and organic solvent content in the micellar solution, which affected the solubilisation and solute retention were studied. These solution parameters were then harnessed to demonstrate sample enrichment using a tripeptide as model analyte. A method using CTAB as pseudophase was developed for pesticides and using SDS for antioxidants. For each method, the analytical figures of merit and application to real (environmental water or processed food) samples analysis were assessed. In addition, comparison between a reversed-phase LC and OT-LC with CTAB for the analysis of a pharmaceutical drug combination was conducted.

4.3 Materials and Methods

4.3.1 Reagents and general equipment

All chemicals (test analytes, buffer compounds, surfactants, salts, polyelectrolytes and organic solvents) were obtained from Sigma-Aldrich (New South Wales, Australia) or Fluka Analytical (St. Louis, MO, USA) and used as delivered. Hexadecyltrimethylammonium bromide (or cetyltrimethylammonium bromide, CTAB) was obtained from bioWORLD (Dublin, OH, USA). Purified water was from a Milli-Q system (Millipore, MA, USA). The pH and conductivity of solutions were measured using a bench top meter (Sper Scientific, Australia). Stock solutions of buffers (0.2 M ammonium formate pH 4.5, 0.2 M ammonium acetate pH 8.5 and phosphate buffers pH 2-10), surfactant stock solutions (0.2 mM SDS and 0.2 mM CTAB) and 3.5 M NaCl were sonicated and filtered using a 0.45 µm filter prior to use. Mobile phases were prepared by mixing appropriate volumes of buffer, surfactant solution stock, MeOH, ACN with purified water. 10% PDADMAC with average molecular weight of 400-500k was prepared in purified

water. This was used to modify the capillary wall in the SDS experiments. Stock solutions of 0.5 – 1 mg/mL analytes (alkyl phenyl ketones, antioxidants and those listed in Chapter Appendix Table A4.1) were prepared in water or 50% MeOH and were stored at 4ºC when not in use. Sample solutions were prepared by mixing appropriate amounts of analyte stock solutions with the mobile phase or as indicated in the text.

4.3.2 OT-LC procedure

OT-LC was performed on a Beckman P/ACE MDQ (Beckman-Coulter, Brea, CA USA) equipped with a UV detector that was set at 200 nm and with fused-silica capillaries (Polymicro, Phoenix, AZ, USA). The total capillary length was 60 or 120 cm (50 or 110 cm from injection end to on-line UV detector, respectively). The capillary inner diameter (i.d.) (25 – 200 μm) used is indicated in the text. The temperature of the capillary was controlled at 20ºC. Sample injection (2 mm plug) and separation was by applying pressure with the sample and mobile phase at the inlet end of the column, respectively. New capillaries were conditioned by flushing (e.g., at 1500 mbar) with 0.1 M NaOH (10 capillary volumes) followed by purified water (5 capillary volumes). The pressure for conditioning, injection and separation was dependent on the capillary i.d. and length (higher pressures were used for narrower i.d. and 120 cm long capillaries). For CTAB experiments, the capillary was conditioned with purified water (2 capillary volumes), 0.1 M NaOH (3 capillary volumes), purified water (2 capillary volumes) and then the mobile phase (4 capillary volumes) before each sample injection. The negative charge at the fused-silica surface allowed the molecular organization of positively charged CTAB. For SDS experiments, the capillary was conditioned with purified water (2 capillary volumes), 0.1 M NaOH (3 capillary volumes), purified water (2 capillary

volumes), 10% PDDAC solution (3 capillary volumes), purified water (2 capillary volumes) and then the mobile phase (4 capillary volumes) before each sample injection. The PDADMAC formed a positive surface for the molecular organization of negatively charged SDS. Three determinations were made at each concentration of CTAB and SDS, and the average of retention time values (n =3) were reported.

4.3.3 Determination of cmc

The cmc was determined by EOF measurements using CE as described in Chapter 2. The cmc of CTAB and SDS (n = 3) was obtained from using unmodified (Figure 2.3) and polyelectrolyte-modified (Figure 2.5) fused-silica capillary, respectively, and was estimated from the concentration of surfactant that produced a stable and reversed EOF.

4.3.4 Preparation of environmental water and processed food samples

The environmental water samples were collected from Browns river (Kingston, Tasmania) and Dru Point estuary (Margate, Tasmania). The extraction procedure was based on the method of Aranas and co-workers.[32] To each water sample, a 100 mL aliquot was extracted 3 times with 5 mL of dichloromethane. The extracts were pooled, and the pooled extract was dried at 30^{o}C and under vacuum. The residue was reconstituted with 450 µL of the mobile phase or mobile phase that was spiked with the pesticides indicated in Figure 4.5(a). The reconstituted samples were then analysed by OT-LC. The three processed food samples (instant noodles, beef soup flavour mix and chicken flavoured rice crackers) were obtained from a chain supermarket in Sandy Bay, Tasmania. The extraction procedure was based on the method of Darji and co-workers.[33] For each solid sample, a 2 g sample was extracted two times with 5 mL MeOH. The extracts were pooled and then a 3

mL aliquot was dried at 30°C and under vacuum. The residue was reconstituted with 400 µL of the mobile phase or mobile phase that was spiked with the antioxidants indicated in Figure 4.5(b). The reconstituted samples were then analysed by OT-LC.

4.4 Results and discussion

4.4.1 Proof of concept: OT-LC with no solid stationary phase and in wide-bore capillaries

Figure 4.1(a) shows retention of pentyl phenyl ketone (peak 2) with ≥25 µm i.d. empty capillaries, although it is well known that OT-LC is normally performed in <10 µm i.d. capillaries with an ample layer of a chromatographic solid phase with high surface area attached to the wall.[21] Retention was most surprising with the 100 – 200 µm i.d. capillaries. The mobile phases consisted only of dilute surfactant solutions of CTAB and SDS (>cmc) in pH 8.5 buffer. The measured cmc values of CTAB and SDS in the buffer from EOF measurements were 0.45 and 0.75 mM, respectively. These data suggested strongly that there was different solubilising power between the closely arranged interfacial CTAB and SDS micelles and the dispersed solution micelles. The retention time (t_R) of pentyl phenyl ketone was longer than that of the much less hydrophobic methyl phenyl ketone (peak 1) which was eluted at the void time (t_0) and was therefore not retained. Solubilisation into the interfacial micelles (leading to retention) was stronger with the CTAB micelles with 16-carbon monomers compared to the SDS with shorter 12-carbon monomers, as suggested by the retention of pentyl phenyl ketone in the 200 µm i.d. with CTAB but not with SDS. The retention was also

stronger with the narrower capillaries, as shown by the longer t_R for pentyl phenyl ketone in the 25 – 50 μm range i.d. capillaries with CTAB and SDS, which was expected in OT-LC. The retention of a variety of analytes including drugs, pesticides, amino acids, peptides and ubiquitin were also obtained (see Table A4.1).

4.4.2 Fast separations with micellar CTAB

Fast chromatography is typically obtained by using high flow-rates that normally generate high back pressures due to the use of a solid stationary phase or support, but this was not a significant problem in the presented OT-LC mode. Figure 4.1(b) shows the OT-LC using dilute CTAB as mobile phase of structurally similar sulfonamides at different flow-velocities during separation. Good separations were obtained within 2.5 and 3.5 min at flow-velocities of 50 and 25 cm/min, respectively. Resolution was compromised with flow-velocities of >50 cm/min (e.g., 100 cm/min). A decrease in analyte signal intensities with an increase in flow- velocity was also observed. This was due to the analyte band dispersion caused by the parabolic flow profile of the mobile phase, which was stronger at higher flow-velocities.

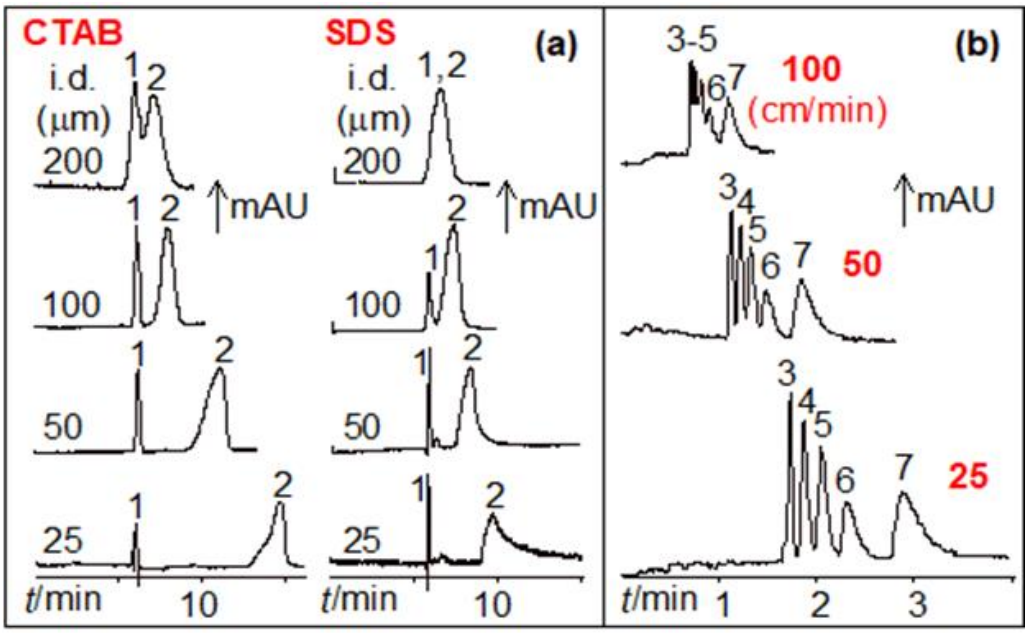

Figure 4.1 (a) OT-LC chromatograms of alkyl phenyl ketones obtained with mobile phases of 0.5 mM CTAB or 0.8 mM SDS in 100 mM ammonium bicarbonate pH 8.5 and different i.d. capillaries. The analytes were methyl phenyl ketone (1) and pentyl phenyl ketone (2) at 0.4 – 1.1 mM, which were adjusted to obtain sufficient sensitivity depending on the capillary i.d. used. Total length of capillaries was 60 cm (50 cm to detector). Applied pressure for separation was adjusted such that the t_0 = 5 – 6 min. For SDS, the capillary wall was coated with a cationic polyelectrolyte. (b) Effect of flow on the OT-LC separation of structurally similar analytes. Capillary i.d. and total length was 50 μm and 60 cm (50 cm to detector), respectively. Mobile phase was 0.8 mM CTAB in 100 mM ammonium bicarbonate pH 8.5 with 10% methanol. The analytes were sulfamerazine (3), sulfamethoxazole (4), sulfadimethoxime (5), sulfamethizole (6) and sulfaquinoxaline (7) at 0.16 – 0.2 mM in the mobile phase. Separation was at different applied pressures from 2.1 – 6.8 bar.

4.4.3 Proposed mechanism for retention

The interfacial CTAB and SDS micelles have a thickness of ~2x the surfactant length[31] which is in the single-digit nm range. These micellar stationary phases are exceptionally thin for OT-LC, and thus the retention contribution by interfacial micelles cannot be explained as traditional chromatography. Solute "distributions" between micelles are proposed here to explain the observed retentions. These are the distributions between: (a) solution micelles, and (b) interfacial micelles. The distributions were facilitated by the micellisation-dissociation equilibrium in ionic surfactant solutions,[34,35] which resulted in a transfer of solubilised analyte from one micelle to another and surfactant monomer exchange. A relaxation time in the milliseconds range has been associated with the above equilibrium[36] that was sufficiently fast for OT-LC. In particular, the distribution between solution micelles improved the transfer of solubilised analytes from the solution micelles to the interfacial micelles, which would otherwise be diffusion-limited and impossible for analyte molecules solubilised in the middle of the wider capillaries. The distributions were also affected by the number of micelles in solution as discussed below.

4.4.3.1 Micellar phase ratio to explain solute retention

The t_R in OT-LC is the distance travelled by a solute from injection end to detector window (L_{eff}) divided by the solute velocity inside the capillary. The weighted average solute velocity (v_{av}) in the experiments is given by equation (4.1), where F_{bulk}, F_{sm} and F_{im} is the fraction of solute in the bulk solution, solution micelles and interfacial micelles, respectively. For the stationary phase, two pseudophases are here at work, the stationary interfacial micelles (*im*), and the

mobile solution micelles (*sm*) moving at same velocity as the mobile phase. Solute velocity is v_{bulk}, v_{sm} and v_{im}, correspondingly.

$$v_{av} = F_{bulk}v_{bulk} + F_{sm}v_{sm} + F_{im}v_{im} \quad (4.1)$$

The v_{bulk} and v_{sm} is equal to the flow-velocity (v_{flow}). The interfacial micelles were assumed to be unaffected by the applied pressure, thus $v_{im} = 0$ and $F_{im}v_{im} = 0$. The $F_{bulk} = 1/1+k_{av}$ and $F_{sm} = k_{av}/(1+k_{av})$, where k_{av} is the averaged retention factor due to the micelles (interfacial and solution) also described as :

$$k_{av} = \frac{F_{av}}{F_{bulk}} = \frac{1-F_{bulk}}{F_{bulk}} \quad (4.2)$$

where F_{av} is the averaged fraction of solute distributed among the solution micelles and interfacial micelles, both acting as stationary phases in the given system. This expression is coherent with the chromatographic definition of retention factor. The k_{av} is a measure of the time the solute resides in the micelles relative to the time it resides in the bulk solution. The rearrangement of equation (4.2) gives $F_{bulk} = 1/(1+k_{av})$. Following stated assumptions and the expression for F_{bulk}, v_{av} from equation (4.1) becomes the v_{flow} which then gives $F_{sm} = k_{av}/(1+k_{av})$.

The fraction of solutes in the solution micelles is related to the micellar phase ratio (β_{mc}) given by equation (4.3), where V_{sm} and V_{im} is the volume of the solution micelles and interfacial micelles, respectively.

$$\beta_{mc} = {}^{V_{sm}}/_{V_{im}} \quad (4.3)$$

The phase ratio has been used to explain a change in a solute's retention.[37,38] As the surfactant concentration is increased after the cmc, the V_{sm} increases as more micelles are formed in solution while V_{im} is constant. The fraction of the solute in the solution micelles is directly proportional to β_{mc}, thus an increase in β_{mc} causes a decrease in t_R as suggested by equation (4.4).

$$t_R = \frac{L_{eff}}{v_{flow}} x \frac{1}{(1/(1+k_{av}))+(\beta_{mc}/(1+\beta_{mc}))} \quad (4.4)$$

The calculated t_R values for analytes with k_{av} in the 0.5 – 5 range is shown in Figure 4.2 (top plot). If the solubilised analytes spend more time in the interfacial micelles due to a very low β_{mc} ($\beta_{mc} \rightarrow 0$), v_{flow} = 10 cm/min and L_{eff} = 50 cm, the t_R values were larger than the t_0. The t_R values approached t_0 as $\beta_{mc} \rightarrow \infty$, where analytes spend more time in the solution micelles. These predictions were verified with OT-LC experiments using different concentrations of surfactant (0.5 – 20 mM CTAB and 1 – 20 mM SDS) to modify β_{mc} and 5 neutral test analytes (alkyl phenyl ketones). The hydrophobicity is related to the chain length, with methyl phenyl ketone and pentyl phenyl ketone as the least and most hydrophobic analyte, respectively. The results are presented in Figure 4.2 (bottom chromatograms). At the lowest micellar concentrations studied (0.5 mM CTAB and 1 mM SDS), there was retention of analytes due to their solubilisation into the interfacial micelles, which is consistent with the Figure 4.2 plot ($\beta_{mc} \rightarrow 0$). As the surfactant concentrations were increased which increased the β_{mc}, the t_R values approached t_0 (see red arrows from t_R directed to the left or t_0). This indicated the preferred solubilisation of analytes into the solution micelles at higher surfactant concentrations. This is also consistent with the Figure 4.2 plot (from $\beta_{mc} \rightarrow 0$ to $\beta_{mc} \rightarrow \infty$). In summary, the β_{mc} provided more insights on the distribution of analytes between the interfacial and solution micelles.

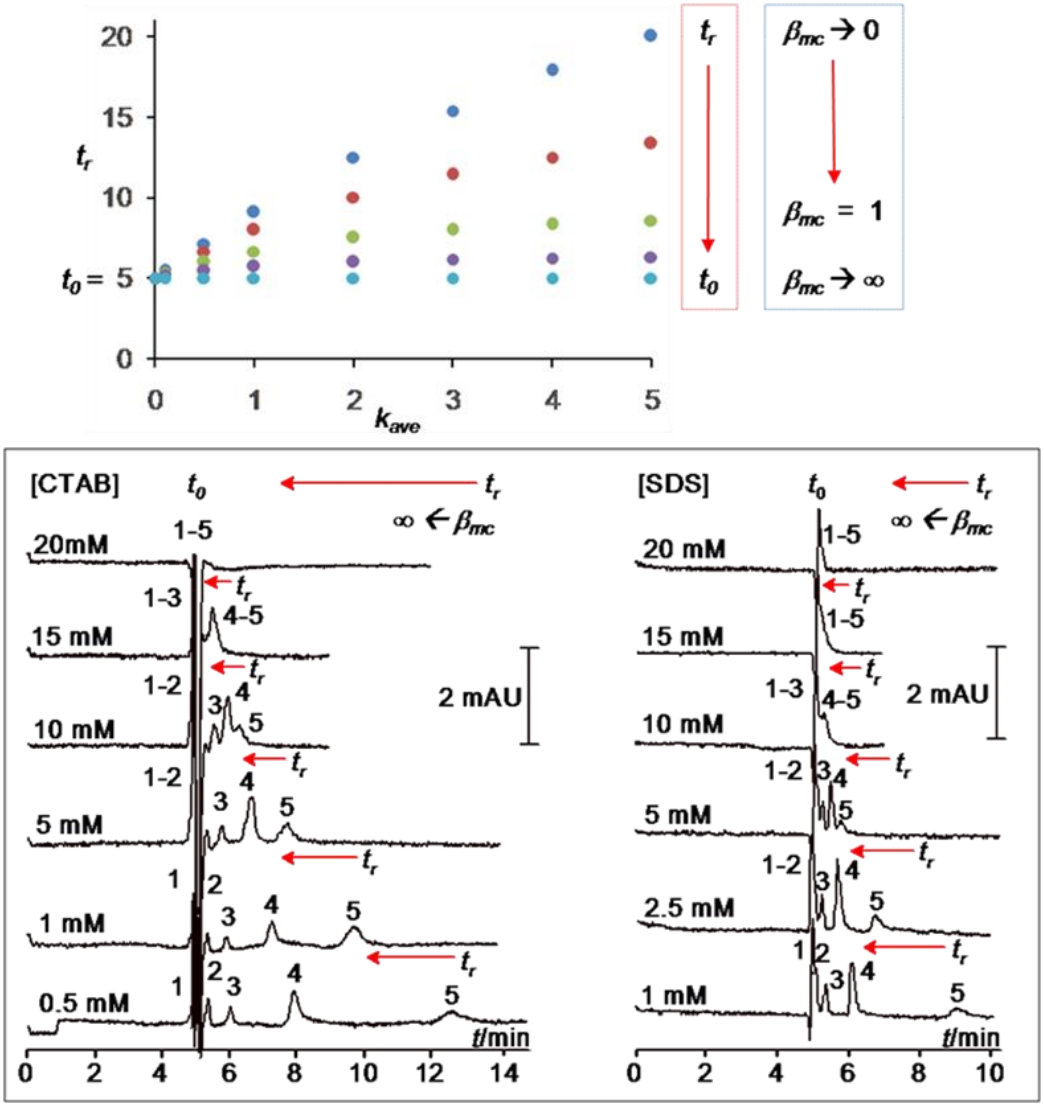

Figure 4.2 (top) The plot of analyte's k_{av} from 0.1 – 5 versus calculated t_R. The $t_R = t_0$ if the analyte was not retained or solubilized into the interfacial micelles. The increase in the micellar phase ratio or $\beta_{mc} \rightarrow \infty$ caused the $t_R \rightarrow t_0$. At $\beta_{mc} = 1$, the micelle solubilized analytes were equally distributed to the interfacial and solution micelles. (bottom) Experimental verification of the trend of $t_R \rightarrow t_0$ as $\beta_{mc} \rightarrow \infty$, using 25 µm i.d. capillaries. The $\beta_{mc} \rightarrow \infty$ when the CTAB concentration [CTAB] or SDS concentration [SDS] in 100 mM ammonium bicarbonate pH 8.5 as mobile phase was increased from 0.5 mM CTAB or 1 mM SDS to 20 mM. The analytes were mostly solubilized in the solution micelles with the 20 mM CTAB or SDS in the mobile phase. The analytes were methyl phenyl ketone (peak 1), ethyl phenyl ketone (peak 2), propyl phenyl ketone (peak 3), butyl phenyl ketone (peak 4) and pentyl phenyl ketone (peak 5), in the order of increasing hydrophobicity or k_{av}. The analyte concentrations were 0.4 – 1.1 mM and injected sample plug was 2 mm. The mobile phases were flowed at a rate of 10 cm/min (180 mbar).

4.4.4 Effect of pH, salt addition and MeOH content on the retention

It was possible to control the number of solubilised solutes into the micelles at the interface or in the solution by changing the surfactant concentration in the mobile phase, as deduced from the chromatographic results in Figure 4.2. The relative retention time (t_R/t_0) for the alkyl phenyl ketones became equal to 1 as the surfactant concentration was increased as shown in Figure 4.3(a) for CTAB. A t_R/t_0 >1 indicated retention or substantive solubilisation into the interfacial micelles. Solubilisation into the solution micelles was significant at CTAB concentrations > 5mM, as more micelles were formed in solution. Other ways to control the solubilisation were investigated using the CTAB and silica system by buffer pH variation as well as NaCl and MeOH addition. The calculated t_R/t_0 values are shown in Figure 4.3(b – d). The solubilising power of interfacial micelles decreased with a decrease in buffer pH (see Figure 4.3(b)). The t_R/t_0 values for the alkyl phenyl ketones were >1 at pH 7 – 10, then were equal to 1 except for pentyl phenyl ketone at pH 2 – 4. This was related to the pKa = 4.9 of the isolated silanol groups in silica.[39] There was a decrease in number of charged sites at the surface for CTAB organisation at below pH 7, and the presence of randomly spaced patchy interfacial micelles at pH = pKa $\pm$ 1 is suspected. Most likely there were no interfacial spherical micelles at pH $\leq$ 3, where the number of charged sites at the surface was very low.

The solubilising power of solution micelles towards the retained analytes increased with an increase in NaCl concentration ([NaCl]) (see Figure 4.3(c)). The t_R/t_0 values decreased from 0.5 to 3.0 M NaCl. This was related to the decrease in the cmc of CTAB caused by the addition of NaCl. The β_{mc} increased as more micelles were formed at high [NaCl]. For the MeOH content study (see Figure

4.3(d)), the observed decrease in retention was due to the increased eluting power of the mobile phase (solution micelles + bulk solution). The t_R/t_0 values decreased as the mobile phase polarity decreased, when the MeOH percentage (MeOH%) was increased from 5 to 70%. This is analogous to the decrease in elution time in gradient elution reversed-phase LC. There was no retention except for pentyl phenyl ketone in the 40-70% range MeOH in the mobile phase. The high MeOH content also increased the cmc that decreased the amount of solution micelles.[40]

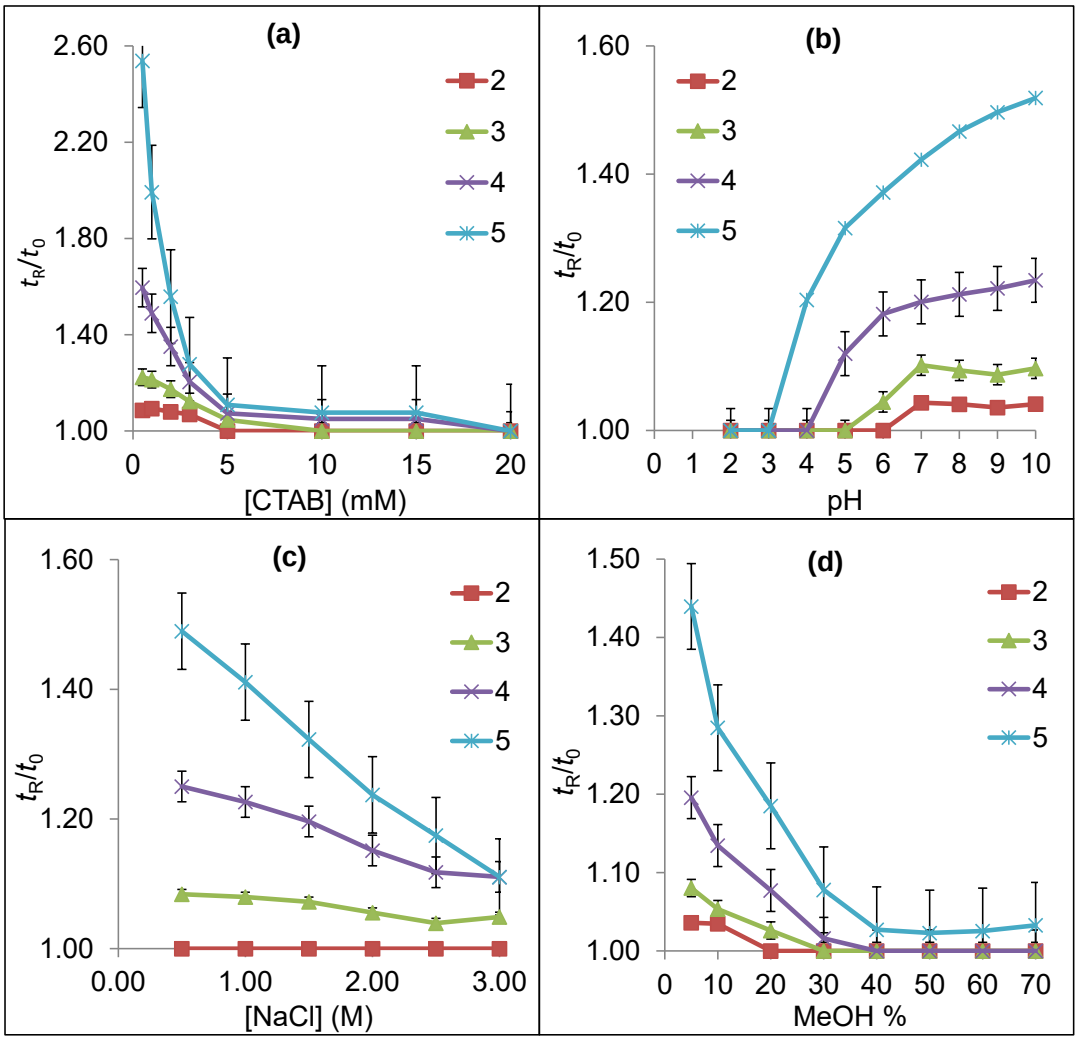

Figure 4.3 Relative retention time (t_R/t_0) versus concentration [CTAB] from 0.5-20 mM (a), pH from 2-10 (b), concentration [NaCl] from 0-3 M (c) and MeOH percentage from 5-70% (d) in the mobile phase in OT-LC using a 50 µm i.d. capillary. The mobile phases contained 100 mM ammonium bicarbonate pH 8.5 except for the pH study. For the pH plot, the conductivity of the mobile phases using phosphate buffers was controlled and equal to 6.0 $\pm$ 0.2 mS/cm. Separation pressure was 500 mbar. The analyte concentrations were 0.4 -1.1 mM. The analytes were methyl phenyl ketone (peak 1, t_0 marker), ethyl phenyl ketone (2), propyl phenyl ketone (3), butyl phenyl ketone (4) and pentyl phenyl ketone (5), in the order of increasing hydrophobicity or k_{av}. For an unretained analyte, $t_R/t_0 = 1$. The analytes were mainly in the mobile phase and spent less time in the stationary phase or interfacial micelles. For a retained analyte, $t_R/t_0 > 1$. The effect of solubilisation of analytes into the interfacial micelles caused the $t_R > t_0$. More explanation in the text.

4.4.5 Analytical figures of merit and application to environmental water and processed food samples

The potential of the proposed separation approach for the determination of pesticides in environmental water samples and antioxidants in processed food samples was investigated. Figure 4.4 (a)i and Figure 4.4 (b)i are separations of the analytes prepared in the mobile phase. These are typical injections of standard solutions. The conditions were optimised by changing the surfactant concentrations, pH and organic solvent content, to achieve the separations within a reasonable time of 20 min. It was not intended to add organic solvent in the final mobile phases, but it can be noted that <0.3 mL of organic solvent was consumed per day for each mobile phase in Figure 4.4. The CTAB and SDS concentration was above the measured cmc (0.20 mM CTAB and 0.75 mM SDS) in the mobile phase used. The cmc values change with the composition of the solution, and thus cmc values should be determined for each buffer that will be used in the preparation of the mobile phase. The analytical figures of merit (linearity, limit of detection (LOD) and interday and intraday (5 days) repeatability of t_R and peak area) are summarised in Tables 4.1 and 4.2 for the CTAB and SDS separation, respectively. The values were considered acceptable, however the LODs were at least an order of magnitude higher than those obtained by other capillary based separation techniques of MEKC and CEC. This is because of the flat profile of the flow (*i.e.*, EOF) in the electrodriven techniques of MEKC and CEC.

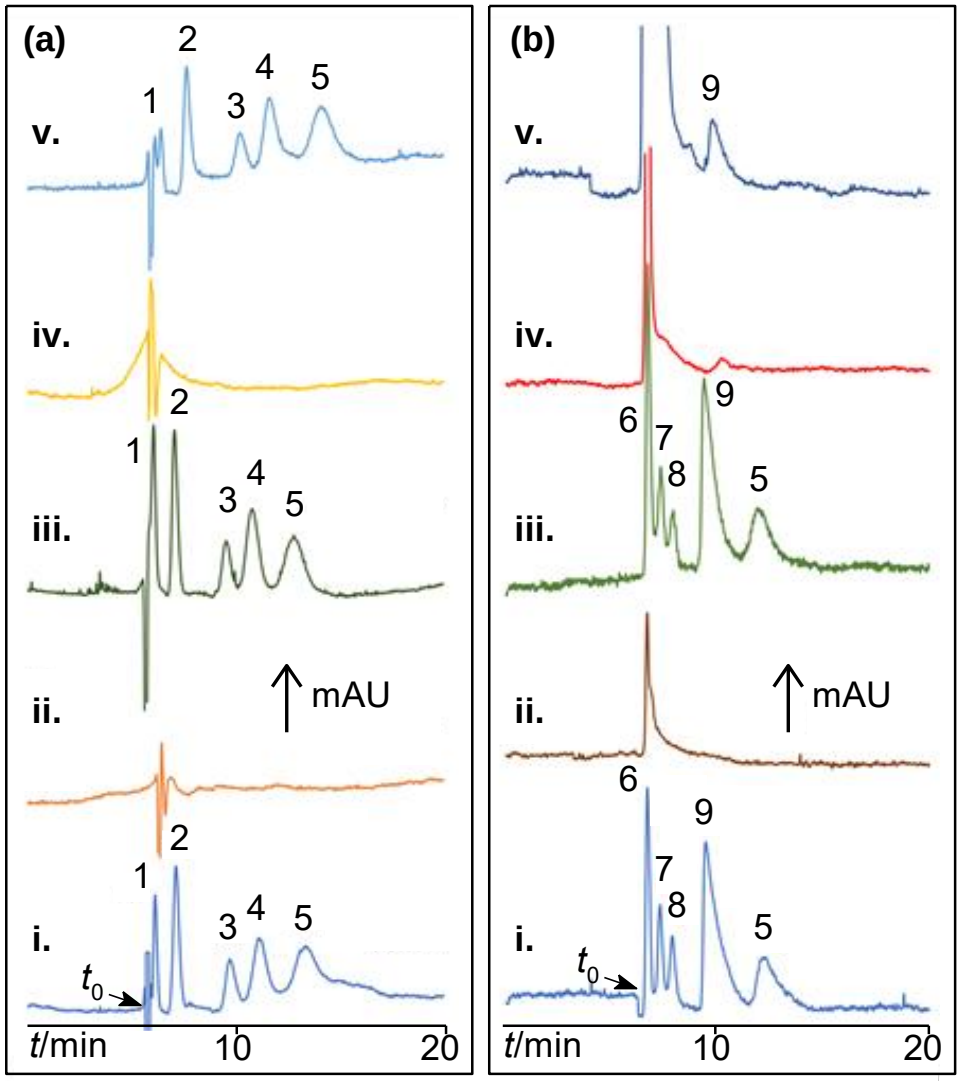

Figure 4.4 OT-LC chromatograms of pesticides (a) and antioxidants (b). Mobile phase was 0.35 mM CTAB in 50 mM sodium borate pH 11 and 5% MeOH (a) and 1 mM SDS in 100 mM sodium phosphate pH 6 and 2% ACN (b). Capillary i.d. and total length was 50 µm and 120 cm (110 cm to detector), respectively. The analytes were atrazine (1), diuron (2), diazinon (3), fenitrothion (4), parathion (5), propylgallate (6), butylhydroxytoluene (7), tert-butylhydroxyquinone (8), and butylhydroxyanisole (9) at 1.77 – 3.43 mM. Separation pressure was 500 mbar. In (a) and (b), (a)i and (b)i were the standards injection of analytes in the mobile phase. In (a), (a)iii and (a)v was fortified sample injection of Browns river water and Dru Point estuary water extract, respectively. (a)ii and (a)iv was injection of unfortified extract, correspondingly. In (b), (b)ii, (b)iv, and (b)v was unfortified sample injection of instant noodle, chicken flavor rice cracker, and beef soup flavor mix extract, respectively. (b)ii was fortified sample injection of instant noodle extract. The chromatograms in each box were drawn on the same scale.

The sample preparation procedures used in this study were based on published methods and are briefly described in Materials and Methods section. This study was aimed primarily to look at the effect of the sample matrix on the OT-LC separations. The results are shown in Figure 4.4(a) and Figure 4.4(b) with CTAB and SDS as pseudophase, respectively. Figures 4.4(a)ii and iv are chromatograms from injections of the water sample extracts from pristine Tasmania, Australia. The analytes tested were not found in the samples. The separations were not affected by the sample matrix, which was deduced from the analysis of the fortified sample extracts in Figures 4.4 (a)iii and v. Recovery values (peak area) of analytes from injection of the standard in Figure 4.4 (a)i/ peak area from injection of the fortified sample in Figure 4.4 (a)iii or v were acceptable (> 80%) except for of the less retained peak 1 since it was eluted too close to the t_0.

Figures 4.4 (b)ii, iv and v are chromatograms from injections of the processed food sample extracts, which are in complex sample matrices. Butylhydroxyanisole (BHA) was identified in one of the samples (*i.e.*, beef soup flavour mix in Figure 4.4 (b)v) based on retention time comparison with the standard injection in Figure 4.4 (b)i. BHA is an additive indicated in the label for the soup flavour mix. The calculated amount of BHA in the soup flavour mix sample was 0.006% (w/w). Figure 4.4 (b)iii was from the analysis of the fortified sample extract in Fig 4.4 (b)ii, showing again that the quantitation of a poorly retained analyte (*i.e.*, peak 6) was difficult due to the matrix constituents, causing the co-elution of peak 6 at the t_0. The same issue was found with the other sample matrices in Figure 4.4 (b)iv and v, and this can be typically solved by developing an additional sample clean-up procedure. Sample preparation is another topic and there are green sample preparation methods available in literature.[41,42]

In summary, although the green aspects of the proposed OT-MLC are clear (*i.e.,* complete removal of chemical waste), the peak shapes, analyte sensitivity, and baseline stability are not as good as in LC. The baseline stability in the developed method was related to the pressure pumping of the instrument we used, which was designed for CE to do electrophoretic separations. The development of instrumentation using more reliable pumping systems should improve the performance of the presented OT-LC with surfactant solutions. The proposed analytical separation approach is also more economical than LC which employs commercially available columns that could cost more than 1500 AUD. In addition, LC columns are packed with stationary phases that are often prepared using organic solvents, with prolonged synthesis time, and chemical waste production from excess and unreacted organic reagents. This contrasts with the proposed OT-LC columns with "soft" stationary phases that are prepared rapidly by simply flushing the capillary with the surfactant solution.

Table 4.1 Analytical figures of merit for the OT-MLC with CTAB of pesticides.

	analyte				
	atrazine	diuron	diazinon	fenitrothion	parathion
Linearity					
concentration range, *x 10*$^{-4}$ M	1.2 – 9.3	1.1 – 8.6	1.5 – 12	1.8 – 14	2.1 – 17
equation of line (y = mx+b)					
slope (m)	14.42	19.31	1.41	1.30	0.50
y-intercept (b)	+ 99.28	+ 9.24	+ 43.76	+ 73.61	+ 66.02
coefficient of variation (R^2)	0.996	0.998	0.996	0.998	0.999
limit of detection, *x 10*$^{-4}$ M (S/N = 3)	0.057	0.067	1.3	0.89	1.3
Repeatability, RSD (%)					
retention time					
intraday (n=3)[1]	0.2 – 0.7	0.1 – 1.1	0.05 – 0.8	0.2 – 0.9	0.3 – 2.0
interday (n=15)[2]	0.8	1.2	2.8	3.2	3.0
peak area					
intraday (n=3)[1]	2.8 – 5.5	1.0 – 5.5	0.2 – 4.2	1.6 – 4.4	0.4 – 6.0
interday (n=15)[2]	5.6	5.4	4.5	4.9	7.6

Table 4.2 Analytical figures of merit for the OT-MLC with SDS of antioxidants.

	analyte				
	propyl gallate	butylated hydroxy-toluene	*tert*-butyl-hydroqui-none	butylated hydroxy-anisole	parathion
Linearity					
concentration range, *x 10*$^{-4}$ M	1.1 – 8.8	1.4 – 11	2.3 – 18	1.7 – 14	1.4 – 12
equation of line (y = mx+b)					
slope (m)	14.6	7.65	4.25	5.71	1.49
y-intercept (b)	+ 241.49	- 19.44	- 56.83	- 26.23	- 3.36
coefficient of variation (R^2)	0.996	1.000	0.998	0.992	0.996
limit of detection, *x 10*$^{-4}$ M (S/N = 3)	0.12	0.31	1.2	0.77	0.58
Repeatability, RSD (%)					
retention time					
intraday (n=3)[1]	0.1 – 2.0	0.2 – 2.1	0.2 – 1.2	0.2 – 3.1	0.3 – 1.9
interday (n=15)[2]	0.7	0.9	1.1	2.8	2.8
peak area					
intraday (n=3)[1]	1.0 – 8.4	1.9 – 5.6	1.0 – 7.3	0.4 – 3.4	0.8 – 9.2
interday (n=15)[2]	5.5	4.7	11.6	5.2	10.1

[1]RSD% range taken within 5 days with three replicates (n=3) per day.
[2]Taken from 15 pooled peak areas (n=15) within 5 days.

4.5 Conclusion

This new analytical chromatographic technique introduced here uses nanosized micellar pseudophases from long-chain ionic surfactants in the solution and at the surface-liquid interface. The pseudophases provided surprising retention and separation of a range of analytes in column i.d.s that are not typical in OT-LC. Fast chromatography was obtained at high flow-velocities. There are limitations encountered with the approach since it is at the early stage of development. These include lower separation efficiencies, low peak capacity, and low analyte detection sensitivity when compared to standard and microLC and CE. These drawbacks were partly attributed to band broadening caused by the parabolic flow of mobile phase as well as the instrumental constraints for the setup used in the present study. A new and green liquid chromatography approach in open-tubes is also presented with the following advantages and/or features: up to zero chemical waste, minimal use of reagents and samples, no preparation of a solid stationary phase, relatively fast separations and reproducible results.

There is still the need to improve separation efficiencies, particularly by employing < 10 μm i.d. capillaries, since mass transport of analytes is improved by decreasing the i.d. of columns. Chromatographic separations in nanochannels[8,43] without a solid phase may even be realized. Separations were currently performed by applying pressure at one end of the capillary, but commercially available nano-pumps should provide better performance. Different separation selectivity will be studied using other surfactants, including bile salts with chiral recognition properties. The sample enrichments with the use of purely aqueous solutions (e.g., by altering the elution pH) will be explored to develop green extraction technologies at the analytical scale or even at larger scales using arrayed columns

or high surface area materials. The fundamental phenomenon of analyte solubilisation into two types of micelles from the same surfactant solution might find use in some industrial processes and products such as in drug delivery, drug formulations, cosmetics and food.[44]

4.6 References

(1) T.M. Arrell, C.L. Marcum, H. Sheng, B.C. Owen, C.J. O'lenick, H. Maraun, J.J. Bozell and H.I. Kenttamaa, *Green Chem.*, 2014, 16, 2713-2727.

(2) F. Svec and Y. Lv, *Anal. Chem.*, 2015, 87, 250-73.

(3) N. Tanaka and D.V. Mccalley, *Anal. Chem.*, 2016, 88, 279-298.

(4) B. Soares, H. Passos, C.S.R. Freire, J.A.P. Coutinho, A.J.D. Silvestre and M.G. Freire, *Green Chem.*, 2016, 18, 4582-4604.

(5) W. Huang, M.- Lan, C.- Qi, S.- Zheng, S.- Wei, B.- Yuan and Y.- Feng, *Chem. Sci.*, 2016, **7**, 5495-5502.

(6) M.J. Andrés-Costa, V. Andreu and Y. Picó, *Trends Anal. Chem.,* 2017, 94, 21-38.

(7) R. Örkényi, J. Éles, F. Faigl, P. Vincze, A. Prechl, Z. Szakács, J. Kóti and I. Greiner, *Angew. Chem. Int. Ed.,* 2017, 56, 8742-5.

(8) H. Shimizu, A. Smirnova, K. Mawatari and T. Kitamori, *J. Chromatrog. A*, 2017, 1490, 11-20.

(9) X. Yuan and R.D. Oleschuk, *Anal. Chem.,* 2018, 90, 283-301.

(10) N. Ganewatta and Z. El Rassi, *Electrophoresis,* 2018, 39, 53-66.

(11) E.R. Major, *LC GC Europe,* 2012, 25, 1-7.

(12) P. T. Anastas, *Crit. Rev. Anal. Chem.* 1999, 29,167-175.

(13) C.J. Welch, *et.al.*, *TrAC - Trends Anal. Chem.,* 2010, 29, 667-680.

(14) E.A. Peterson, *et.al.*, *Green Chem.,* 2014, 16, 4060-4075.

(15) Y. Shen, B. Chen and T.A. Van Beek, *Green Chem.,* 2015, 17, 4073-4081.

(16) M.J. Ruiz-Angel, E. Peris-Garcia and M.C. Garcia-Alvarez-Coque, *Green Chem.,* 2015, 17, 3561-3570.

(17) P.T. Anastas and J.C. Warner, Green Chemistry: Theory and Practice, Oxford University Press, Oxford, UK, 2000.

(18) C.J. Welch, T. Nowak, L.A. Joyce and E.L. Regalado, *ACS Sustainable Chem. Eng.,* 2015, 5, 1000-1009.

(19) X. Yuan, E.G. Kim, C.A. Sanders, B.E. Richter, M.F. Cunningham, P.G. Jessop and R.D. Oleschuk, *Green Chem.,* 2017, 19, 1757-1765.

(20) X. Yuan, B.E. Richter, K. Jiang, K.J. Boniface, A. Cormier, C.A. Sanders, C. Palmer, P.G. Jessop, M.F. Cunningham and R.D. Oleschuk, *Green Chem.,* 2018, 20, 440-448.

(21) G. Desmet and S. Eeltink, *Anal. Chem.,* 2013, 85, 543-556.

(22) W.J. Cheong, F. Ali, Y.S. Kim and J.W. Lee, *J. Chromatogr. A,* 2013*,* 1308, 1-24.

(23) R. De Pauw, T. Swier, B. Degreef, G. Desmet and K. Broeckhoven, *J. Chromatogr. A,* 2016, 1473, 48-55.

(24) T. Hara, *et.al.*, *Anal. Chem.,* 2016, 88, 10158-10166.

(25) D.W. Armstrong and F. Nome, *Anal. Chem.,* 1981, 53, 1662-6.

(26) S. Terabe, K. Otsuka, K. Ichikawa, A. Tsuchiya and T. Ando, *Anal. Chem.,* 1984, 56, 111-3.

(27) M. Ye, H. Zou, Z. Liu, J. Ni and Y. Zhang, *J. Chromatogr. A,* 1999, 855, 137-145.

(28) T. Tegeler and Z. El Rassi, *Electrophoresis,* 2002, 23, 1217-1223.

(29) F. Reiss-Husson and V. Luzzati, *J. Phy. Chem.*, 1964, 68, 3504-3511.

(30) S. Manne and H.E. Gaub, *Science*, 1995, 270, 1480-1482.

(31) S. Manne and G.G. Warr, *ACS Symposium Series*, 1999, 736, 2-23.

(32) T. Aranas, A.M. Guidote Jr., P.R. Haddad and J.P. Quirino, *Talanta,* 2011, 85, 86-90.

(33) V. Darji, M.C. Boyce, I. Bennett, M.C. Breadmore and J.P. Quirino, *Electrophoresis,* 2010, 31, 2267-71.

(34) E.A. Aniansson, *et.al., J. Phys. Chem.,* 1976*,* 80, 905-922.

(35) Y. Rharbi, M. Karrouch and P. Richardson, *Langmuir,* 2014, 30, 7947-7952.

(36) J. Lang, *et.al., J. Phys. Chem.,* 1975, 79, 276-283.

(37) T. Hara, H. Kobayashi, T. Ikegami, K. Nakanishi and N. Tanaka, *Anal. Chem.,* 2006, 78, 7632-7642.

(38) N.P. Dinh, T. Jonsson and K. Irgum, *J. Chromatogr. A,* 2013, 1320, 33-47.

(39) H.- Fan, F. Li, R.N. Zare and K.- Lin, *Anal. Chem.,* 2007, 79, 3654-3661.

(40) A.M. Guidote and J.P. Quirino, *J. Chromatogr., A*, 2010, 1217, 6290-6295.

(41) J. Płotka-Wasylka, M. Rutkowska, K. Owczarek, M. Tobiszewski and J. Namieśnik, *TrAC - Trends Anal. Chem.,* 2017, 91, 12-25.

(42) Z. Niu, W. Zhang, C. Yu, J. Zhang and Y. Wen, *TrAC - Trends Anal. Chem.,* 2018, 102, 123-146.

(43) Smirnova, H. Shimizu, Y. Pihosh, K. Mawatari and T. Kitamori, *Anal. Chem.*, 2016, 88, 10059-64.

(44) R. Zhang and P. Somasundaran, *Adv. Colloid Interface Sci.,* 2006, 123-126, 213-229.

Chapter 4 Appendix

Table A4.1 Relative retention time (t_R/t_0) of selected analytes in the proposed OT-MLC.

pseudophase	CTAB t_R/t_0	SDS t_R/t_0		CTAB t_R/t_0	SDS t_R/t_0
cations			*anions*		
nicardipine	1.71	-	flufenamic acid	2.51	1.11
labetalol	1.63	1.39	mefenamic acid	2.30	1.06
imipramine	1.57	-	4-bromophenol	1.96	1.50
verapamil	1.54	-	fenbufen	1.82	-
dibucaine	1.49	-	fenoprop	1.79	-
propranolol	1.40	-	ibuprofen	1.72	-
naphthylamine	1.26	1.51	dichlorprop	1.63	-
diphenhydramine	1.23	-	4-vinylbenzene-sulfonic acid	1.63	-
alprenolol	1.17	2.84	sulindac	1.57	-
chlorpheniramine	1.14	2.73	4-nitrophenol	1.56	-
3-hydroxypyridine	1.06	-	furosemide	1.31	-
pindolol	1.04	1.47	chloramphenicol	1.09	1.06
nadolol	1.04	1.07	4-methoxyphenol	1.08	1.04
dibenzoquat	-	4.02			
diquat	-	1.16	*amphiphilic*		
neostigmine	-	1.04	sulfaquinoxaline	1.74	1.08
			sulfamethizole	1.60	-
p-nitroaniline	-	1.17	sulfadimethoxine	1.55	-
p-toluidine	-	1.04	sulfamethoxazole	1.39	-
ranitidine	-	1.03	sulfamerazine	1.12	-
neutrals			*amino acids/peptides/protein*		
chlorpyriphos	2.16	-	tyr-tyr-tyr	1.74	-
biphenyl	1.70	-	ubiquitin	1.44	-
acenaphthene	1.64	-	glu-val-phe	1.43	1.02
parathion	1.59	2.76	tryptophan	1.23	-
fenitrothion	1.52	2.13	phenylalanine	1.05	-
diazinon	1.46	1.66	bradykinin	-	1.27
prednisolone	1.40	1.08			
hydrocortisone	1.33	1.11			
azinphos-methyl	1.32	2.06			

Mobile phase was 1 mM CTAB or 1 mM SDS in 100 mM ammonium bicarbonate pH 8.5. Capillary was 50 µm i.d. and was unmodified (CTAB) or modified (SDS) with a cationic polyelectrolyte PDADMAC. Injection length was 2 mm. Separation was by pressure at a flow velocity of 10 cm/min. Detection was at 200 nm. More analytes were retained with CTAB as pseudophase.

Chapter 5

Conclusion and future direction

A major research interest for separation sciences continues to be the development of column stationary phases in chromatography and its associated areas that are efficient, robust, and selective. This has spurred the advancement of diverse novel materials as SPs made from nanomaterials, MOFs and COFs, novel functionalised polymers, and even biomaterials. A new and green approach for LC and CEC has been developed here in open-tubular capillary format that exploits the retentive behaviour of molecular aggregates of long-chain surfactants at the solid-solution interface below and above their cmc. Open-tubular admicellar liquid chromatography and electrochromatography (OT-AMLC and OT-AMEC) utilise surfactant aggregates below the cmc but above the csac as soft, immobile stationary pseudophases to demonstrate chromatographic and electrochromatographic separations. Open-tubular micellar liquid chromatography employs surfactant interfacial and solution micelles formed above the cmc, manifesting unexpected retention behaviour.

Surfactant micelles have long been used in pressure-driven (MLC) and electrodriven (MEKC) separations requiring surfactant solutions to be above the cmc. Surfactants are introduced in the mobile phase in chromatography and electrochomatography, thereby modifying or affecting their cmc values. Thus, determining the cmc of surfactants in the BGS is necessary, especially for OT-AMLC, OT-AMEC and OT-MLC. The significance of cmc, including csac, of surfactants in the BGS draws from the fundamental understanding of mechanism of molecular aggregation of surfactants on a solid-solution interface introduced by

Somasundaran and Fuerstenau.[1] Thus, in Chapter 2, the generation of adsorbed surfactant aggregates of CTAB and SDS by self-assembly onto a fused-silica surface were characterised using electrophoretic methods based on CE. The decrease in the EOF magnitude as surfactant concentration was increased at initial stages was depicted as the formation of surface hemimicelles. The transition from zero EOF to reversal of polarity was described as the slow formation of bilayer aggregates called admicelles. The surfactant concentration at the transition was denoted as the csac. The gradual increase of the reversed EOF mobility signified charge build-up from further bilayer formation. The reversed μ_{EOF} reached a constant value indicating surface saturation with adsorbed admicelles and morphological change. This also inferred the formation of bulk micelles in solution and the surfactant concentration at this point was denoted as the cmc. The csac and cmc values of CTAB were varied (csac-cmc: 0.04-0.20 mM in 50 mM sodium tetraborate at pH 9.5; 0.09-0.50 mM in 100 mM ammonium bicarbonate at pH 8.5) due to buffer effects (pH, ionic strength or added electrolyte). Determining the csac and cmc for SDS (0.16-0.75 mM in 100 mM ammonium bicarbonate at pH 8.5) required column precoating with cationic PDADMAC to generate the positively-charged surface necessary for SDS adsorption. The electrophoretic method employed can be regarded as a straightforward and simple procedure for cmc and/or csac determination, especially for the study and application of OT-AMLC/AMEC/MLC with surfactants in the actual mobile phase environment being used.

The concentration range between the csac and the cmc of CTAB was used as a basis for OT-AMLC and OT-AMEC in Chapter 3. Pressure-driven and voltage-driven separations of neutral alkylphenones were depicted in the increase of their

RRT at CTAB concentrations from the csac and above the cmc, showing the retentive abilities of admicelles. The retention of alkylphenones were differentiated by their RRTs based on their hydrophobicity. This behaviour was explained in the light of the phase ratio (β) parameter in open-tubular chromatography, where β would decrease as retention increases with addition of surfactants. The similarity of RRT values in both pressure- and voltage-driven separations confirmed that formed admicelles acted as immobile pseudophases even in the presence of an electric field, thus the dubbing of the methods as OT-AMLC and OT-AMEC. These separations were again demonstrated using five neutral pesticides. The better chromatographic profile (i.e. sharper peak shapes) in OT-AMEC showed the advantages of having the flat plug profile of the EOF. A new method for cmc determination was also developed from pressure-driven (OT-LC) separations of alkyl phenyl ketones (*e.g.* pentyl phenyl ketone) based on highest RRT attained at varying surfactant concentrations and replicated in different column i.d. (25 – 200 μm). Increased retention with smaller i.d. columns reinforced expectations with open-tubular chromatography.

Mobile phase parameters were also essential to fully depict separation performance of OT-AMLC. pH effects on retention showed influence on the degree of surface ionisation to control surfactant adsorption, *i.e.* minimal retention at pH 6 – 8 attributed to insufficient ionised surface for adsorption, but highest and constant at alkaline conditions (pH ≥ 8) due to complete surface ionisation and maximum surface charge. Addition of salt (NaCl) affected retention due to lowering of the csac (and the cmc), thus increasing admicelle formation and also the chromatographic retention. Addition of MeOH produced a reversed-phase mechanism on the CTAB admicelles resulting in decreased retention. Problems

with longer analysis time from pH effects on the EOF, and high running currents resulting from increasing salt on the BGS were obviously unfavourable for studying further the mobile phase effects by voltage-driven OT-AMEC. The OT-AMLC of anionic sulfonamides was shown feasible at the optimised BGS of pH 8.5 at high buffer concentration (400 mM ammonium bicarbonate) and 0.20 mM CTAB (determined as below the cmc by similar OT-LC methods) and 2% MeOH. The OT-AMEC of sulfonamides showed retention of the analytes close to the EOF indicating affinity with the admicellar pseudophase, as confirmed by loss of retention in the PDADMAC-coated capillary. The analytical figures of merit of OT-AMLC using neutral (pesticides) and anionic (sulfonamides) analytes were deemed to be acceptable, although performance can be further improved by using more appropriate instrumentation optimised for open-tubular separations. No adverse effects of sample matrices (from local environmental surface water samples) on the LC technique showed applicability to real samples but these may require some sample clean-up and preconcentration.

Surfactant concentration at and above the cmc governed the experimental conditions for OT-MLC as elaborated in Chapter 4. The RRT profile of pentyl phenyl ketone against surfactant concentration showed a decreasing trend past the cmc (with maximum RRT) for pressure-driven separations (OT-MLC) and an increasing trend above the cmc for voltage-driven separations (MEKC). The decreasing pattern is reflected by the phase ratio in the micellar conditions, where increasing elution caused by increasing solution micelles led to a decrease in retention on the interfacial micelles. For electrodriven separations, the increase in RRT was attributed to the migration of micelles under an applied electric field, which is a major factor in MEKC separation. In OT-MLC, the interesting retentive

action of CTAB near the vicinity of its cmc is attributed to the solubilisation of solutes among dense spherical interfacial micelles on the solid surface and the dispersed solution micelles and its distribution among them through rapid micellisation-demicellisation equilibrium processes. This proposed mechanism was rationalised by the micellar phase ratio β_{mc} illustrating a solute's changing retention behaviour when surfactant concentration is varied. This was used to explain the unexpected retention of methyl- and pentyl phenyl ketones in capillaries of i.d. $\geq$ 50 μm and relatively fast analysis of sulfonamides at high flow rates, achieving good separations.

Mobile phase conditions just above the cmc were also shown to affect the separation and retention behaviour of test solutes (alkyl phenyl ketones) and control over solute solubilisation among interfacial and solution micelles. Similarly, pH influenced the degree of surface ionised sites for surfactant adsorption, thus minimal interfacial micelles at lower pH resulted in decreasing analyte solubilisation and therefore retention. Salt effects on the lowered cmc increased the solubilisation by predominant solution micelles which decreased solute retention. Increase in added organic solvent enhanced the eluting power of the less polar mobile phase, resulting in decreasing retention. The separation performance of OT-MLC of neutral pesticides using CTAB and anionic food-grade antioxidants using SDS at optimised mobile phases demonstrated that good separations can be achieved within 20 min. The analytical figures of merit were considered acceptable despite LODs being an order of magnitude higher when compared to MEKC or CEC techniques. Similarly, the absence of negative matrix effects obtained from real samples of local environmental surface waters qualifies the acceptability of OT-MLC. BHA, a common food additive, was even confirmed present from the

food sample matrix (identified as present in the product label) based on retention time comparison with the standard.

The three techniques introduced in this thesis, being in the initial stages of development, still show some serious limitations, particularly with regard to chromatographic efficiencies (on peak shape and peak width), peak capacities, and analyte detection sensitivity when comparted to developed standard and micro-LC and CE/CEC approaches. Band broadening is particularly a concern for the pressure-driven techniques as well as the need for appropriate instrumentation to meet the requirements of open-tubular capillary formats, *e.g* use of efficient nano-pumps to improve separation performance. Improved separation efficiencies are anticipated when employing capillaries of < 10 μm i.d. due to the expected increased mass transport and improved phase ratios. Further investigations are needed in the use of other surfactants, perhaps exhibiting potential selectivity and chiral separation abilities (*e.g*. bile salts), narrower i.d. capillaries, real or more complex sample matrices, and performance comparison with other related separation techniques. Studies could be extended to use other flow micro- or nanochannels, *e.g*. microfluidic platforms, multichannel capillaries and photonic crystal fibers. Green extraction methodologies can be established in analytical scale or high-surface-area column arrays based on the working principle as was already demonstrated by the sample enrichment examples using purely aqueous solutions and simple alteration of elution pH.[2] The same principle of analyte solubilisation can find use in industrial process and products like drug delivery and formulation, cosmetics and food. Despite some apparent limitations, these new techniques have demonstrated strong characteristics in the greening of analytical chemistry – up to

zero chemical waste, minimal use of reagents and samples, no preparation of a solid stationary phase, relatively fast separations and reproducible results.

References

(1) Somasundaran, P.; Fuerstenau, D. W. *J Phys Chem* **1966**, *70*, 90-96.

(2) Quirino, J. P.; Tarongoy, F. M. *Green Chemistry* **2018**.